Experimental Performance Analysis of Heat Exchanger-Evacuated Tube Assisted Drying System (HE-ETADS) under Various Operation Conditions

Ph.D. Thesis Submitted

in Partial Fulfillment of the Requirement for the

Degree of

DOCTOR OF PHILOSOPHY

in

MECHANICAL ENGINEERING

by

Anand Kushwah

(2K20/Ph.D./ME/505)

Under the supervision of

Dr. Anil Kumar
(Associate Professor)
Supervisor

Dr. Amit Pal
(Professor)
Jt-Supervisor-I

Dr. Manoj Kumar Gaur
(Professor)
Jt-Supervisor-II

Department of Mechanical Engineering

DELHI TECHNOLOGICAL UNIVERSITY

(Formerly Delhi College of Engineering)

Shahbad, Daulatpur, Bawana Road, Delhi-110042, India

JANUARY, 2024

DELHI TECHNOLOGICAL UNIVERSITY
Sahbad Daulatpur, Main Bawana Road
Delhi-110042 (India)

DECLARATION

I hereby declare that thesis entitled **"Experimental Performance Analysis of Heat Exchanger-Evacuated Tube Assisted Drying System (HE-ETADS) under Various Operation Conditions"** submitted by me in fulfillment of the requirement for the degree of Doctor of Philosophy to Delhi Technological University (Formerly Delhi College of Engineering) is a record of bonafide work carried out by me under the supervision of Dr. Anil Kumar, Associate Professor, Department of Mechanical Engineering, Delhi Technological University, Dr. Amit Pal, Professor, Department of Mechanical Engineering, Delhi Technological University and Dr. Manoj Kumar Gaur, Professor, Department of Mechanical Engineering, Madhav Institute of Technology & Science,Gwalior, M.P (India).

I further declare that the work reported in this thesis has not been published and will not be submitted, either in part or in full, for the award of any other degree or diploma in any other Institute or University.

(ANAND KUSHWAH)
Roll No: 2K20/ Ph.D./ME/505
Department of Mechanical Engineering
Delhi Technological University, Delhi (India)

Date: April 12, 2024
Place: Delhi, India

DELHI TECHNOLOGICAL UNIVERSITY
Sahbad Daulatpur, Main Bawana Road
Delhi-110042 (India)

CERTIFICATE

This is to certify that the work embodied in the *Thesis* entitled **"Experimental Performance Analysis of Heat Exchanger-Evacuated Tube Assisted Drying System (HE-ETADS) under Various Operation Conditions"** is a record of *bona fide research work* carried out by **Mr. Anand Kushwah** (**2K20/Ph.D./ME/505**) in fulfillment of requirements for the award of degree of **Doctor of Philosophy** in **Mechanical Engineering** specialization in **Thermal Engineering**. He has worked under our guidance and supervision and has fulfilled the requirements which, to my knowledge, have reached the requisite standard for submitting the thesis.

The results in this thesis have not been submitted in part or full at any other University or Institute for the award of any degree or diploma.

(**Dr. Anil Kumar**)
Associate Professor
Mechanical Engineering Department
Delhi Technological University
Delhi-110042 (India)
(Supervisor)

(**Dr. Amit Pal**)
Professor
Mechanical Engineering Department
Delhi Technological University
Delhi-110042 (India)
(Joint Supervisor-I)

(**Dr. Manoj Kumar Gaur**)
Professor
Mechanical Engineering Department
Madhav Institute of Technology & Science
Gwalior (M.P)-474005 (India)
(Joint Supervisor-II)

DELHI TECHNOLOGICAL UNIVERSITY
Sahbad Daulatpur, Main Bawana Road
Delhi-110042 (India)

ACKNOWLEDGEMENT

I would like to express my heartiest gratitude to my research supervisor Dr. Anil Kumar and Joint Supervisors Dr. Amit Pal, and Dr. Manoj Kumar Gaur for their supervision. Special thanks to my mentor and guide Dr. Anil Kumar for his advice and continuous guidance from the conception of this research as well as for imparting extraordinary experiences throughout the work. His advice on both research and my career has been priceless. He has been a tremendous mentor for me. If I was proud of my achievements, he is the main creditor. It is my privilege to be under his tutelage. Perseverance, exuberance, and positive approaches are just some of the traits he has imprinted on my personality. I thankfully acknowledge him for his vital contribution, which made him the backbone of this research and this *Thesis*. These lines are dedicated to my Guide:

"गुरुर्ब्रह्मागुरुर्विष्णुर्गुरुर्देवोमहेश्वरः
गुरुः साक्षातपरब्रह्मातस्मैश्रीगुरवेनमः"

I would like to express my gratitude to Prof. Prateek Sharma, Honorable Vice Chancellor, Delhi Technological University, Delhi, for providing this opportunity to carry out this work in this prestigious institute.

I would like to express my gratitude to Prof. S.K. Garg, DRC Chairperson and Head of the Department of Mechanical Engineering, for his kind support in accomplishing this work.

I express my special thanks to Dr. Ravi Kant, Associate Scientist, Solar Energy Division, Sardar Patel Renewable Energy Research Institute, Gujarat -388 120 (India), for helping me with difficult time and providing unflinching moral support.

My words fail to express my appreciation to my respected parents Shri Ram Singh Kushwah and Smt. Sheela Kushwah whose blessings have helped me to achieve my goal. My wife Mrs. Renu Kushwah and son Lakshya Kushwah deserve thanks for their inseparable support and patience. At last, I would like to thank everyone who helped with the successful realization of this thesis and express my regret that I could not mention them personally one by one.

DELHI TECHNOLOGICAL UNIVERSITY
Sahbad Daulatpur, Main Bawana Road
Delhi-110042 (India)

I would like to extend my thanks to everybody who was essential to the successful realization of this Thesis, as well as express my regret that I could not mention them individually. Finally, I would like to express my gratitude to Almighty 'ॐ ' for giving me patience and strength to achieve such a blissful moment in life.

ANAND KUSHWAH

Roll No: 2K20/ Ph.D./ME/505

Department of Mechanical Engineering

Delhi Technological University, Delhi (India)

DELHI TECHNOLOGICAL UNIVERSITY
Sahbad Daulatpur, Main Bawana Road
Delhi-110042 (India)

ABSTRACT

Food is one of the essential needs of human for their existence. With the increase in population, the food requirement also increases. The food requirement can be met either by growing more food or by conserving the produced one. The edible items (fruits, vegetables, cereals, etc.) mostly get spoiled due to high moisture content in them. The effective method to preserve the crop from being deteriorated is drying it up to a safe moisture level. Solar drying is considered an efficient method of using solar radiation. Solar drying of crops prevents crop deterioration and helps in storing it for longer time. The dried produce has various advantages like better quality, low after harvest losses and longer storage time. To fulfill these criteria an advanced heat exchanger-evacuated tube-assisted drying system (HE-ETADS) has been fabricated at the rooftop of Madhav Institute of Technology and Science, Gwalior (26° 14' N, 78° 10' E) and tested under unload conditions in active mode at different water flow rates (10, 20, and 30Ltr/h). The purpose of testing in unload conditions is to record the maximum temperature and dehydrate the agricultural product that has moisture content in the range of 90 ± 5% to 70 ± 5%. Maximum heat consumption factor (0.775) was calculated during the third day for Category-III (ventilation window is open) at 30Ltr/h. Higher coefficient of performance was 0.902 on third day of experiment for Category-I at 30Ltr/h water flow rate whereas 0.940 was on first day of experimentation for Category-II at 10Ltr/h flow rate. Category-III achieved 0.97 at 10Ltr/h water flow rate during first day of experiment. Response surface methodology (RSM) is applied in the optimization of drying parameters i.e. drying chamber temperature (◦C), water flow rate (Ltr/h), and geometry (cm^2). Optimal operational parameters are observed 89.99°C (drying cabin temperature), 14.0 Ltr/h (water flow rate), 0.9998 (circular geometry), and 0.24004 kg (product mass). Optimum responses were 7.55% db. (moisture content), 5.54 kW/h (energy consumption), and 69.54% (shrinkage). Highest value of drying rate is 1.48 kgH_2O/kg dry solid/h and the maximum efficiency of solar collector and solar dryer is 43.62% and 55.28%, respectively, at 30 Ltr/h water flow rate. Garlic dehydrated from 70% to 8% (wb) moisture content. The maximum exergy efficiency and minimum exergy loss were 57.64% at 30 Ltr/h water flow rate and 4.58 W at 10 Ltr/h water flow rate. Future,

investigations carried out in three different drying methods named HE-ETADS (Heat exchanger- evacuated tube assisted drying system), greenhouse solar dryer (GHSD), and open sun drying (OSD) to compare thin layer drying kinetics, concept of mass transfer, and quality assessment of banana slices. Initial moisture content of banana slices was obtained 78 ± 2.0% (wb), which decreased to 23.2 ± 2.0% (wb), 25.6 ± 2.0% (wb), and 28.8 ± 2.0 % (wb) in all three drying systems respectively in 9hours of drying time. Weibull model (WM) defines thin layer drying kinetics of banana slices in all three drying processes. Maximum hardness and shrinkage factor of dried banana slices were obtained as 373.6g and 75%, respectively, in HE-ETADS. Effective moisture diffusivity, activation energy, and mass transfer coefficient were computed as 1.11E-07 to 2.48E-07m^2s^{-1}, 30.25kJ/mole, 3.21E-04 to 1.0E-04m/s, in HE-ETADS. System mitigates 77, 45.52, and 126 tons of CO_2 & 42.68, 24.62, and 39.21 tons of CO_2 in its lifetime for Case-I and Case-II for garlic cloves, banana slices and peppermint leave correspondingly. Energy payback time for garlic cloves, banana slices, and peppermint leaves is 0.85, 1.1 and 2.45 years less in Case-I compared to Case-II. The drying system is more sustainable in Case-I, with a higher Environmental Sustainability Index (ESI) value of 2.92, while in Case-II, the drying system has a lower value (1.25).

Keywords: *Solar dryer; Evacuated tube solar collector; Drying rate; Efficiency; Exergy; Quality assessment; Mass transfer; Activation energy; Water activity*

DELHI TECHNOLOGICAL UNIVERSITY
Sahbad Daulatpur, Main Bawana Road
Delhi-110042 (India)

TABLE OF CONTENT

DELHI TECHNOLOGICAL UNIVERSITY
Sahbad Daulatpur, Main Bawana Road
Delhi-110042 (India)

LIST OF FIGURES

DELHI TECHNOLOGICAL UNIVERSITY
Sahbad Daulatpur, Main Bawana Road
Delhi-110042 (India)

LIST OF TABLES

NOMENCLATURE

Symbol	Description
A_c	Area of ventilation (m^2)
A_i	Area of inlet hole (m^2)
A_v	Area of vent (m^2)
$A_{Collector}$	Area of Evacuated tube solar collector in m^2
A_{dry}	Area of Dryer (m^2)
B_i	Biot number
C	Constant
C_d	Coefficient of diffusion
C_{pa}	Specific heat of air (kJ/kg-K)
D	Diameter of collector in mm.
D_{eff}	Effective moisture diffusivity, m^2s^{-1}
E_e	Embodied energy (kWh)
E_a	Annual thermal energy output (kWh)
E	Exergy
E_a	Activation energy, kJ/mole
h_m	Mass transfer coefficient, m/s
h	Heat transfer coefficient, $W/m^2/K$
h_c	Convective heat transfer coefficient ($W/m^2°C$)
I_g	Direct solar radiation (W/m^2)
L	Half plane or slabs thickness in meter, m
L_{lv}	Latent heat of vaporization, J/kg
L	Length of collector in mm.
m_c	Total mass of product (kg)
M_d	Mass of dried crop per batch, kg/batch
m_a	Mass of air (kg)
M	Moisture content, %
n	Positive number
P(T)	Pressure of air at temperature T (N/m^2)
ΔP	Pressure difference between drying cabin and air temperature (°C)

q	Quantity of energy used (kW/h)
Q_{ab}	Quantity of heat is immersed (kJ)
Q_n	Amount of heat for drying processes in kJ
R	Universal gas constant, kJ/(mol.K)
R^2	Determination coefficient
t	Time in seconds
T	Temperature in Kelvin (K)
V_T	Total volume of water (m^3)
V_w	Volume of water (m^3)
ρ_{water}	Density of water (kg/m^3)
η_c	Collector efficiency (%)
ρ_{water}	Density of water (kg/m^3)

Subscripts

f	final
i	initial
loss	losses
t	at time t
$t + \Delta t$	at time $t + \Delta t$
Xo	output
Xi	input

Greek symbols

β	Tilt angle, degree
$\chi 2$	Chi-Square
Δt	Total hour of drying, s
θ	Incidence angle, degree

Abbreviations

COP	Coefficient of performance
CHTC	Convective heat transfer coefficient
DR	Drying rate
ETSC	Evacuated tube solar collector
EMC	Equilibrium moisture content
ETC	Evacuated tube collector

EBPT	Energy payback time
FPC	Flat plate collector
HCF	Heat consumption factor
H.E	Heat exchanger
HE-ETADS	Heat Exchanger evacuated tube assisted drying system
ITLEF	Instantaneous thermal loss efficiency factor
MC	Moisture content
MTC	Mass transfer coefficient
RH	Relative humidity
RSME	Root mean square error
RSM	Response surface methodology
SD	Solar dryer
SC	Solar collector

CHAPTER-1

1. Introduction

According to previous investigations, energy utilization in the whole world increased (doubled) every 20 years [1-2]. Therefore, the expenditure on renewable energy is still less than fossil fuel, which is responsible for several environmental pollution and problems worldwide. Hence, the need for renewable energy, particularly solar power (solar energy), has grown recently [3]. Significant amount of whole world energy, nearly 30%, is consumed in farming areas and around 3.59% is utilized in dehydrating crops and foodstuffs [4-5]. One suitable technique for preserving farming products such as fresh vegetables and fruits is dehydrating them via well-designed machines with optimal energy utilization. It could be in the absence of dehydrating process and free water is responsible for spoils or rots in the foodstuff. Hence, removing free water in terms of moisture from the surface of vegetables and fruits improves shelf life of agricultural products and makes those products easy to package and transport. Solar drying is one of greatest techniques for dehydrating farming produce that comprises two industrial as well as traditional processes. In traditional ways, because of dehydrating agricultural products in the front of sun on open roof or floor, the quality of dried products in terms of color index is less than in industrial technique [6]. Food is one of the essential requirements of living beings for their existence. With the increase in population, the food requirement also increases. Produced food needs to be conserved by reducing the various post-harvest losses to meet the food requirement. Solar dryers are the setup to harness solar energy for drying crops or grains or other non-agricultural products. Edible items (fruits, vegetables, cereals, etc.) are mostly spoiled due to their high moisture content. Effective method to preserve the crop from

being deteriorated is drying them up to a safe moisture level [7-8]. During drying, the moisture level at which the crop is considered safe for storage with a minimum loss in its nutritious qualities is termed a safe moisture level [9]. Dried agricultural produce had various advantages like better quality, low after-harvest losses, and longer storage time[10-11]. Various artificial dryers are developed, providing the required velocity and temperature to achieve good quality products in less time [12]. However, these dryers consume energy generated from conventional sources and are not eco-friendly [13]. Solar drying is considered a proficient method of using solar insolation for drying purposes as the energy from the sun is a clean source of energy and is available in ample quantity [14]. Solar drying is not a very new concept from ancient times. Natural sun drying is used for drying crops and other non-agricultural produce [15-16]. Open sun drying requires less investment, but the dried product is contaminated easily by birds, insects, pests, dirt, grit, rain, etc [16-19]. Hence, solar dryers were developed to prevent crop deterioration and store it for a longer time [20]. Solar dryers are also sustainable as they emit very low or even negligible carbon [21]. Solar drying systems are classified into three different categories i.e. direct, indirect, and mixed-mode types [22]. Greenhouse dryers (direct type) emerged as the best means to utilize solar energy for bulk drying and space heating [23]. The greenhouse solar dryers function on the greenhouse effect principle as enclosing material like glass, polythene, polycarbonate sheets, etc., allowing short-wavelength radiation coming from sun through it and trapping for drying non infrared or long-wavelength radiations inside it. Greenhouse temperature increases because longwave thermal radiation cannot escape [24]. Greenhouses are utilized for different purposes like crop drying, crop cultivation, space heating, etc. These dryers are mainly used to dry agricultural produce and non-

agricultural produce like paper, rubber, sludge, surgical cotton, etc. Greenhouses are a direct type or hybrid type operating in active or passive mode [25]. Many solar drying systems have been developed for dehydrating the product at various topographical places assisted with flat plate collector (FPC) [13]. Limited number research has been carried out for dehydrating the farming products constructed with evacuated tubes solar collector (ETSC) [26]. Solar flat plate collector dryers are extensively used to generate hot air to dehydrate food stuff products in comparison to evacuated tube collectors (ETC). It is observed from literature that, due to abundant, low cost and unlimited amount of solar energy, it is being used in dehydrating farming produces. For example, this technique has been used for dehydrating banana chips and garlic cloves.

1.1 Classification of solar drying system

Solar drying technology is divided into two different categories namely open sun drying (OSD) and closed. Kumar et al. evaluated convective heat transfer coefficient (CHTC) for open sun drying and also observed that convective heat transfer coefficient is directly proportional to mass of drying products. All kinds of solar drying systems operate in two modes only such as active mode and passive mode [14]. Fig 1.1 shows classification of solar drying system.

In passive method, buoyancy force plays an important role in the flow of air through the drying product. The hot air flows in upward direction because of thermosiphon effect and it escapes out through the ventilation. These types of drying systems are more suitable for low moisture content and less quantity. Jain et al. have fabricated greenhouse drying system under passive mode to dehydrate the cabbage and also compared the observed data with open sun drying as presented in Fig 1.2. Results

indicate that drying rate is higher in natural convection compared to open sun drying [27].

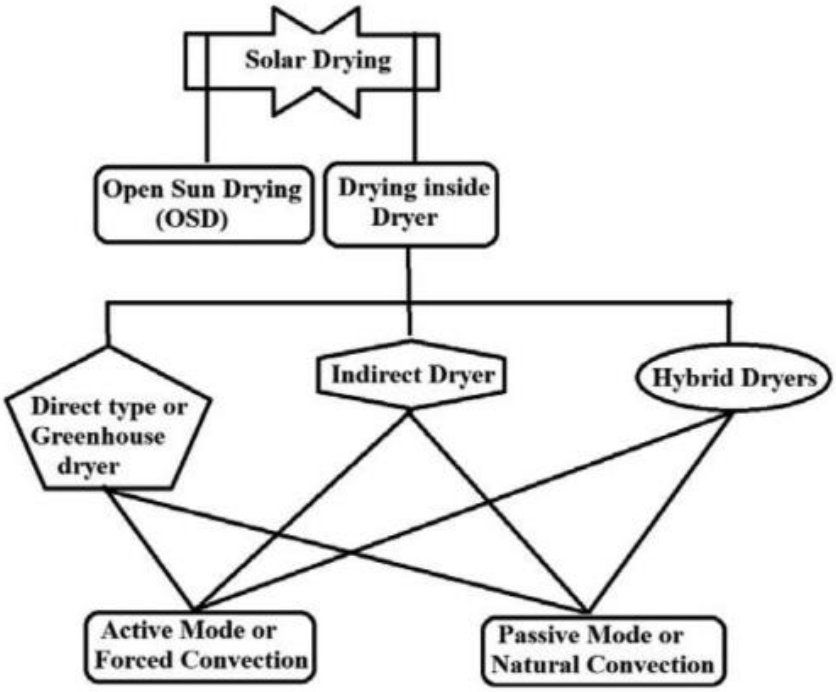

Fig 1.1 Classification of solar drying systems

Fig 1.2 Passive greenhouse dryer and the open sun drying [27]

In active method, the product was dehydrated by the force circulation produced through a blower/fan operated by grid. This objective is fulfilled through PV modules or grid energy. Kumar et al. have determined the thermal model in active method for jaggery drying. Fig 1.3 indicates the developed drying system operating under active mode. These types of dryers are more suitable for high moisture content crops and large quantities. Also, passive dryers are cheaper than active ones due to no external devices like fans, PV panels, blowers, etc. [1].

Fig 1.3 Representation of drying sytem operating in active mode [1]

1.1.1 Direct type solar dryers

In direct type solar drying system, the solar intensity is used directly for dehydrating the food stuff products kept inside the drying cabin. The whole setup is covered through transparent materials i.e. polyethylene sheet and glass. Some part of solar intensity is absorbed and transmitted by covering material, therefore some part of solar

radiation gets reflected back. Solar radiation transmitted inside the drying cabin gets trapped and increases inside temperature of drying system. As the room temperature increases, moisture begins to evaporate from the crop surface. Gbaha et al. developed a direct-type solar drying system to evaluate the performanc analysis and also observed the drying as well as heat balance behavior of cassava, mango, and bananas. The demonstration of direct type solar drying system is shown in Fig 1.4 [28].

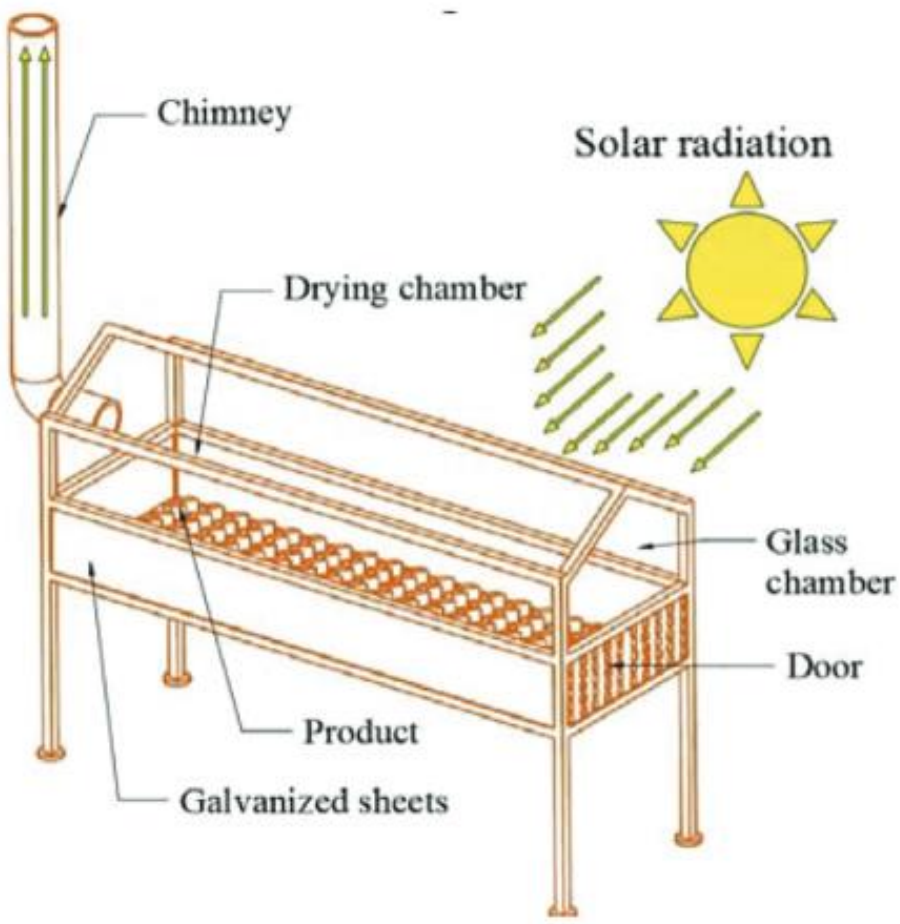

Fig 1.4 Direct type solar dryer [28]

1.1.2 Indirect type solar dryer

In this type of drying system, solar collectors were used to heat outdoor air using solar radiation and then circulate this heated air into an opaque drying chamber. Mohanraj

and Chandrasekar developed such types of drying systems that assisted with different sensible heat storage materials for chilli drying [29]. Fig 1.5 shows the schematic view of indirect type of solar drying system. The main advantage of this type drying system is that higher temperature can be maintained inside the drying cabin compared to direct solar drying system.

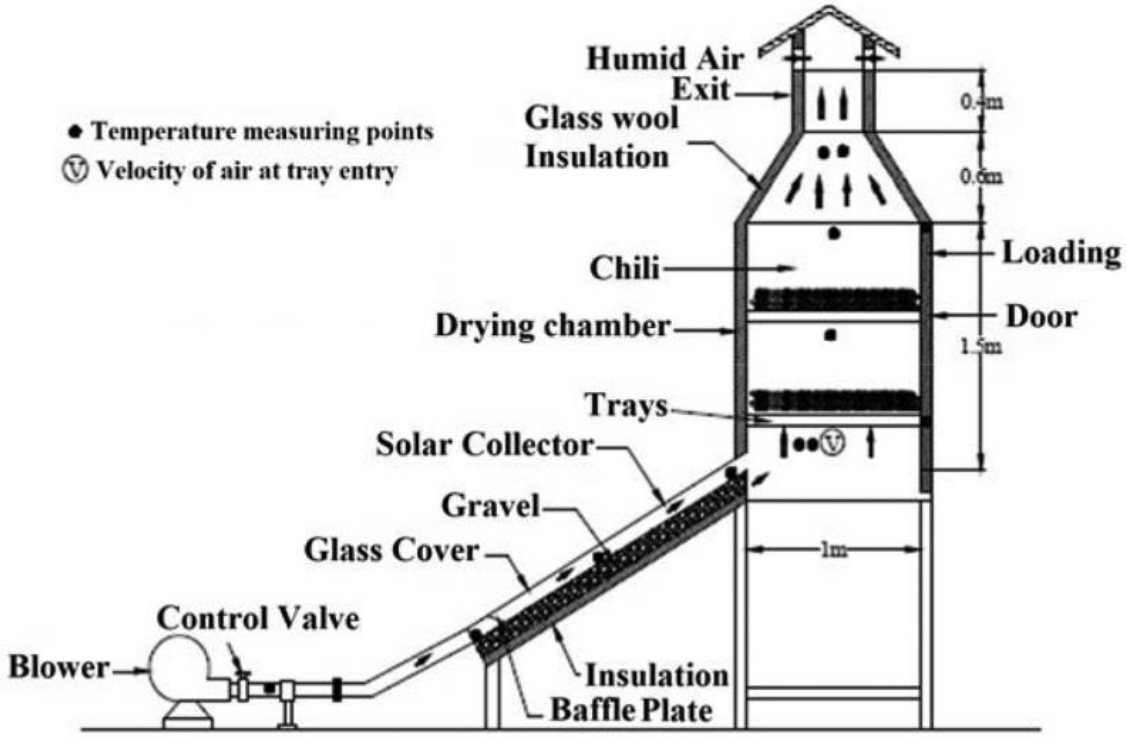

Fig 1.5 Indirect types solar drying system [30]

1.1.3 Mixed-mode or hybrid dryers

This type of drying system was developed for a faster drying rate. It is a combination of both direct and indirect types of solar drying systems. In such a drying system, solar radiation is absorbed in both flat plate air collectors and in the drying cabin. The photographic view of the mixed mode type drying system is shown in Fig 1.6. The DC fan or blower should be provided to maintain air circulation. In PVT hybrid drying system the fan is operated by electricity generated through PV modules.

Fig 1.6 Mixed mode type solar drying system [31]

1.1.4 Advancement in solar drying system

Efforts are made to make solar drying systems more efficient by overcoming their limitations. A limitation of the solar drying system is that it cannot be used in hours away from sunlight, and the solar intensity is also not the same at all locations. Therefore, this limitation can be reduced by storing the thermal energy of solar radiation in the form of storage as sensible or latent heat [32]. Figs 1.7–1.8 indicate the several modifications implemented on the drying system.

Fig 1.7 PVT integrated drying system [33]

Fig 1.8 PVT integrated drying system[34]

CHAPTER-2

2. Literature Review

Open sun drying now seems obsolescent, as it is weather-dependent and labor-intensive, and fruit crops are exposed to rain, insects and dirt [35-36]. Greenhouse drying is environmentally friendly because higher cost of fossil fuels and scarcity of wood have led to an emphasis on using alternative renewable energy sources [37-38]. Preferred solar drying systems (including greenhouse solar drying systems) should decrease impurity, dry faster and more evenly, and produce better than open-air techniques. Therefore, conventional greenhouse solar drying system become hybrid by assisting some external source of energy like photovoltaic thermal devices (PV/T), solar collectors (ETSC and FPC), biomass, and LPG burners, etc. Hybrid dryers are suitable for drying crops with high moisture due to high temperature inside the greenhouse [39]. Convective and evaporative heat transfer coefficients significantly affect moisture evaporation rate from banana slice surface. Indoor air temperature and airflow rate also strongly affect the drying rate [40]. Hassanain et al. developed and estimated a novel solar drying system to dehydrate the banana pulp. Solar collector was attached at 30° throughout year and drying cabin was flexible for the horizontal axis between 0° to 90°. In this study, it is observed that horizontal drying cabin accelerated banana drying compared to vertical drying cabin. Maximum drying cabin temperature was recorded 54℃. Developed dryer was capable of dehydrating banana pulp in 25 hours under sunny conditions (in clear sky) from initial moisture content (MC) of 66–67% (wb) to final moisture content (MC) of 22% (wb) [41]. A new hybrid solar dryer (HSD) for drying bananas was developed and fabricated [42]. The solar collector (SC) was installed above the drying cabin of HSD. Developed dryer used

power of sun under sunny days, but on hazy days, this operated as a HSD. Drying cabin air temperature was 30 to 40℃ more than atmospheric air. Lingayat et al. fabricated a solar dryer (SD) to dehydrate the bananas [43]. It consisted of a solar FPC with corrugated V-shape copper absorber mounted horizontally at an angle of 23.50° to insulated drying cabin, and the exhaust was hooked to the chimney for air. MC of banana crops was reduced from initial 56% (db) to final about 22% (db) in 18 hours. Similarly, Pruengam et al. calculated the performance of a V-groove, FPC in a solar drying system to dry banana slices [44]. Maximum efficiency of the SC (56.23%) and the thermal efficiency of the SD (16.90%) was estimated. Genobiagon et al. designed and developed a prototype model of low-cost solar cabinet drying system to dehydrate green bananas. The system was fabricated with two types of SC: a solar air heater and a water heater with heat exchanger and a storage tank. Maximum drying cabin temperature was noted at 48℃. The efficiency of SD (18%) and drying rate (0.27 kg/h) were evaluated. Pruengan et al. developed and tested a double side solar collector (SC) assisted drying system having both side drying chamber for dehydrating banana chips. MC decreased from 68.5% (wb) to 17.4% in 40 hours[45]. Higher dying cabin temperature was observed 62.7℃, which was 13.6℃ high than atmospheric temperature. Lingayat and Chandramohan conducted the computational analysis of indirect type solar drying system coupled with solar air collectors[46]. The average thermal efficiency of drying system (55.30%) and solar collector (64.5%) were calculated. Moisture content was decreased from initial 3.555 to final of about 0.2604(db) during the experimentation.Lamnatou et al. integrated an evacuated tube air heating collector and evaluated the thermodynamic performance of the system. Experiments conducted on drying apples, carrots, and apricots showed that the

temperature levels suitable for drying agricultural products are achieved through warm outlet air from the collector without preheating [47]. Solar vacuum tubes were used to heat the stream of ambient air to a higher temperature by Mahesh et al. Drying setup was tested to dry different fruit and vegetable samples. Results indicate that open sun drying consumes more drying hours in comparison to the developed drying system, and maximum drying air temperature was achieved at 45.5°C in this system. Heat provided by the evacuated tube was enough to replace the usage of auxiliary electric heating after certain hours of sunshine [48]. Ubale et al. evaluated the performance of ETSC for drying grapes under the force convection mode of heat transfer. Overall efficiency of the solar collector was attained at 24.3% as compared to 16–22% for flat plate collectors [49]. Singh et al. evaluated the performance of heat exchanger-assisted drying system and found that maximum temperature difference (35.4 °C) between ambient air and hot air and 55% maximum efficiency of the setup was noticed. It is operated in solar light hours for dehydrating the garlic in current topographical locations [50].

Majdi and Esfahani proposed a new technique for the numerical simulation of systems and this technique was optimized using Taguchi algorithm to observe optimum drying conditions to reduce drying period and energy utilization. Control parameters included drying temperature, air flow rate, and thickness ratio. Following optimal conditions were computed drying temperature (60°C), air flow rate (0.1 m/ s), and thickness ratio (0.1) [51]. Sumic et al. dehydrated fresh red currants using vacuum drying method with RSM and evaluated the physical properties (MC, color indices, stability, and water activity) and chemical properties (contamination of whole phenols, flavonoids, monomeric anthocyanins as well as ascorbic acid and antioxidant activity) of

dehydrated products. The temperature from 48℃ to 78℃, pressure from 30 to 330mbar and drying period varying from 8 to 16 h were considered independent factors in their research work and increased concurrently. The best-fit outcomes of responses were obtained at temperature of 70.2℃, a pressure of 39 mbar and dehydrating period of 08 h [52]. Han et al. used an arrangement of vacuum system and microwave for dehydrating apple slices and studied the effects of innumerable independent parameters and their connections on response parameters by applying RSM. The best-fit results were achieved at 12.0 W/g microwave power, 0.089 MPa vacuum levels (VL), and 0.692 kg/db. initial MC [53]. Esfahani et al. experimented on a convective solar dryer and also applied the RSM to improve the method for convective dehydrating of apple slices with desirable purpose. Interface of independent variables together with ambient temperature in a range of 70–90 ◦C, air flow velocity 4–5 m/sec, and apple slice dimensions such as circle, square, & triangle through the dependent parameters comprise of dehydrating period, energy consumption rate (ECR), shrinkage factor (SF) was calculated. The best-fit result was obtained on 90 ℃, 5 m/s and 0.781 temperature, AFV and Square geometry, respectively [54]. Emmanuel et al. experimented with an indirect solar dryer and used RSM to optimize the dryer for dehydrating the unblanched and blanched aerial yam. The results observed that the optimum process variable was attained on 71 gm, 3.2 mm and 1.5 m/sec, & 70 gm, 3.0 mm and 1.5 m/sec for blanched and unblanched samples, correspondingly [55]. Abano et al. calculated the optimal drying factors for tomato slices [56]. Abdeen et al. employed response surface methodology to optimize solar drying systems for thermal comfort [57]. Their outcomes agreed with Gorji and Ranjbar who also applied the same technique (RSM) for geometric optimization of

nano-fluid based direct absorption solar collectors [58]. Obajemihi et al. to modelled and optimize the process conditions for tomato hot air drying. The ideal drying circumstances were found using a graphical overlaying method [59]. Dalvand et al. optimized the drying parameters of a solar electrodynamic drying system based on a sustainability approach [60]. Response surface model relieved minimization of experiment cost and was also concluded to be effective, comparatively simple, drying period as well as material saving. Related characteristics were described by employing RSM by Raju et al. in optimization of process parameters of drying button mushrooms [43].

To compare the performance of drying systems, authors have given several models to predict the moister ratio (MR) of dry products using only time as a dependent variable. Lingayat and Chandramohan fitted six dry kinetics models to find a good fit model for dehydrating banana chips in a direct type solar dryer coupled with solar air collectors. Midilli et al. model gives a good fit as it gave highest R^2 (0.9982) and lowest X^2 (0.00031). Tunckal and Doymaz experimented with dehydrating the banana chips in heat pump coupled drying system. The drying behavior of banana slices was observed with 6 mathematical relations. Midilli et al. and Kucuk model was found to good fit for experimental drying data. It gave higher R^2 (0.9989 – 0.9996) and lower X^2 (0.000031– 0.000085) for both models [46]. Mewa et al. used 8 drying kinetics models in HSD to dehydrate the beef; it was dehydrated from initial weight 20kg to a final weight of 7.5kg inside the drying system in 11 hours. Page model was best fit for the drying behavior of beef [13]. Sallam et al. fitted nine mathematical models for active and passive drying mode of mint. Verma et al. model was a good fit for experimental drying data [61].

Tripathy et al. evaluated that mixed mode type drying system will decrease the 23% CO_2 emission and also analyzed that conventional energy consumption can be minimized in the range of 28-81% with a minimum of 39% efficient solar drying system [62]. Singh and Tiwari developed a mixed-mode type solar drying system and observed that maximum CO_2 mitigation was attained using solar energy in place of coal. This drying system mitigates CO_2 178–612 kg annually with a volumetric dimension of 0.19 m^2 [63]. Prakash et al. fabricated a greenhouse solar dying system and computed the CO_2 mitigation as well as emission by dehydrating the capsicum, potato and tomato in active and passive methods. This drying system mitigates nearby 28–35 kg of CO_2 per annum and emits 4.15kg of CO_2 more in active than passive method [32]. Prakash and Kumar developed a modified greenhouse drying system to dehydrate the tomato flakes under active method and determined that CO_2 mitigation nearby 38.1 tons per annum. The earned carbon credit by drying system differs from $171.8 to $687.1[64]. Elkhadraoui et al. developed a newly mixed mode type drying system and dehydrated the red pepper. This drying system mitigates 25–30 kg CO_2 yearly [17]. Tiwari and Tiwari evaluated thermal performance of a newly developed PVT-based solar drying system for different sun-shine periods. This drying system earned carbon credit of about $817.50 annually. The CO_2 mitigation and CO_2 emission were attained 81.7 tons and 170.1 kg/year, respectively [65]. Ndukwu et al. explained the role of different designed drying system's performance on environmental sustainability by decreasing CO_2 mitigation and CO_2 emission into environment. The earned carbon credit was around $2,908 annually [66]. Singh and Gaur developed a hybrid drying system coupled with auxiliary device (evacuated tube collector) and determined the performance analysis by drying tomato, ginger and bottle gourd. This

system mitigates 88.1, 50.5 and 135.1 tons of CO_2 and 49.6, 26.6 and 41.2 tons of CO_2 with and without auxiliary devices, respectively [67]. Gupta et al. discussed economic and environmental aspects of PVT-based solar drying system under different system life (10, 20, and 30 years). The CO_2 emission of the PVT system reduces to 136.9, 68.5, and 45.6 kg/year for different system life (10, 20, and 30 years), respectively. CO_2 mitigation rises to 18.2, 39.6, and 60.9 tones for different system life (10, 20, and 30 years). This PVT system earned carbon credits earned about $182.4, $395.8, and $609.1 for 10, 20, and 30 years for different system life[68]. Simo-Tagne.M and Ndi-Azese designed and developed a new drying system and placed a solar collector on the top of drying cabin. The results indicated that this system mitigates the 58.433 tons of CO_2 [69]. Madhankumar et al. evaluated the performance analysis of indirect solar dryer in 03 different modes. The energy payback period (1.42 years), CO_2 mitigation (20.13 tons), CO_2 emission (23.88kg/year), and earned carbon credit ($100.642 to $402.569) were calculated for indirect solar drying system [70].

2.1 Research Gap

The research gaps are enumerated and explained briefly in the following section. Based on the literature review following research gaps were identified for carrying out the research work.

- Many researchers have done thermodynamic investigations on ETC-based solar drying systems. However, no one has design hybrid solar drying system based on heat exchanger evacuated tube assisted drying system (HE-ETADS) and water as heat transfer fluid for the dehydrating of product. Design consideration and assumption play a significant role in thermal performance of

solar drying. It is very first developed drying system for dehydrating high moisture content crops.

- It has been observed from the literature review that a no of researchers have used air as a heat transfer fluid in various drying systems. However, water as a heat transfer fluid inside the drying cabin has not been discussed in literature.
- The insulation material has not been used in heat exchanger-evacuated tube assisted drying system for dehydrating agricultural products that have moisture content in the range of 90 ± 5% to 70 ± 5%.

2.2 Objective of Research Work

Specific objectives are as follows:

i. To design and develop an evacuated tube assisted drying system (HE-ETADS).
ii. To investigate the performance characteristic of heat exchanger-evacuated tube-assisted drying system in loaded and unloaded conditions.
iii. Thermodynamics analysis of heat exchanger-evacuated tube-assisted drying system.
iv. To study drying kinetics of different crops in drying system at different water flow rate.
v. To optimize the operational parameters for maximizing the performance of heat exchanger-evacuated tube-assisted drying system.
vi. To analyse the economic aspects of heat exchanger-evacuated tube-assisted drying system.

CHAPTER-3

3. Research Methodology

This chapter explains the methodology that has been adopted to find the objectives. For a detailed discussion, it has been divided into five sections. Section 3.1 Design and development of heat exchanger-evacuated tube assisted drying system, in section 3.2 Performance characteristic of heat exchanger-evacuated tube-assisted drying system in unloaded condition, in section 3.3 Optimization of drying parameters for drying system using response surface methodology, in section 3.4 Thermodynamics analysis of heat exchanger-evacuated tube-assisted drying system, in section 3.5 Evaluation of drying kinetics, quality assessment, and heat and mass transfer, in section 3.6 Environmental analysis of HE-ETADS

The methodologies adopted in the research work are as follows:-

3.1 Design and development of novel drying system

Fig.3.1 describes Heat exchanger- Evacuated tube-assisted drying system that has been designed and constructed in solar energy lab of MITS, Gwalior Madhya Pradesh, India (26° 14' N, 78° 10' E). The outer structure of proposed drying system is made of hollow rectangular-shaped iron rods which are joint together at each corner by welding (in Fig.3.2). Make it air-tight to reduce loss, and fill joints properly by M-sealing and welding. Polycarbonate sheet is used to cover the drying system. During forced mode operation, 04 DC fans are provided to propel the air inside drying cabin of the system. 02 PV panels are also installed on the roof of the drying system to supply electricity to operate the DC fan and DC pump.

DC pump is used to circulate the hot water from ETSC to the copper tube of wire & tube type heat exchanger, which is kept in side drying cabin. In current research, the

dryer is made hybrid by using single source only i.e. solar energy. Solar is simultaneously used for heating water in evacuated tube solar dryer and also for heating air inside dryer by greenhouse effect. Heat of hot water is further transferred from hot water to air getting inside dryer. Therefore, temperature of air is here not increasing only due to greenhouse effect but also due to heat exchange between hot water and air. Hence, drying cabin temperature is obtained more than other dryers and this will reduce the drying time of crops. As more is the temperature, the drying rate will be faster. Thus this dryer is more suitable for drying high moisture content crops in less time without compromising their quality.

Fig 3.1 Pictorial view of experimental set-up

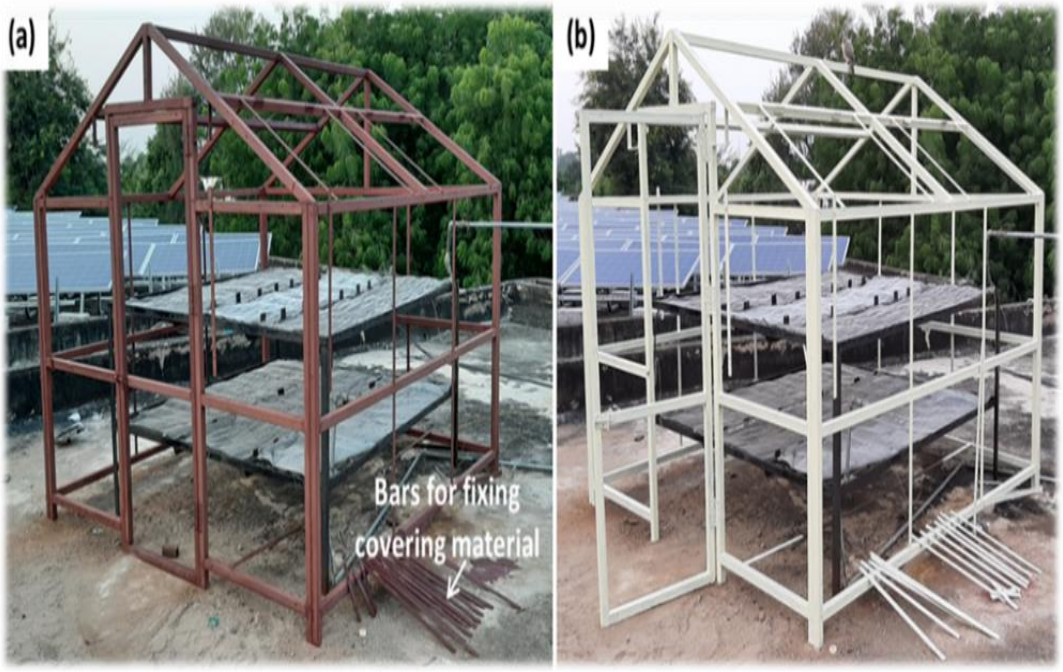

Fig 3.2 Outer structure of propsed drying system

A complete installed experimental setup is displayed in Figs. 3.3 and 3.4 It is made of frame type drying platform kept inside the drying system with two layers of floor area 183 × 199 cm each. Each layer of drying platform has 17 arrays of U-shaped copper tubes, each having length of 196 cm for a series flow of heated water. Steel wire mesh with holes of 1.2 × 1.2 cm and wire diameter 0.3 cm is placed over the copper tubes. Wire mesh gains heat by direct contact with copper tubes and transfers it to the drying product placed over it. Greenhouse environment air also receives this additional secondary heat (primary source is greenhouse heating). Fresh air enters from a 15 cm height wire mesh. Design specifications of advanced HE-ETADS are listed in Table 3.1.

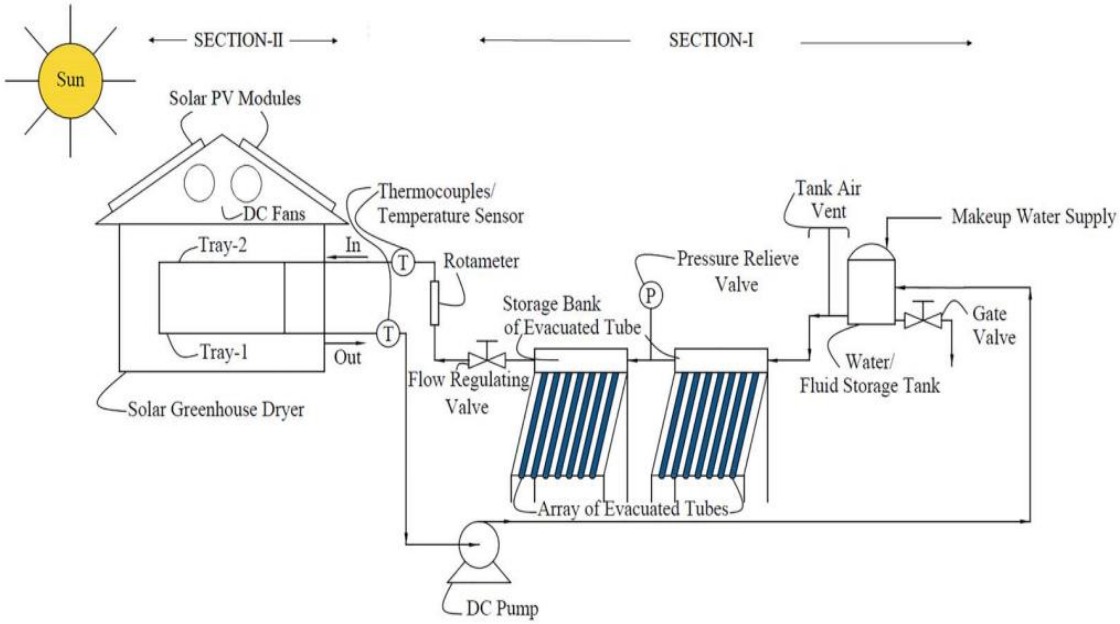

Fig 3.3 Layout of drying system

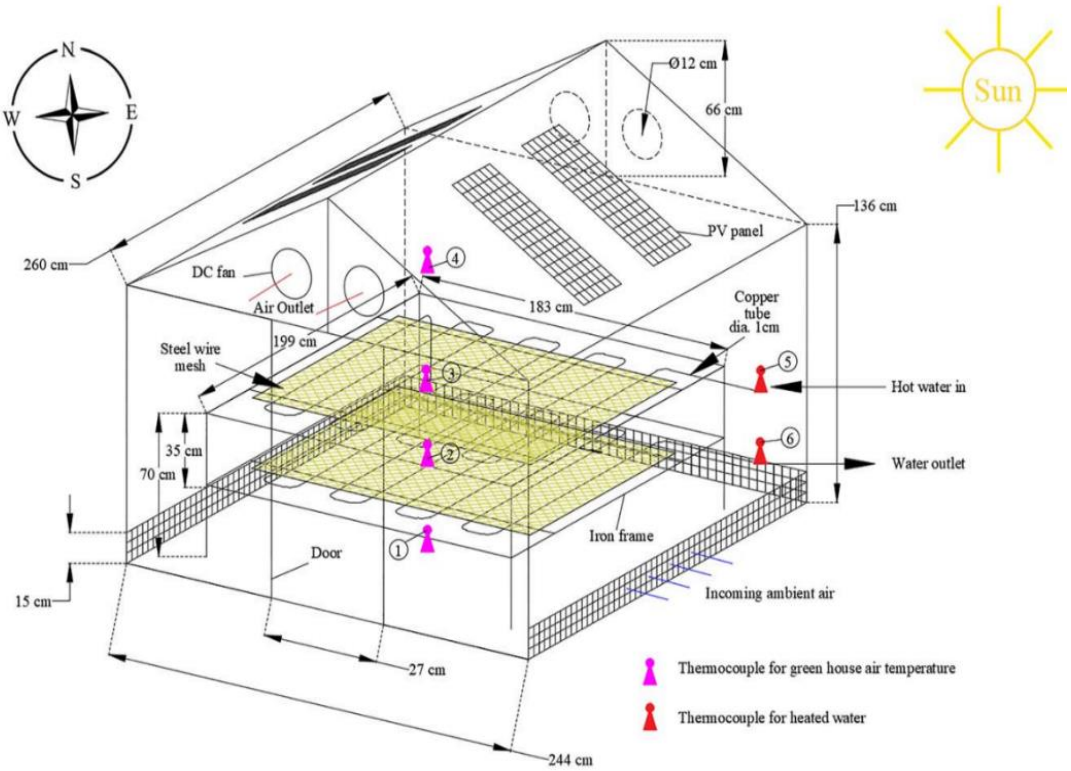

Fig 3.4 Arrangement of drying tray inside drying system

Table 3.1 Design specifications of advanced HE-ETADS

Component	Explanation
Solar Collector	
Type	Evacuated Tube collector
No. of Tubes	20
Diameter	58 mm (outer) ;47mm (inner)
Material	Double Walled Borosilicate
Capacity	200litre per day (LPD)
Quantity	Two
Length	1647mm
Absorptance	0.92
Insulation	PUF insulation (50mm)
Efficiency	65%
DC Pump	
Type	12V DC solar powered + Brushless magnetic
Material	Abs (acrylonitrile butadiene styrene)+Stainless steel
Drying Cabin	
Area needed for drying of agricultural product	4.41m^2
Measurement of drying tray	2.1 m×2.1 m
Number of Drying Tray	02
Collector Area	1.59 m^2
Water flow rate	10,20,30Ltr/h.
Usual solar intensity (in April)	850W/m^2
Types of SD	Active
Insulation Material	Polycarbonate Sheet
β	51.84◦
θ	2.39◦

3.1.1 Heat exchanger configuration

Wire and tube type heat exchanger is designed for the present application. It consists of copper condenser tubes used for airconditioning systems and is readily available in the local market. Wire meshed sheets are used to construct drying platforms to increase the heat transfer area to greenhouse air. These are directly placed on the copper tubes

carrying heated water, as shown in Fig 3.5. Copper material is selected for fabrication of heat exchanger due to its favourable mechanical and thermal properties.

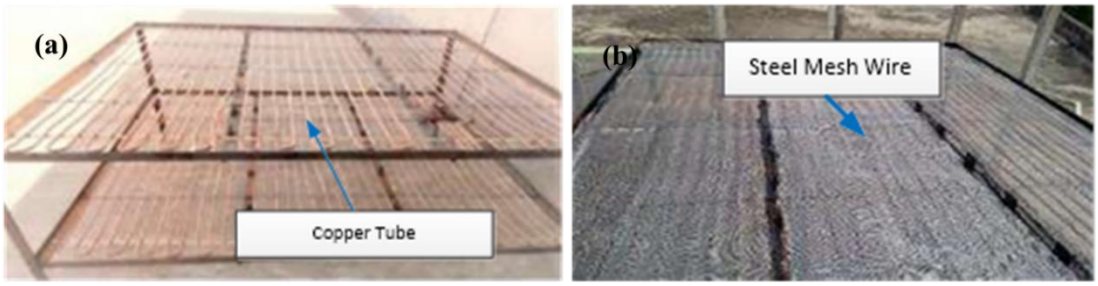

Fig 3.5 Drying platform (a) copper tubes/coils (b) Complete setup with wire mesh

3.1.2 Instrumentation for ambient data recording

i. Data-logger (Data Taker DT85 series 3, Australia) was installed and recorded relative humidity (Rh) and atmospheric air temperature inside and outside the drying cabin. Experiment was performed from 09:00 to 18:00h.

ii. Anemometer (Dynalab DLAW 8701) was used to measure airflow rate (m/s) over the banana slices inside and outside the drying cabin.

iii. Solarimeter (Megger PVM 210) was mounted and used to record direct beam radiations as well as diffused solar radiations.

iv. Digital weight machine (having accuracy ±0.001kg and a range of 0 - 20kg) was used to measure the weight of dehydrated crops.

3.1.3 Uncertainty analysis

The instrument used for evaluating drying air properties along with their accuracy, range, standard uncertainty, and uncertainty in measured variables, are given in Table 3.2.

If X_1, X_2 ……X_n are the independent variables affecting the observed parameter Y, then uncertainty in observed variable U(Y) was computed using Eq. 3.1: [71].

$$U(Y) = \left[\left(\frac{\partial Y}{\partial x_1}\right)^2 u^2(x_1) + \left(\frac{\partial Y}{\partial x_2}\right)^2 u^2(x_2) + \cdots \ldots \ldots + \left(\frac{\partial Y}{\partial x_n}\right)^2 u^2(x_n)\right]^{1/2} \qquad (3.1)$$

where, U(Y) is the total uncertainty, $u^2(x_1), u^2(x_2)$, ….,$u^2(x_n)$ are uncertainty of independent variables

Table 3.2 Uncertainty of instruments

Instruments	Accuracy	Range	Standard uncertainty (σ)	Uncertainty of observed parameters	Uses
K-types thermocouple (PT-100 and PT-1000 sensor)	±0.1℃	-140 to 990℃	0.0567℃	±0.265℃	Measuring the temperature at different locations
Infrared Temperature gun (HTC, MTX-2)	±1℃	-40 - 500℃	1.143℃	±1.175	Measuring the banana slice's surface temperature
Solarimeter (PMV-210)	11 W/m^2	0-2000W /m^2	5.67 W/m^2	5.67 W/m^2	Measuring the solar insolation
DYNALAB DLAW-8701 Digital Anemometer	±1m/s	0-45m/s	0.566m/s	0.645m/s	Measurement of ambient air flow velocity
MEXTECH TM-1 Digital Hygrometer	2%	5-85%	1.72%	1.69%	Measurement of Relative humidity
Digital weight Machine	0.001kg	0-35kg	0.00058kg	0.270kg	Dehydrated banana slices weight

3.2 Performance characteristic of heat exchanger-evacuated tube-assisted drying system in unloaded condition

In this section, experimental work was conducted in three different categories under

unload condition. **Category-I:** drying system in stagnation condition, **Category-II:** all fans are in operating condition and **Category-III:** ventilation window is open. Coefficient of performance (COP), HUF, coefficient of diffusion, and CHTC have been calculated in thermal performance analysis of advanced system.

Based on temperature achieved inside the drying cabin of advanced drying system during experimentation works, agricultural produce i.e. crops, vegetables, and fruits are selected that have a moisture content in the range of 90 ± 5% to 70 ± 5%.

Following parameters have been calculated and analysed to estimate the thermal performance of HE-ETADS under active mode.

3.2.1 Convective heat transfer coefficient (CHTC)

CHTC is a measurement of heat loss from roof surface to the drying cabin and can be computed using Eq.3.2 [1].

$$h_c = 0.884 \times \left[(T_{rs} - T_{dc}) + \frac{[P(T_{rs}) - Rh_a P(T_{dc})](T_{dc}+273)}{268900 - P(T_{dc})}\right]^{1/3} \quad (3.2)$$

3.2.2 Coefficient of diffusion (C_d)

Moisture removal rate is the key parameter responsible for dehydrating farming products in the drying cabin of HE-ETADS. As moisture removal rate is higher, it decreases the dehydrating period of agricultural produce. It is called instantaneous thermal loss efficiency factor [72]. This term is also defined as follows:

Rate of instantaneous thermal loss efficiency factor from cover (polycarbonate sheet) is indirect loss parameter and can be evaluated using Eq.3.3 [73].

$$\eta_{itlef} = \frac{U \sum A_i (T_{rs} - T_{dc})}{I_g A_c} \quad (3.3)$$

where, η_{itlef} instantaneous thermal loss efficiency factor.

Experimentation work was performed under unload conditions. It is assumed that the sum of loss factor through cover and ventilation equals 1. Following this assumption,C_d can be determined using Eq.3.4 [32]:

$$C_d = \frac{(1-\eta_{itlef})I_g A_c}{(nA_v\sqrt{\frac{2\Delta P}{\rho}}\Delta P)} \quad (3.4)$$

3.2.3 Heat loss factor

This heat loss occurs due to a surplus amount of intake air inside the HE-ETADS; because of it, hot air escapes outside through the vent due to density difference. This factor can be calculated using Eq.3.5 [74]:

$$Q_{hlf} = C_d A_v \sqrt{\frac{2\Delta P}{\rho}} \Delta P \quad (3.5)$$

3.2.4 Heat utilization factor (HUF)

HUF is defined as the ratio of temperature reduced due to cooling throughout dehydrating and increases due to heating. HUF can be expressed by Eq.3.6 [74]:

$$HCF = \frac{(T_{rs}-T_{dc})}{(T_{rs}-T_{air})} \quad (3.6)$$

3.2.5 Coefficient of performance (COP)

It is defined as ratio of temperature difference b/w HE-ETADS drying cabin temperature and air temperature to temperature difference between roof surface temperature and air temperature. It can be evaluated by following Eq.3.7 [72]:

$$COP = \frac{(T_{dc}-T_{air})}{(T_{rs}-T_{air})} \quad (3.7)$$

3.3 Optimization of drying parameters for drying system using response surface methodology

This section mentions methodology to be adopted for experimentation.

3.3.1 Sample preparation

Fresh bananas are bought from the supermarket in Morar, Gwalior. Before the experiment, bananas are peeled off and cut into 1cm thickness by a cutting machine. In each experiment, banana was cut into two geometries, circle and square, to ensure the product volume remained unchanged. Dimensions of the square slices were 2cm, the diameter of the circle pieces was 2.5cm, and their thickness was 1cm. Oven method is used to compute initial moisture content (74.8 ± 0.4% on wet basis) of banana slices at 105℃ for 24 hours.

3.3.2 Investigation process

The experiments were conducted via an indirect hybrid solar dryer assisted by a control unit to regulate temperature and flow of water inside. A fully functional weather station with a hygrometer, anemometer, Pyranometer, and 12 channel thermocouples was used to record the measurements using a computerized data logger, and Universal data Taker DT85 integrated with dEX software. Along with this, portable measuring equipment, including a temperature gun, a weight machine, and an anemometer, was also employed for measurement. There was no need for pre-treatment with a fresh food product. Experimentation work was performed on various air temperatures, water flow rates, and banana slice geometries. In each experiment, banana was cut into two geometries, circle and square, to ensure the product volume remained unchanged. Dimensions of the square slices were 2cm, the diameter of the circle pieces was 2.5cm, and their width was 1cm. The digital weight machine was used to measure the weight loss at regular intervals of time, and it was also attached to computer to record the data with uncertainty of ± 0.0001 kg (0.1gm). During the drying process, the obtained value of Rh was 8 ± 1.0%. MC in the banana slices before drying was measured 74.8 ± 0.4%

on wet basis (wb.) or about 3.33 ± 0.07 % on dry basis (db.) The dehydration of the product was unreliable until their EMC was at each operating condition. Guggenheim-Anderson-de Boer model was used to find out EMC. Its value on dry basis (db) at dehydrating temperatures of 70–90°C was around 0.01gm water/gm dry matter [75].

3.3.3 Drying

Experiments were carried out and repeated for different water flow rates, product mass and sample geometry. Hence, Moisture content (MC) of product on dry basis was evaluated by following Eq.3.8 [75-76].

$$\mathrm{MC} = \frac{\mathrm{m_i} - \mathrm{m_f}}{\mathrm{m_i}} \times 100 \qquad (3.8)$$

where

m_i and m_f = intial and final moisture content of the product

3.3.4 Utilization of energy

Amount of energy consumed in drying system at various operating parameters such as water flow rates and temperatures are evaluated with Eq.3.9. It was denoted as drying energy used and employed as one of dependent parameters in optimization process variables [51].

$$q = MC_p \Delta T.\, t \qquad (3.9)$$

$$q = Q\rho C_p \Delta T.\, t \qquad (3.10)$$

where q = quantity of energy used (kW/h), t = Drying period (h)

3.3.5 Response surface methodology (RSM)

RSM is an arithmetical technique that increases dependent variables as yield variables. All response (dependent variable) is changed through several input parameters. A central-composite design (CCD) is used in RSM. Also, the CCD is best suitable for

fitting a quadratic surface that normally works well for the method optimization and includes the least number of experiments to be carried out. The CCD technique adopted the no. of tests to be executed to optimize the process variables. Design Expert Version.11.0 software was used to enhance drying method. Table 3.3 displays experiment's range and levels of control factors. Similarly, Response surface methodology is influential in describing the relationship between responses and control parameters [77]. Every response in response surface methodology has a mathematical correlation.

This equation can be conveyed as

$$Res = \alpha_0 + \alpha_1 A + \alpha_2 B + \alpha_3 C + \alpha_{11} A^2 + \alpha_{22} B^2 + \alpha_{33} C^2 + \alpha_{12} AB + \alpha_{13} AC + \alpha_{23} BC \quad (3.11)$$

where, Res denotes the response (dehydrating period, energy consumption (EC) and shrinkage).

In the present work, Eq.3.11 is written via quadric model of response surface methodology and mathematical correlation among the control parameters.

Desirability function is also known as objective function $\left(\mathrm{D(X)}\right)$ and was evaluated for optimization of multiple variables using Eq.3.12 [78].

$$D(X) = (Y_1 \times Y_2 \times Y_3 \times Y_4 \ldots \ldots . Y_n)^{\frac{1}{n}} \quad (3.12)$$

where, Yi (i = 1, 2… n) are the control variables and ‘n’ is total no. in study. The rate of ‘D’ differs from 0 - 1. The ‘D’ is the desirability (objective) function demonstrating how desired (fit-matched) control variables are at particular levels of independent parameters.Fig.3.6 illustrates the procedures that must be followed to correctly implement this approach.

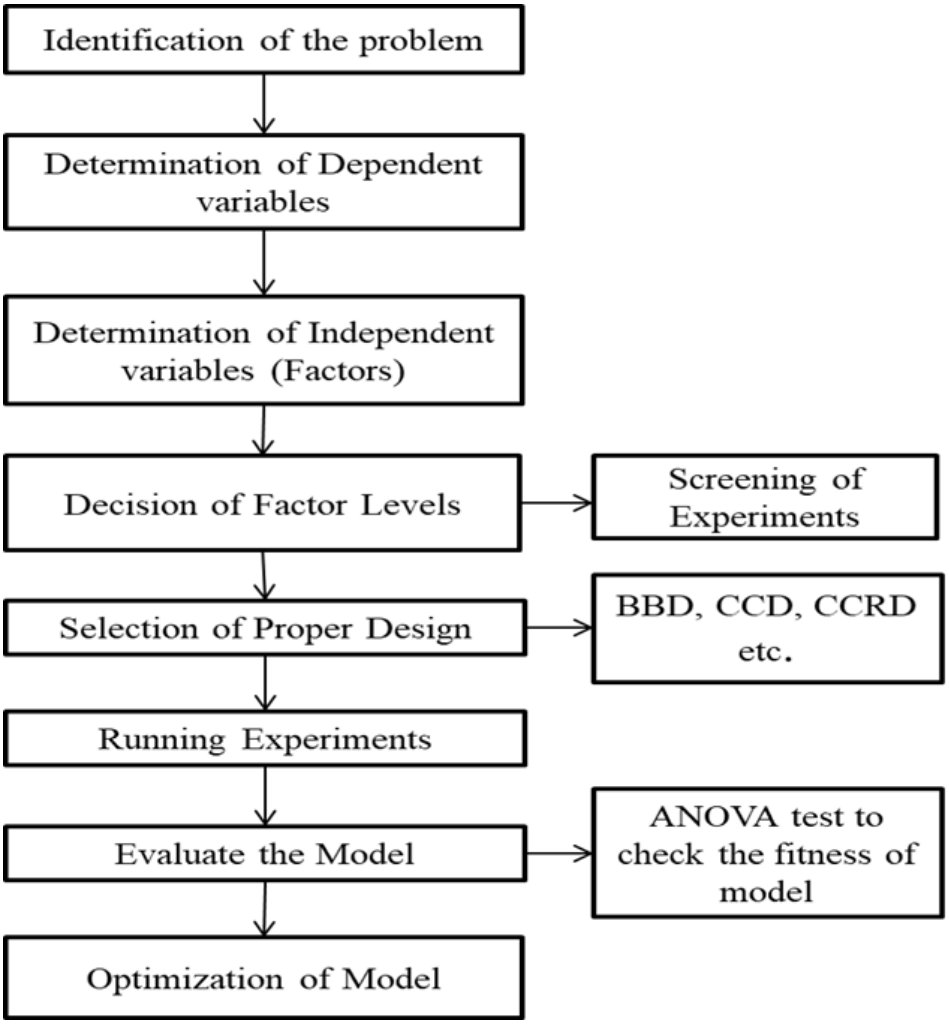

Fig 3.6 Steps for response surface methodology

Table 3.3 Experiments range and levels of the control factors for banana drying

Control Parameters	Units	Symbols	Level-1	Level-2
			Lower-Range	Higher-Range
Temperature	°C	A	70	90
Water Flow Rate	Ltr/h.	B	10	30
Geometry of Product	cm^2	C	Circular	Rectangular
Mass of product	kg	D	0.24	1.0

3.4 Thermodynamics analysis of heat exchanger-evacuated tube-assisted drying system

In this section, solar collector's efficiency, drying system efficiency, and energy balance equations were used for room air and crop surface temperature in a heat exchanger evacuated tube assisted drying system discussed.

3.4.1 Design of evacuated tube solar collector (ETSC)

Initial moisture content in the garlic is calculated by Eq.3.13 [1]:

$$M_{tw} = \frac{M_T \times m_i}{100} \tag{3.13}$$

where M_{tw} is total moisture existing in crop (kg), M_T is total mass of crop (kg), and m_i is percentages of the initial moisture content of product (wb). Moisture content must be removed to obtain desirable moisture from the expected amount of product for safe storage is given by Eq.3.14 [79]:

$$M_w = \frac{M_T \times (m_i - m_f)}{100 - m_f} \tag{3.14}$$

where M_w is removable moisture content during drying in kg. Average drying level of product was dignified according to the desired MC within a particular period that can be evaluated by using the following Eq.3.15 [64]:

$$D_R = \frac{M_w}{t_d} \tag{3.15}$$

Amount of heat required is calculated from Eqs.3.16 and 3.17 [80]:

$$Q = M_T \times C_P \times (T_p - T_a) + M_W \times h_{fg} \tag{3.16}$$

$$h_{fg} = 4.186 \times 10^3 \times (597 - 0.56T_p) \tag{3.17}$$

where Q is total amount of heat needed for sensible heating as well as for evaporation of water in kJ, C_P is specific heat (kJ/kg K), Tp is temperature of product (K), T_a is air

temperature (K). Overall amount of required heat for product drying can be determined using Eq.3.18 with an assumption of 10% heat loss during the experimental process [26]:

$$Q_{overall} = Q + Q \times 10\% \quad (3.18)$$

Heat energy needed for drying the garlic per hour was estimated by Eq.3.19:

$$Q_{overall/h} = \frac{Q_{overall}}{t_d} \quad (3.19)$$

The required amount of water (heat transfer fluid) removed from crop batch drying can be calculated by heat energy balance Eqs.3.20-3.23 [49]:

$$M_w \times h_{fg} = M_{water} \times C_p(T_{co} - T_o) \quad (3.20)$$

$$M_w \times h_{fg} = \rho_{water} \times C_p \times V_T \times (T_{co} - T_o) \quad (3.21)$$

$$T_f = T_a + 0.25 \times (T_{co} - T_o) \quad (3.22)$$

$$V_T = \frac{M_w \times h_{fg}}{\rho_{water} \times C_p \times (T_{co} - T_o)} \quad (3.23)$$

Water flow rate needed for drying garlic can be calculated by Eq.3.24 [49]:

$$V_w = \frac{V_T}{t_d} \quad (3.24)$$

where V_w water flow rate in m^3/h is, V_T is total volume of water in m^3, t_d is total drying time in hours. Total quantity of heat energy immersed by ETSC should be equal to amount of heat needed for dehydrating product within exact time. Therefore, evacuated tube solar collector area as well as number of evacuated tubes needed for drying method can be estimated by following Eqs.3.25- 3.26 [49]:

$$Q_{ab} = Q_n = A_{Collector} \times I_g \times \eta_c \quad (3.25)$$

$$A_{Collector} = \frac{\pi}{2} \times D \times L \times N \quad (3.26)$$

where Q_{ab} total quantity of heat is immersed by ETSC in kJ, Q_n is needed quantity of heat for dehydrating processes in kJ, $A_{Collector}$ is area of evacuated tube solar collector in m^2, η_c is collector efficiency. Thermal efficiency of collector and performance of solar dryer depends on tilt angle (β) and incidence angle(θ). These can be evaluated by following Eqs.3.27-3.28 [38]:

Assessment of tilt angle (β)

$$\beta = [\varphi - \delta] = \left[\varphi - 23.45 sin\left\{(284 + n) \times \frac{360}{365}\right\}\right] \quad (3.27)$$

Incidence angle (θ)

$$\theta = \cos^{-1}\{\sin\delta.\sin(\varphi - \beta) + \cos\delta.\cos(\varphi - \beta).\cos\omega\} \quad (3.28)$$

3.4.2 Thermal performance of HE-ETADS

3.4.2.1. Quantity of moisture escaped

MC is amount of water available in the sample at an instant and can be calculated in percentage of MC. MC on wet basis (%wb) can be determined by following Eq.3.29 [37]:

$$MC = \frac{m_i - m_f}{m_i} \times 10 \quad (3.29)$$

3.4.3 Drying performance

It can be defined as mass reduction from inside the drying chamber of HE-ETADS. Drying performance can be evaluated in terms of following Eq.3.30 [81]:

$$D_p = \frac{M_t - M_{t+\Delta t}}{\Delta t} \quad (3.30)$$

where D_p is drying performance (kg H_2Odry solid/h), M_t is the MC at an instant of time (t).

3.4.4 Drying kinetics modeling

MR of product can be calculated from Eq.3.31:

$$MR = \frac{M_t - M_e}{M_i - M_e} \tag{3.31}$$

where M_e is equilibrium moisture contented, and M_t is moisture contented at any time t in the product. Equilibrium moisture contented (EMC) is more important factor of the dehydrating products, specifically in a tropical nation where RH is very high. EMC of crop was calculated in the range of 35–55 ◦C temperature and 0–100% RH. Halsey Eq. is the greatest fit of EMC of crop [72]:

$$R.H = exp\left(\frac{-11.08492}{RT_{abs}} \times M_e^{-0.886330}\right) \tag{3.32}$$

3.4.5 Solar collector efficiency (η_C)

Ratio of heat energy absorbed by water to received solar energy on the collector as written in the form of Eq.3.33 [26]:

$$\eta_C = \frac{Q_{ab}}{A_c \times I_G}$$

$$Q_{ab} = M_{water} \times C_p(T_{co} - T_a)$$

$$\eta_C = \frac{M_{water} \times C_p(T_{co} - T_a)}{A_c \times I_G} \tag{3.33}$$

3.4.6 Efficiency of solar drying system

Thermal efficiency plays a significant role in evaluating thermal behavior of solar dryers. It is determined using Eq.3.34 [26]:

$$\eta_D = \frac{(m_i - m_f) \times L_w + C_{pw}(T_o - T_a)}{Q_s} \times 100 \tag{3.34}$$

where η_D is dryer efficiency, L_w is the LH of evaporation (kJ/kg), Q_s is thermal energy absorbed by ETSC.

3.4.7 Drying cabin

According to law of conservation, mass balance can be written as Eq.3.35 [26]:

$$\sum\left(M_f\gamma_i + M_w\right) = \sum\left(M_f\gamma_o\right) \quad (3.35)$$

Energy balance inside the drying cabin can be written as Eq.3.36 [26]:

$$\sum\left(M_f h_{wi} + M_w q_i\right) = \sum\left(M_f h_{wo} + M_w q_o\right) \quad (3.36)$$

3.4.8 Exergy efficiency of developed solar drying system

Exergy inflow, exergy outflow, exergy loss, and exergy efficiency are necessary to estimate for 2nd law thermodynamic analysis of solar dryer. Experimentation on the developed dryer was carried out for exergy efficiency optimization. The exergy efficiency was determined by Eqs 3.37-3.40 [66]:

Exergy Inflow of the drying cabin

$$Ex_i = m_a C_{pa}\left[(T_i - T_a) - T_a \ln\frac{T_i}{T_a}\right] \quad (3.37)$$

Exergy outflow of the drying cabin

$$Ex_o = m_a C_{pa}\left[(T_o - T_a) - T_a \ln\frac{T_o}{T_a}\right] \quad (3.38)$$

Exergy losses

$$Ex_{ls} = Ex_i - Ex_o \quad (3.39)$$

Exergy Efficiency (EE)

$$\eta_{EE} = \frac{Ex_o}{Ex_i} \quad (3.40)$$

where, Ex_i = Exergy inflow, Ex_o = Exergy outflow

3.5 Investigation of drying kinetics, quality assessment, and heat and mass transfer

This section deals with the sample preparation, procedure of experimentation work, and performance analysis in terms of effective moisture diffusivity, mass transfer, activation energy and quality assessment.

3.5.1 Sample preparation

Fresh bananas were bought from the supermarket in Morar, Gwalior. Before the experiment, bananas were peeled off before cutting into 3mm thickness by a cutting machine. Oven method was used to compute initial MC (78 ± 2% on wet basis) of banana slices at 105℃ for 24 hours.

3.5.2 Procedure of experimentation

Banana slice drying experiments were carried out under three different modes of drying as follows::

- Experiment is carried out in HE-ETADS. Where heated water (heat transfer fluid) comes from evacuated tube collectors circulated in copper tubes of heat exchanger.
- Experimentation is performed in greenhouse solar dryer.
- Banana slices are dehydrated in open sun drying.

At the same time, banana slices are dehydrated inside HE-ETADS, greenhouse drying, and open sun drying. In all three conditions, 5kg banana slices are spread for dehydration and weighed at 1 hour intervals.

3.5.3 Performance analysis

Thermal performance analysis of HE-ETADS with and without load conditions: This section deals with the thermal performance of drying system under loaded and unloaded conditions

Drying kinetics: Evaluation of initial and final MC, MR, drying rate (DR), and fitting of drying kinetics mathematical models in drying curves of banana slices.

Quality and color index assessment: This comprises the assessment of product in terms of quality (hardness, rehydration ratio) and color index.

Concept of mass transfer: This evaluates effective moisture diffusivity, mass transfer and activation energy.

3.5.3.1 Drying kinetics

The linearized forms of Verma Model, Wang and Singh, Two-term exponential, Prakash and Kumar, Midili-Kucuk Model, Lewis Model, Page Model, Modified Henderson and Pabis, Henderson Model, Weibull Model are given in Table 3.4. Moisture ratio is defined as:

$$MR = \frac{M_t - M_e}{M_i - M_e} \tag{3.41}$$

It is dimensionless parameter and was computed to compare the drying performance of any drying system for banana slices [82].

Equilibrium moisture content (M_e) is a significant factor in drying crops, mainly in tropical nations with a larger relative humidity. M_e of agricultural produce was computed in ranges of 25-75℃ temperature and 0-100% relative humidity. Halsey's Equation. is the best fit of M_e of agricultural produce.

$$RH = exp\left(\frac{-11.08492}{RT_{abs}}(M_e^{-0.886330})\right) \quad (3.42)$$

Equation (3.42) can be modified as Eq.4 to determine the M_e of agricultural produce:

$$M_e = \left[\frac{-11.8492}{RT_{abs} \times ln(RH)}\right]^{1.128} \quad (3.43)$$

Linear regression analysis was performed using MATLAB-2018, and Chi-square ($\chi 2$), root mean square error (RMSE), and coefficient of determination(R^2) values were computed. R^2 was used to compute experimentally and predicted moisture ratio values. All these factors can be evaluated using following relations (Eq. 3.44,3.45 and 3.46) [82]- [83].

$$R^2 = \frac{\left(\sum_{i=1}^{N} MR_{exp,i} MR_{pre,i}\right)^2}{\sum_{i=1}^{N} MR_{exp,i^2} - \sum_{i=1}^{N} MR_{pre,i^2}} \quad (3.44)$$

$$\chi 2 = \frac{\sum_{i=1}^{N} (MR_{pre,i} - MR_{exp,i})^2}{N - n,} \quad (3.45)$$

$$RSME = \sqrt{\frac{1}{N}} \sum_{i=1}^{N} (MR_{pre,i} - MR_{exp,i})^2 \quad (3.46)$$

Table 3.4 Models tested for drying kinetics[28-30]

Name of model	Abbreviation	Models
Verma Model	VM	$MR = a.\exp(-kt) + (1-a)\exp(-gt)$
Wang and Singh Model	WSM	$MR = 1 + at + bt^2$
Two-term Model	TTM	$MR = a\exp(-k_0 t) + c\exp(-k_1 t)$
Prakash and Kumar Model	PKM	$MR = at^3 + bt^2 + ct + d$
Midili-Kucuk Model	MKM	$MR = a\ \exp(-kt^n) + bt$
Lewis Model	LM	$MR = \exp(-kt)$
Page Model	PM	$MR = \exp(-kt^n)$

Henderson and Pabis Model	HPM	$MR = a\exp(-kt)$
Weibull Model	WM	$MR = a - b\exp(-kt^n)$
Henderson Model	HM	$MR = a\exp(-kt) + C$

3.5.3.2 Moisture content and drying rate

It is defined as the quantity of water present in sample (agricultural produce) at an instant of time and was calculated based on percentage of MC escape and conveyed on wet basis and can be evaluated using Eq.3.47 [83]:

$$MC = \left(\frac{M_i - M_f}{M_i}\right) 100 \quad (3.47)$$

Overall drying rate, which can be defined as the ratio of the differences between initial and final moisture content to the time interval, was evaluated using following relations [83]:

$$DR = \frac{M_t - M_{t+\Delta t}}{\Delta t} \quad (3.48)$$

3.5.3.3 Quality evaluation of dried agricultural produces

3.5.3.3.1 Rehydration ratio

Rehydration ratio of product was evaluated in two steps; in Step-I 100gm dried product were boiled in water with 1% salt for a time period of 10 min. In step-II final weight was obtained. It can be calculated using the following relation [83]:

$$\text{Rehydration Ratio} = \frac{W_{final}}{W_{intial}} \quad (3.49)$$

3.5.3.3.2 Shrinkage

It is defined as the percentage change in volume of dehydrated food product compared to actual volume of fresh food product. It was evaluated using following relations [28-31]:

$$\text{Shrinkage} = \left(\frac{S_{actual} - S_{final}}{S_{final}}\right) 100 \quad (3.50)$$

3.5.3.3.3 Hardness

It is a key parameter and vital in quality assessment of dehydrated product. Hardness is greatest force applied during first bites (in kg_f). Hardness of dried product was evaluated afterward rehydration through CT3 Texture Analyzer. The outcome of hardness was concluded by taking average of 10 readings [28-31].

3.5.3.4 Colour index

Colour index plays a significant role in quality assessment of dried products for acceptance by end-user. This factor for dried product was obtained using a colorimeter and observations were recorded at an interval of 1h. Color standards of the product were described in terms of Commission International Eclairage (CIE) chromaticity coordinates L_o, a_o, and b_o. Total Colour Difference (**Δ**E) was obtained using Eq.3.51 [84-86]:

$$\Delta E = \sqrt{(\Delta L_o)^2 + (\Delta a_o)^2 + (\Delta b_o)^2} \quad (3.51)$$

where

$$\Delta L_o = (L_0 - L)$$

$$\Delta a_o = (a_o - a)$$

$$\Delta b_o = (b_o - b)$$

where ΔE is total colour changes during the drying process. Significance of all coordinates is summarized in Table 3.5 These factors play an important role in deciding the color combination in terms of huge angel (h) estimated from Eq.3.52.

Table 3.5 Significance of L_o, a_o, and b_o

Coordinates	Color difference/change	
L_o	Lightness	Darkness
	(L_o = 100 for white)	(L_o = 0 for black)
a_o	Redness	Greenness
	(a_o>0 for red)	(a_o<0 for green)
b_o	Yellowness	Blueness
	(b_o>0 for yellow)	(b_o<0 for blue)

$$h = \begin{Bmatrix} \tan^{-1} & (b_0/a_o)\ (\text{when } a_o > 0) \\ & 180° + \tan^{-1}(b_0/a_o)\ (\text{when } a_o < 0) \end{Bmatrix} \quad (3.52)$$

where h is the huge angle

3.5.3.5 Water activity

Water activity is a key factor and plays an important role in storing dried food products and signifies microbiological stability during storage. It is defined as the ratio of vapour pressure in food concerning pure water vapour pressure. A water activity meter was used to determine water activity of dried banana slices at 60 min intervals of time and can be calculated from Eq.3.53 [84]:

$$A_w = 1 - \exp[-0.0193(T + 44.36)M_e^{0.3316} \quad (3.53)$$

3.5.3.6 Concept of mass transfer

This section deals with the phenomena of mass transfer throughout the drying process. The following sub sections are discussed.

3.5.3.6.1 Effective moisture diffusivity ($\mathbf{D_{eff}}$)

It plays a significant role in understanding the concept of moisture removal along with mass transfer throughout the dehydrating process. Mass transfer occurs through molecular diffusion. Fick's second law was used to evaluate molecular diffusion[84]. The following assumptions allow for the solution of Fick's second law of diffusivity equation: [87]:

- Drying process is diffusional.
- Banana slice temperature and diffusivity are both constant.
- There is very little shrinkage throughout the drying process [88].

Fick's second law for unsteady-state diffusion (Eqs.3.54-3.56) was used to compute the MR (Eq. (39)).

$$\frac{\partial MR}{\partial t} = \nabla\left[D_{eff}(\nabla MR)\right] \tag{3.54}$$

$$\frac{\partial MR}{\partial t} = \nabla\left[D_{eff}\nabla\left(\frac{M_t - M_e}{M_i - M_e}\right)\right] \tag{3.55}$$

$$\frac{\partial MR}{\partial t} = \left[D_{eff}\nabla^2\left(\frac{M_t - M_e}{M_i - M_e}\right)\right] \tag{3.56}$$

To simplify, Eq. 3.56 boundary conditions can be considered from 0 to ∞.

$$MR = \frac{M_t - M_e}{M_i - M_e} = \frac{8}{\pi^2}\sum_{n=0}^{\infty}\frac{1}{(2n+1)^2}\exp\left(-\frac{(2n+1)^2\pi^2 D_{eff}t}{4L^2}\right) \tag{3.57}$$

For long drying period, Eq.3.57 can be further rewritten as:

$$MR = \frac{M_t - M_e}{M_i - M_e} = \frac{8}{\pi^2}\exp\left(-\frac{\pi^2 D_{eff}t}{4L^2}\right) \tag{3.58}$$

Eq.3.58 can also be simplified using natural logarithmic form Eq.3.57 as:

$$ln(MR) = ln\left(\frac{8}{\pi^2}\right) - \left(\frac{\pi^2 D_{eff}t}{4L^2}\right) \tag{3.59}$$

Or

$$ln(MR) = A - B \quad (3.60)$$

Eq.3.60 is the natural logarithmic form of Eq.3.58, slope (B) can be obtained from linear regression of *ln(MR)* versus time curves, and effective moisture diffusivity **(**EMD) can be evaluated as (Eq.3.61):

$$B = -\frac{\pi^2 D_{eff}}{4L^2} \quad (3.61)$$

3.5.3.6.2 Activation energy (AE)

Activation energy transfers water from the surface of foodstuff, i.e. fruits and vegetables, into the atmosphere in the form of moisture content. Relation between D_{eff} and air temperature was assumed to be an Arrhenius-type Eq.

$$D_{eff} = D_o exp\left(-\frac{E_a}{RT}\right) \quad (3.62)$$

where D_{eff} is EMD (m^2s^{-1}), D_o is Arrhenius factor (m^2s^{-1}), E_a is AE (kJ/mole)

Equation (3.62) further simplifies as:

$$lnD_{eff} = lnD_o - \left(\frac{E_a}{R}\right)\frac{1}{T} \quad (3.63)$$

3.5.3.6.3 Mass transfer coefficient (MTC)

MTC signifies moisture diffusion during dehydrating process. Therefore, Biot number states that resistance offered to moisture removal from product's surface to drying medium. It can be estimated using Eqs.3.64-3.66.

$$h_m = \frac{(D_{eff})(B_i)}{H} \quad (3.64)$$

$$B_i = \frac{24.848}{Di^{0.375}} \quad (3.65)$$

$$D_i = \frac{v}{kL} \quad (3.66)$$

3.6 Environmental analysis of HE-ETADS

This section deals with the environmental sustainability and exergetic based sustainability indicators of drying system in two different cases.

3.6.1 Experimental procedure

Garlic clove, banana slices, and peppermint leaves were brought from local market of Morar Gwalior (M.P.) India. Experimentation was carried out in HE-ETADS on March 8-10, 2022, in the solar energy lab from 6:00 to 19:00 hours. The observation was noted at an interval 30 min. Experimentation work was continued until product achieved its final moisture level. Flow chart of drying process is shown in Fig 3.7. The experimental work was categorized into two Cases, as mentioned.

Case-I: *HE-ETADS coupled with ETC. In this case, system was operated for 13h every day (6:00 to 19:00 h) because the heat energy is stored in hot water that circulates from ETSC through wire & tube-type heat exchanger to maintain temperature inside drying cabin after sunset.*

Case II: *HE-ETADS without ETC. In this case, the drying system is operated 13h every day until sunset (6:00 to 19:00 h).*

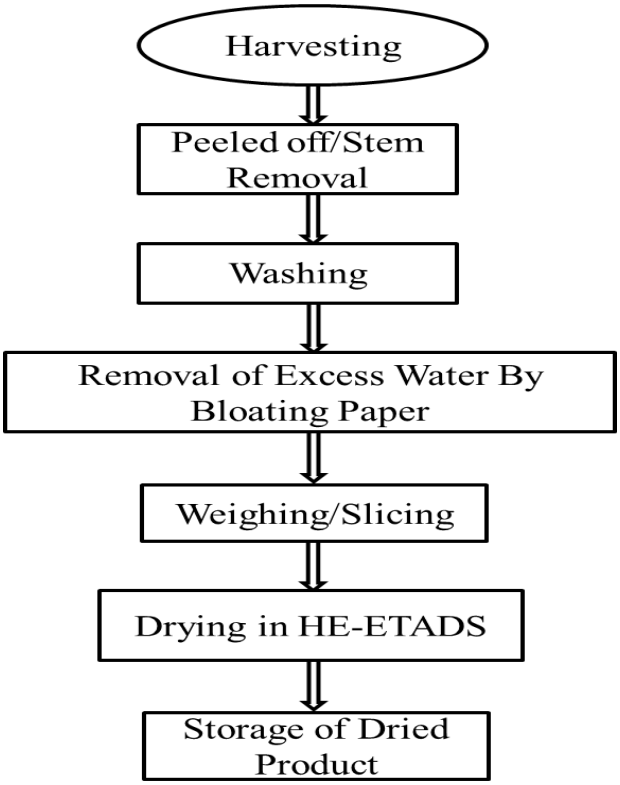

Fig 3.7 Flow chart of drying process

Environmental analysis plays a significant role in showing the impact of advanced developed drying system on the atmosphere. Solar drying systems are the best example of sustainable system and do not affect the atmosphere in any manner. The first step in environmental analysis is to compute embodied energy of a newly developed drying system. It is amount of energy devoted to any product, from extraction and dispensation of its raw material to final product in hand. Table 3.6 indicates amount of embodied energy used for different materials to fabricate drying systems for both Cases. The value of energy density for different used material to fabricate drying system is preferred from previous research work [89]. Therefore, assumption and relations used in calculation of environmental analysis are discussed in Table 3.7.

Table 3.6 Embodied energy for different used material to fabricate drying system

Materials used	**Embodied Energy (kWh/kg)**	**Mass (kg)**	**Case-I** **Total Embodied Energy (kWh)**	**Case-II** **Total Embodied Energy (kWh)**
Cast iron L-shape angel for structure	8.90	225	2002.5	2002.5
Cast iron L-shape angel for drying platform	8.90	80	712	00
Copper tube	19.85	40	794	794
Stainless steel wire mesh	9.50	5	47.5	47.5
Al duct tap	56.21	0.055	3.091	3.091
Polycarbonate sheet	10.50	20	210	210
Fitting materials	56.12	2.1	117.85	117.85
DC fan made of plastic	19.54	0.4	7.816	7.816
Oil paint	25.25	2	50.5	50.5
PV panels	740	02 no.	1480	1480
ETSC	423.25kwh/m^2	4.0m^2	1693	00
Electricity wire	19.59	0.1	1.959	1.959
Al T and L-shaped joint	55.25	26	1436.5	00
Total embodied energy			**8556.71**	**4633.21**

3.6.2 Energy Payback Time (EPBT)

The time is taken by system to recover quantity of energy invested for fabricating experimental setup known as energy payback period of drying system.

3.6.3 CO_2 emission

It may be defined as the investment of embodied energy in fabricating a complete assembly of drying system in proportion to system life. Electricity generation from coal gives average CO_2 equivalent intensity of around 0.98 kg per kWh [31].

3.6.4 Net CO_2 mitigations

The equivalent CO_2 emissions mitigated by system in comparison to conventional fossil fuel are determined as [68]:

3.6.5 Carbon credits

The carbon credits corresponding to the carbon mitigations obtained under various life span period of the present drying system is obtained as [90]:

$$\begin{aligned}\text{Life Time Carbon Credit in tons} \\ &= \text{Lifeteime } CO_2 \text{ mitigation in tons} \\ &\times \text{Cost of carbon credit per tons}\end{aligned}$$

The cost of CO_2 emission in 2020 is being traded at an average cost of 20 USD per tones of CO_2 mitigation [67]. The conversion rate of 1 USD in Indian currency is nearly 80 rupees [67].

3.6.6 Exergetic indicators for evaluating sustainability

To ensure sustainable development and appropriate energy resource consumption, it is essential to identify where energy is wasted. Decreasing fossil fuel exergy losses can lead to attaining sustainability [91].

3.6.6.1 Environmental Sustainability Index (ESI)

Environmental sustainability of energy systems is a key factor for ecologists and researchers. ESI is a key factor for exergetic sustainability of solar drying methods in terms of II^{nd} law of thermodynamics. Environmental Sustainability Index (ESI) measures overall progress in environmental sustainability. Therefore, reducing energy emissions will increase the system's energy efficiency. The value of ESI for an advanced drying system can be determined as [92]:

$$\text{Environmental Sustainability Index (ESI)} = \frac{1}{(1-\eta_{ex})} \quad (3.67)$$

3.6.6.2 Environmental destruction coefficient (EDC)

EDC plays a significant role in showing the reduction of positive impact of solar drying methods on exergetic sustainability. Theoretically, EDC varies in the range of 0 and 1. Therefore, the value of EDC was obtained as 1. Thus, reference point is better way to improve the efficiency of system. The value of EDC for a newly developed drying system can be obtained as [92]:

$$\text{EDC} = \frac{1}{\eta_{ex}} \quad (3.68)$$

3.6.6.3 Environmental impact factor (EIP)

EIP of solar drying system also plays a vital role in representing whether or not it harms the ecosystem due to its inadequate waste exergy and exergy destruction. It can be reordered in the following form for solar drying system in the range of 0 to + ∞.

EIP for solar drying system can be calculated as [92]:

$$\text{EIP} = \frac{E_{Xloss}}{E_{Xin}} \times \text{ED} \quad (3.69)$$

3.6.6.4 Environmental Effect Factor (EEF)

EEF of solar drying system indicate the effect of unusable waste energy on the atmosphere. Consequently, EEF is directly proportional to waste energy ratio. EEF for solar drying system can be calculated as [93]:

$$EEF = \left.\frac{\frac{E_{Xloss}}{E_{Xin}}}{\frac{E_{Xo}}{E_{Xi}}}\right. \quad (3.70)$$

where, E_{Xin} = Exergy inflow, E_{Xloss}= Exergy loss

Table 3.7 Relations used in environmental analysis

Equations	Ref.	Eq.
Energy Payback Period $= \frac{\text{Emboided Energy } (E_e)}{\text{Annual Thermal Energy Output } (E_a)}$ where E_a is annual thermal energy output evaluated from HE-ETADS, it can be computed as: $E_a = E_d \times N_{sd}$ where E_d is daily thermal energy output of HE-ETADS and N_{sd} is no. of sunshine day per annum. Following relation was used to calculate daily thermal energy output of system: $E_d = \frac{M_{me} \times L_{lv}}{3.6 \times 10^6}$ L_{lv} is considered as 2.26×10^6 J/kg. The amount of moisture (kg) evaporated from crop surface can be determined as: $M_{me} = \frac{m_c(M_i - M_f)}{100 - M_f}$	[64]	(3.71) (3.72) (3.73)
CO_2 emission per year $= \frac{E_e}{L} \times 0.98$ kg Considering domestic appliance losses (L_a) and transmission losses (L_t), then CO_2 emissions through the advanced HE-ETADS are described as: CO_2 emission per year $= \frac{E_e}{L} \times \frac{1}{1 - L_a} \times \frac{1}{1 - L_t} \times 0.98$ kg If $L_t = 0.40$ and $L_a = 0.20$ due to old appliances, then Eq. (42) becomes as follows:	[64]	(3.74) (3.75)

$\text{CO}_2 \text{ emission per year} = \frac{E_e}{L} \times 2.042 \text{ kg}$		(3.76)
$\text{CO}_2 \text{ mitigation per year} = \text{E}_{\text{system}} \times \frac{1}{1-\text{L}_\text{a}} \times \frac{1}{1-\text{L}_\text{t}} \times 0.98 \text{ kg}$ $\text{CO}_2 \text{ mitigation per year} = \text{E}_{\text{system}} \times 2.042 \text{ kg}$ For a life span of N years, it would be $= \text{E}_{\text{system}} \times \text{N} \times \frac{1}{1-\text{L}_\text{a}} \times \frac{1}{1-\text{L}_\text{t}} \times 0.98 \text{ kg}$ For a life span of N years, it would be $= \text{E}_{\text{system}} \times \text{N} \times 2.042 \text{ kg}$ Net CO_2 mitigation = Lifetime CO_2 mitigation - Lifetime CO_2 emission $= (\text{E}_{\text{system}} \times \text{N} - \text{E}_\text{e}) \times \frac{1}{1-\text{L}_\text{a}} \times \frac{1}{1-\text{L}_\text{t}} \times 0.98\text{kg}$ $= (\text{E}_{\text{system}} \times \text{N} - \text{E}_\text{e}) \times 2.042\text{kg}$ The conversion rate of 1 USD in Indian currency is nearly 80 rupees.	[16]	(3.77) (3.78) (3.79) (3.80) (3.81)

CHAPTER-4

4. Results and Discussion

The thermal performance of heat exchanger-evacuated tube-assisted drying system (HE-ETADS) is evaluated under unload and load conditions, optimise the drying parameters and also evaluates the drying kinetics and environmental sustainability of novel drying system. Results of the research work are discussed in this section:

4.1 Evaluation of performance of HE-ETADS under no-load condition

4.1.1 Impact of solar insolation and air temperature on drying cabin and ground (floor surface) temperature

Direct solar insolation plays an important role in the rising air temperature, drying cabin temperature and ground (floor surface) temperature inside the HE-ETADS because solar insolation is directly proportional to the temperature. Figs. 4.1(a), 4.1(b), and 4.1(c) indicate the variation in drying cabin temperature, inside ground (floor surface) temperature of HE-ETADS, and atmospheric air temperature in all three categories. In Category-I, inside drying cabin and ground (floor surface) were always greater than Category-II and III. Maximum temperature difference between drying cabin and atmospheric air was 54.97℃, 68.74℃, and 57.48℃ at 11h, 10h, and 11h for Category-I, at different water flow rates (10, 20, and 30Ltr/h) for all three days of experiments. Inside drying cabin temperature of the proposed HE-ETADS is 66.25%, 69.25%, and 67.44% greater than the atmospheric air temperature for all days of experiment, respectively, for Category-I. Similarly, in Category-II maximum temperature differences of 34.19℃, 30.42℃, at 43℃ at 12h, 12h, and 11h were recorded for 1^{st}, 2^{nd}, and 3^{rd} days of experiment. Inside drying cabin temperature is 57.37%, 54.38%, and 62.31% greater than atmospheric temperature at all water flow

rates (10, 20, and 30Ltr/h) for 1st, 2nd, and 3rd days of experiment. Similarly, for Category-III, it was found at 37.4℃, 34.28℃, and 33℃ at 15h, 12h, and 15h at different water flow rates and on all days of experiment.

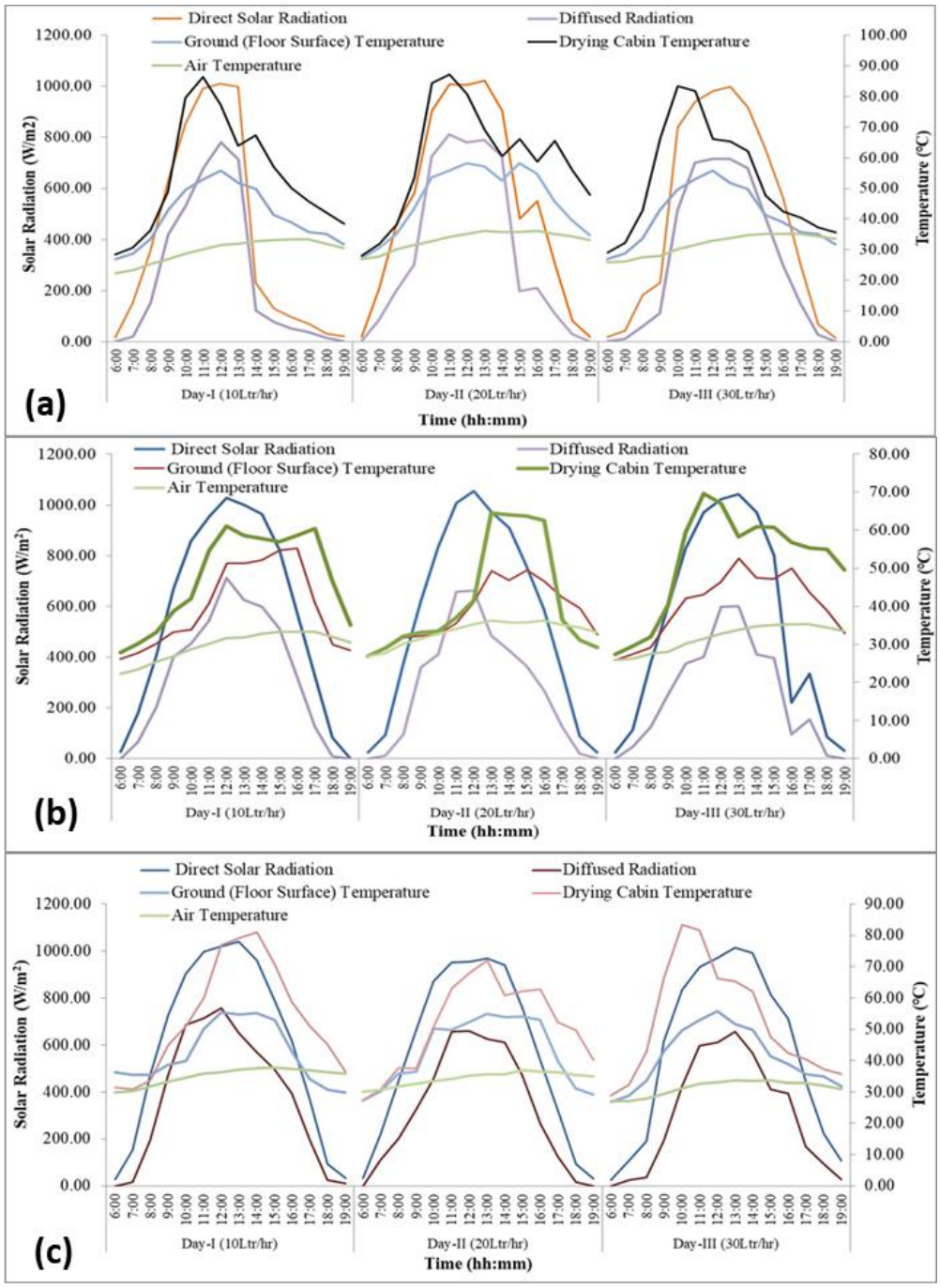

Fig 4.1 Variation of different temperatures with respect to time of day (a) for Category-I, (b) for Category-II, and (c) for Category-III

Drying cabin temperature is 52.85%, 53.84%, and 53.22% higher than atmospheric temperature. Inside drying cabin temperature of newly developed HE-ETADS for Category-I is 8.88%, 14.87%, and 5.13% greater than Category-II; in a similar manner, 13.4%, 15.41%, and 14.22% greater than Category-III for all three days of experiment at 10,20, and 30Ltr/h water flow rate. These outcomes represent efficiency and thermal performance of HE-ETADS.

Inside ground (floor surface) temperature also plays a vital role in enhancing the drying cabin temperature and reducing inside relative humidity. Figs. 4.2(a), 4.2(b), and 4.2(c) show the relationship between drying cabin temperature and inside ground (floor surface) temperature at 10, 20, and 30Ltr/h water flow rate for all three days of experiment. For Category –I maximum ground (floor surface) temperature was 44.13°C, 46.39°C, and 44.13°C at 14h, 15h, and 14h, while in Category-II it was recorded 43.86°C, 39.86°C, and 41.30°C at 16h, 15h, and 13h. Likewise, maximum inside ground (floor surface) was observed at 46.17°C at 14h, 47.62°C at 15h, and 40.39°C at 15h for 1^{st}, 2^{nd}, and 3^{rd} days of experiment at different water flow rates. ETSC is responsible for enhancing the inside drying cabin temperature of advanced HE-ETADS flowing hot water at different flow rates (10, 20, and 30Ltr/h) through a heat exchanger kept inside the dryer. The combined effect of all units has a greater influence on efficiency and thermal performance of HE-ETADS in terms of faster moisture removal rate.

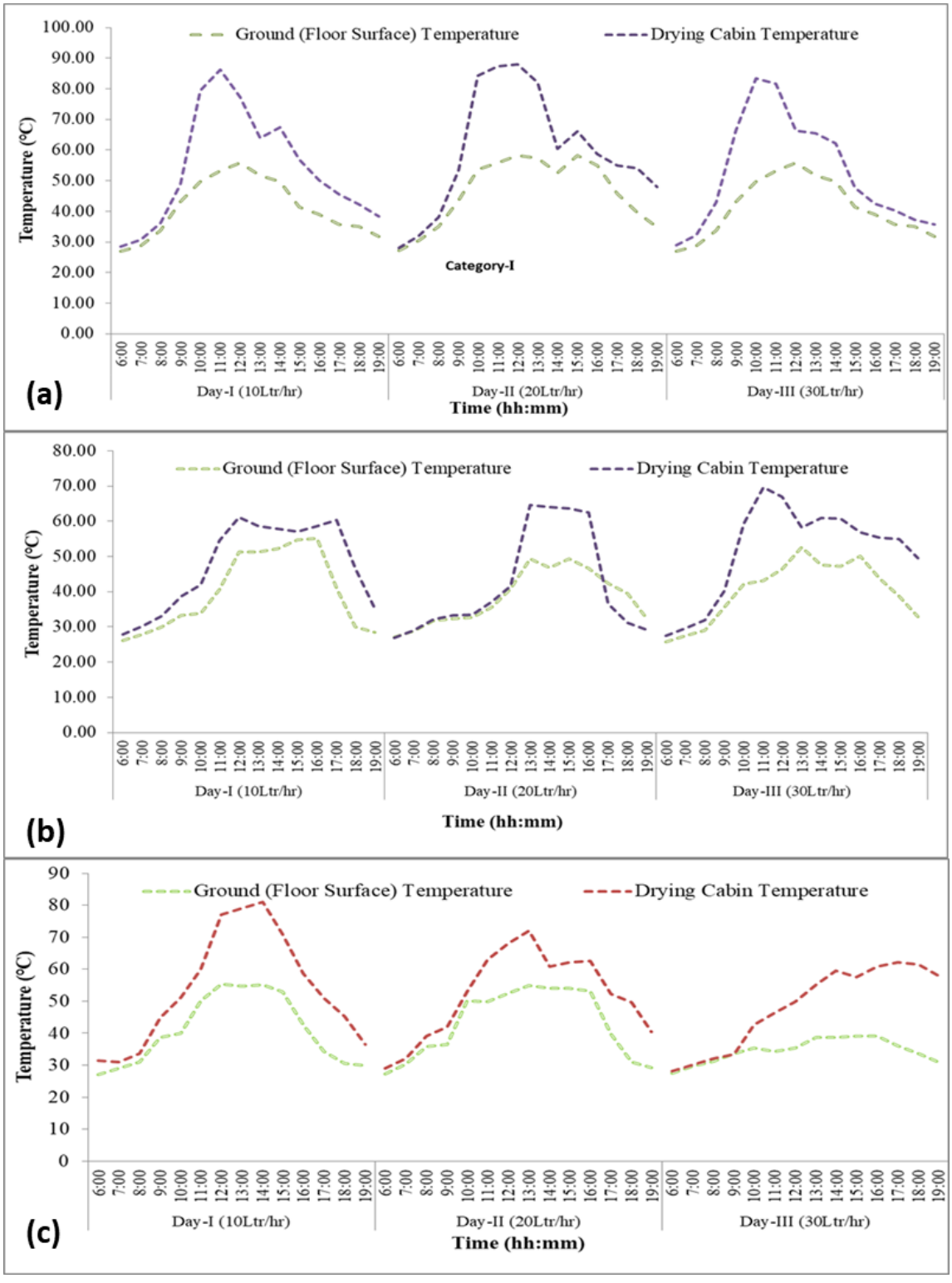

Fig 4.2 Variation in ground (floor surface) and drying cabin temperature of HE-ETADS with respected to time of day (a) for Category-I, (b) Category-II, and (c) Category-III

4.1.2 Comparative analysis of CHTC of HE-ETADS for Category-I, II, and III

Fig. 4.3(a) illustrates the variation of CHTC for ground (roof surface) and drying cabin air for all three categories. CHTC is greater for Category-I than Category-II, III due to stagnation approach of HE-ETADS. Maximum CHTC for Category-I was observed 37.32W/m^2°C, 44.52W/m^2°C, and 47.542W/m^2°C at 14h, 14h, and 15h, respectively for 1st, 2nd, and 3rd days of experiment at different water flow rate, whereas in Category-II it was found 22W/m^2°C at 12h, 18.94W/m^2°C at 13h, and 19.85W/m^2°C at 13h for all days during experiment. Due to presence of clouds or hazy days, the CHTC lower for day-2 in Category-II. For Category-III, CHTC 18.60W/m^2°C,19.781W/m^2°C, 21.65W/m^2°C at 13h, 14h, and 14h for three days during experiment at 10, 20, and 30Ltr water flow rate. Maximum CHTC (47.542W/m^2°C) was evaluated on 2nd at 14h for Category-I, 22W/m^2°C at 12h on 1st for Category-II whereas in Category-III it was 21.65W/m^2°C at 14h on day-III during experimentations. CHTC of north wall insulated greenhouse dryer (NWIGHD) for ground to drying cabin air was 46.622W/m^2°C [94], while for advanced HE-ETADS it was found 47.542 W/m^2°C, that is 1.98% greater than NWIGHD. It indicates the thermal performance or efficiency of proposed HE-ETADS.

4.1.3 Comparative analysis of coefficient of diffusion (C_d) in HE-ETADS (for all Categories)

Coefficient of diffusion can be evaluated using Eq.3. Dependent parameters of C_d are atmospheric air temperature solar insolation, and HE-ETADS cabin temperature. From Fig. 4.3(b) it is clear that C_d varies with respect to solar insolation and is directly proportional to solar insolation. In general C_d was observed maximum during noon

and minimum in the evening. Maximum value of coefficient of diffusion (0.220) was observed during day-I of experimentation at 14h in Category-III.

4.1.4 Heat losses from HE-ETADS for Category-I, II, III

Hourly heat loss through HE-ETADS can be evaluated using Eq.4. Hence, C_d plays a vital role in calculation of heat loss for all categories. It is clear from Fig.4.3(c) that the heat loss through system was maximum in Category-II than Category-I and III. Therefore, for high efficiency and thermal performance of HE-ETADS heat loss should be less as possible. For Category-I, maximum heat loss by the system was 383.01W,377.366W, and 285.895W at 11h,12h, and 15h for all three days during experiment at different water flow rate, whereas in Category-II 403.02W, 397.477W, and 295.906W at 13h,12h, and 14h respectively. Similarly, for Category-III, it was 320.701W, 447.477W, and 337.616W during all days of experiment. Using ETSC coupled with dryer makes the whole system more effective for dehydrating farming products.

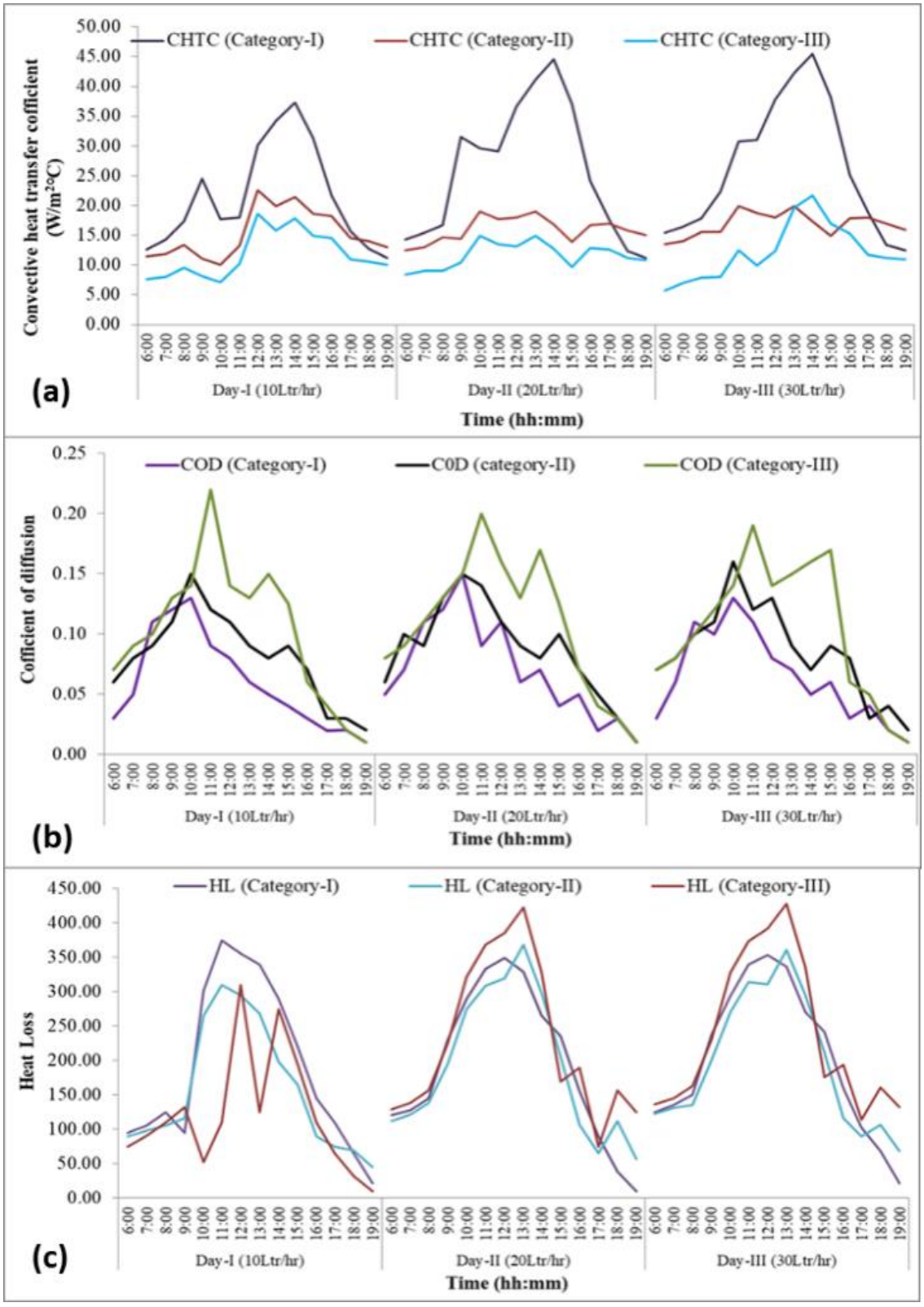

Fig 4.3 (a) CHTC with respect to time of the day, (b) Coefficient of diffusion with respect to time of day, and (c) Heat loss with respect to time

4.1.5 HUF and COP for HE-ETADS

Figs. 4.4(a), 4.4(b), and 4.4(c) illustrate variation of HUF and COP for three successive days of experimentation under all three Categories at different water flow rates (10, 20, and 30Ltr/h). For Category-I HCF differs in the range of 0.185-0.560, 0.154-0.615,and 0.110-0.376 for three consecutive days of experiment at 10, 20, and 30Ltr/h water flow rate, whereas in Category-II it varied from 0.120-552, 0.125-619, and 0.198-542 for all three days. In similar way for Category-III, it differs from 0.046-0.550, 0.16-0.928, and 0.0701-0.769 for all three successive days, respectively.

COP variations of Category-I, Category- II, and Category-III were 0.303-0.801, 0.353–0.904 & 0.601-0.901 and 0.62–0.94, 0.302–0.862 & 0.220–0.909 and 0.45-0.970, 0.35-0.880 & 0.20-0.920 during the experiment for first, second and third day at different water flow rate (10, 20, and 30Ltr/h) respectively. Maximum HUF (0.60) is achieved during the IInd day for Category-I at 20Ltr/h, and for Category-II it is 0.775 during the IIIrd day of experimentation at 30Ltr/h. whereas in Category-III it is 0.782 at 10Ltr/h water flow rate during Ist day of experiment. Higher COP(0.902) is obtained during IIIrd day of the experiment for Category-I at 30Ltr/h water flow rate, whereas 0.940 is obtained on Ist day for Category-II at 10Ltr/h flow rate. For Category-III, it achieved 0.97 at 10Ltr/h water flow rate during first day of experiment.

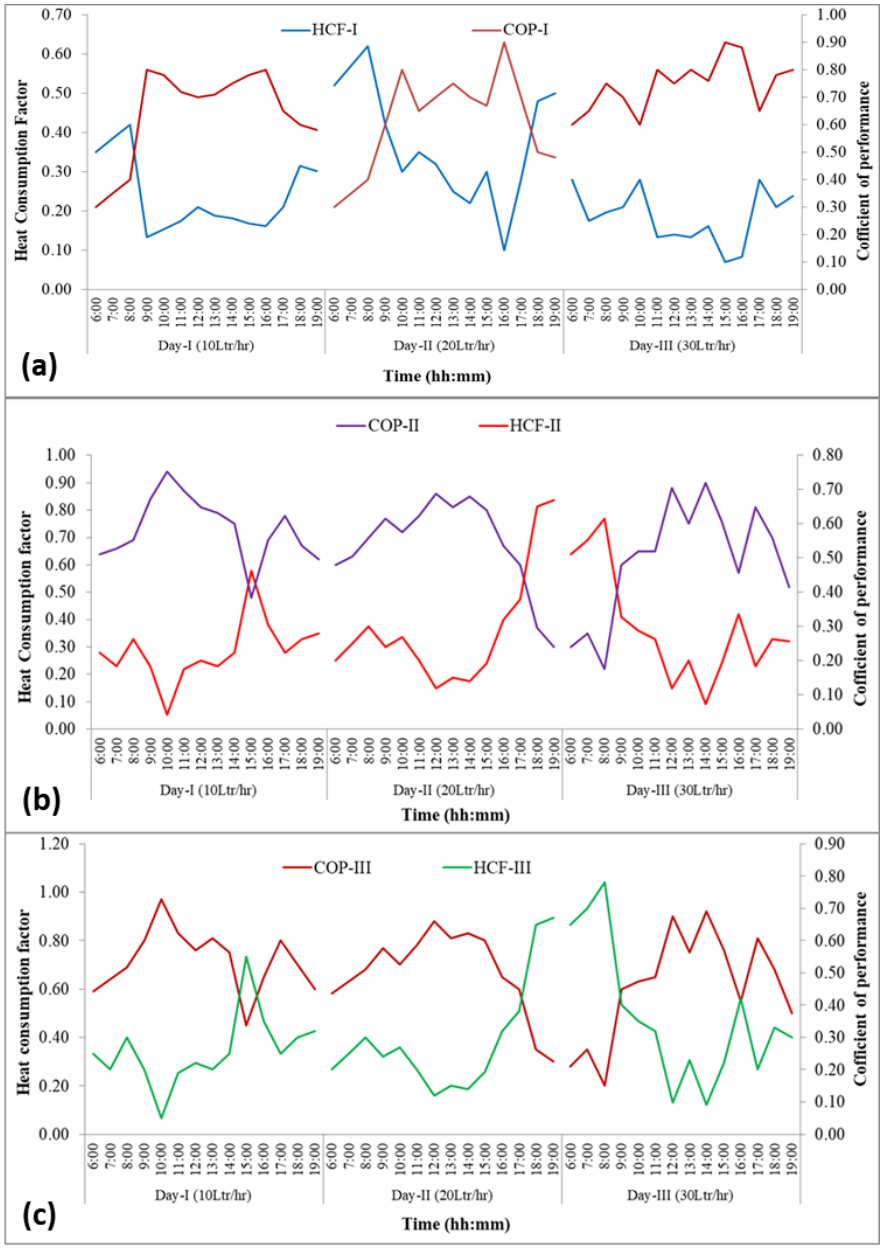

Fig 4.4 Heat consumption factor and coefficient of performance with respect to time of day

4.2 Optimization of drying parameters for drying system using response surface methodology

4.2.1 Design Research

30 runs and 29 degree of freedom (DOF) are estimated to complete an optimization

study using response surface methodology corresponding to 3- levels of dependent parameters. Inside temperature (°C), water flow rate (Ltr/h.), geometry of product (cm^2), and mass of the product (kg) have been considered as input parameters for this analysis. In addition, the drying period (hours), EC (kW/h), and moisture content (% db) are taken as control variables. Hence, the purpose of drying method optimization was accompanied by having the lowest response standards. Table 4.1 displays run of the CCD and 30 experiments performed in the optimization method.

Table 4.1 Numbers of runs of the CCD

Run	**Variable 1**	**Variable 2**	**Variable 3**	**Variable 4**	**Response 1**	**Response 2**	**Response 3**
No.	A:Temperature	B:Water Flow Rate	C:Geometry of the Product	D:Mass of product	M.C for Product	Energy consumption	Shrinkage
	°C	Ltr/h.		kg	%	kW/h	%
1	80	20	0	0.62	11.09	6.448	61.6041
2	90	30	1	1	63	5.88	68.4544
3	90	30	-1	0.24	6.8	7.0985	71.6352
4	70	10	-1	1	68.5	7.94	76.2395
5	80	10	0	0.62	33.3	6.448	60.2143
6	80	20	0	0.62	30.2	6.584	72.6454
7	90	20	0	0.62	33.25	6.548	72.9584
8	70	30	-1	0.24	6.2	8.264	74.9922
9	80	20	0	0.62	30.12	6.448	61.6048
10	80	30	0	0.62	29.15	6.58	71.7346
11	80	20	0	0.62	30.1	6.458	72.4211
12	80	20	0	0.62	30.01	6.398	72.1250
13	90	10	1	0.24	7.5	5.86	73.9008
14	90	10	-1	1	66.8	5.484	69.0157
15	70	20	0	0.62	30.25	8.502	60.4779
16	70	10	1	0.24	7.58	7.137	70.9282
17	70	10	1	1	68.45	7.13	70.8214
18	80	20	-1	0.62	29.98	7.639	72.6744
19	90	10	1	1	64.25	5.485	72.9852
20	70	30	1	0.24	6.18	5.48	69.5256
21	70	30	1	1	62.58	7.188	69.4142
22	80	20	0	0.24	6.41	8.045	61.5247
23	70	10	-1	0.24	6.13	7.985	75.9541
24	90	30	1	0.24	6.75	5.85	68.2514
25	80	20	1	0.62	29.99	6.447	68.3921

26	90	30	-1	1	62.95	7.0125	71.5213
27	70	30	-1	1	67.52	8.12	74.5241
28	80	20	0	1	66.52	6.347	61.2582
29	90	10	-1	0.24	7.51	5.352	65.2028
30	80	20	0	0.62	29.95	7.98	72.1428

4.2.2 Study of variance (ANOVA) and predictable regression

Freedman et al. Studied that variance was executed to confirm the model precision. Several factors are used to check the efficiency of model, such as mean squares, DOF, sum of squares, model F-value and, model P-value. Resolution of model F-value expects the variance of statistics around the mean. Moreover, model P-values approve the model from the arithmetical. By following the variance study, the variables have additional accuracy at the model F-values > 1. In addition, for the model P -value < 0.05 the model is accepted and fit according to statistical approach [95].

4.2.3 Drying

The analysis of variance for solar drying is presented in Table 4.2. Model F- value (47.20) proposes that the model is in an acceptable range or significant. Model P - value is < 0.0001 specifies that the model relations are significant. A, B, C, and D are significant model relationships in this circumstance. Therefore, P values greater than 0.1 show the model relations are not significant. In present study, A*B, A*C, A*D, A^2, B^2, C^2 and D^2 are inconsequential model relationships. Hence, the Predicted R^2 (0.9628) is inequitable covenant with the Adjusted R^2 (0.9571). Adeq Precision dealings with the signal to noise ratio. If the ratio is more than 4, then it is acceptable. The value of ratio is 60.09 shows an acceptable signal to noise-ratio. However, present developed model can be used to pilot the design space.

Table 4.2 Variances for solar drying

Source	**Sum of Squares**	**DOF**	**Mean of Square**	**F-value**	**p-value**	
Model	16008.81	14	1143.49	47.20	< 0.0001	significant
A-Temperature	1.17	1	1.17	0.0481	< 0.0001	
B-Water Flow Rate	19.82	1	19.82	0.8182	< 0.0001	
C-Geometry of Product	2.07	1	2.07	0.0856	< 0.0001	
D-Mass of product	15576.71	1	15576.71	642.91	< 0.0001	
AB	0.1640	1	0.1640	0.0068	0.9355	
AC	0.0625	1	0.0625	0.0026	0.9602	
AD	9.80	1	9.80	0.4044	0.5344	
BC	0.9025	1	0.9025	0.0372	0.8495	
BD	5.24	1	5.24	0.2164	0.6484	
CD	4.91	1	4.91	0.2025	0.6591	
A^2	4.54	1	4.54	0.1873	0.6713	
B^2	1.65	1	1.65	0.0682	0.7975	
C^2	0.5048	1	0.5048	0.0208	0.8872	
D^2	94.48	1	94.48	3.90	0.0670	
Residual	363.43	15	24.23			
Lack of Fit	63.00	10	6.30	0.1049	0.9985	not significant
Pure Error	300.43	5	60.09			
Cor Total	16372.24	29				
Predicted R^2		**Adjusted R^2**		**Adeq Precision**		
0.9628		0.9571		18.3860		

The externally studentized residuals are shown in Fig 4.5(a) indicated reasonably adjacent to the sloping line denotation once the highest precision of the model describes the correlation b/w the dependent parameters and drying. In data, studentized residuals are proportion resultant from the division of a residual by an estimate of its drying. The Box-Cox transformation is shown in Fig 4.5(b), a method to advance standardization of distribution by endorsing it to the power and altering it for arithmetical study. The power-transform is suitable for forming a monotonic

transformation of data through power functions [96]. The random dissemination of the residuals between −5 and +5 can also be found in Fig 4.5(c).

Fig 4.5(d) shows relationship between external studentized residuals and trial run numbers for drying.

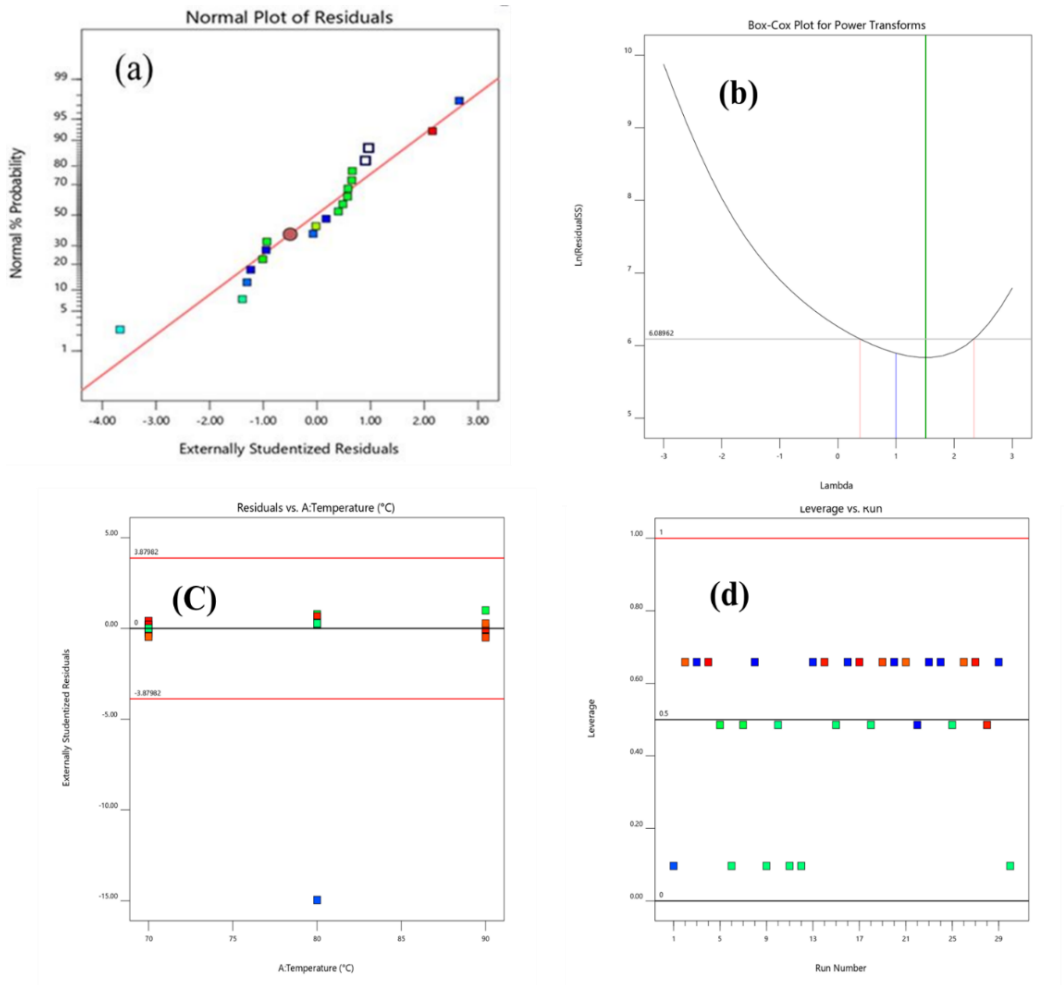

Fig 4.5 (a) Relationship of Normal probability curve vs. extremely studentizedresiduals (b) Box-Cox curve for power transforms (c) Relationship between residuals and predicted response (d) Relationship between residuals and run no.

The coded equation for drying can be written in the following form:

$$\boldsymbol{M}.\text{C of Product} = 28.67 - 0.2544\text{a} - 1.05\text{B} - 0.3394\text{C} + 29.42\text{D} + 0.1013\text{AB} + 0.062\text{AC} - 0.782\text{AD} \ -0.237\text{BC} - 0.5725\text{BD} - 0.5537\text{CD} + 1.32\text{A}^2 + 0.7986\text{B}^2 \pm 0.4414\text{C}^2 + 6.04\text{D}^2 \quad (4.1)$$

Fig 4.6 represents the relationship between objective function versus the control factors. The figure shows that the most suitable temperature for drying is 89.99℃.

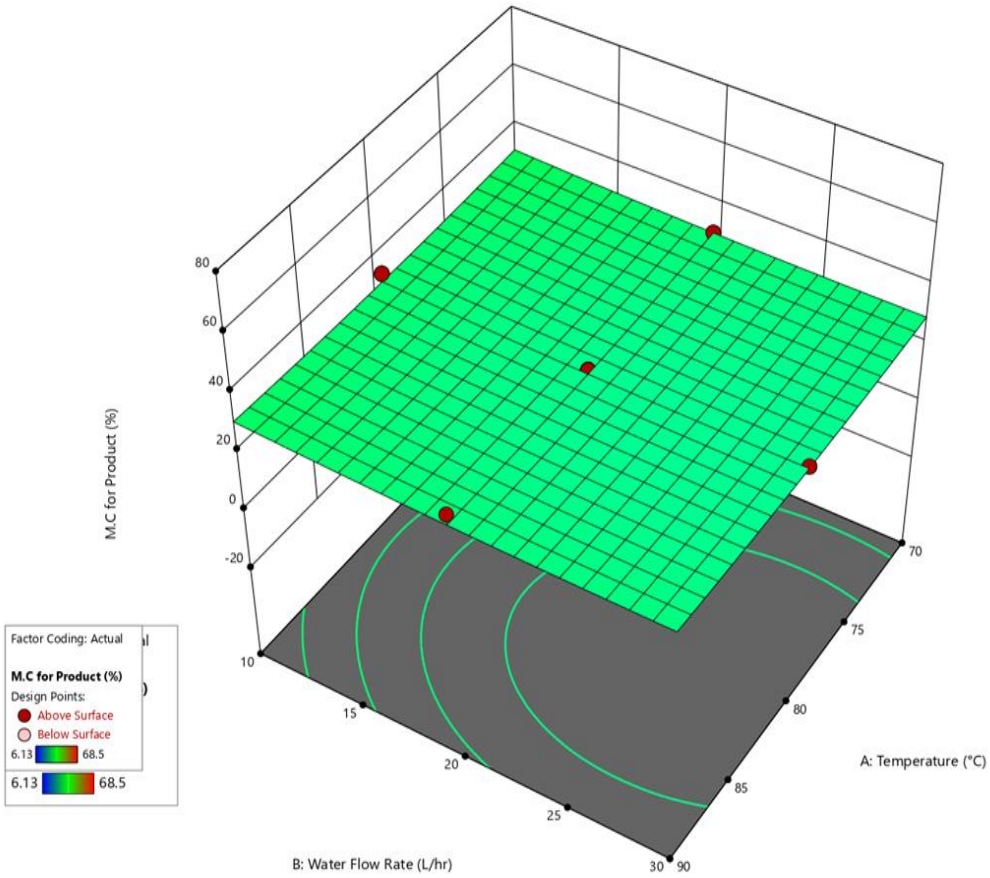

Fig 4.6 Objective functions vs. the control factors relationship

4.2.4 Energy Consumption (EC)

Study of variance for EC is shown in Table 4.3 The Model F value is 8.18 which indicates that model is significant. The Model P value is < 0.0001, which indicates the suitability of model. A, B, C, and D, are the most significant model terms in present

study. The Predicted R^2 is 0.9530. That is in equitable agreement through the Adjusted R^2 of 0.9974. Adeq Precision measures the signal to noise ratio. If the value of ratio is more than 4, however, it is desirable. Adeq Precision of 10.2937 specifies an acceptable signal to noise ratio. Due to these causes, this model can be utilized to optimize this response.

Table 4.3 Study of variances for energy consumption

Sources	**Sum of Square**	**DOF**	**Mean of Square**	**F-value**	**p-value**	
Model	14.00	4.0	3.50	8.18	0.0002	significant
A-Temperature	9.64	1.0	9.64	22.52	< 0.0001	
B-Water Flow Rate	0.3907	1.0	0.3907	0.9124	0.3486	
C-Geometry of the Product	3.96	1.0	3.96	9.24	0.0055	
D-Mass of product	0.0131	1.0	0.0131	0.0305	0.8627	
Residual	10.71	25	0.4283			
Lack of Fit	8.78	20	0.4390	1.14	0.4862	not significant
Pure Error	1.93	5.0	0.3853			
Cor Total	24.71	29				
Predicted	**R^2**	**Adjusted**	**R^2**	**Adeq**		**Precision**
0.9530		0.9974		10.2937		

The Box-Cox plot also accepted the consistent predictability of the model; later transformation to lambda is 1 for the response completed. The style documented in Fig 4.7 makes it comprehensible that the advanced model can precisely predict the investigational data. Figures 4.8(a) and 4.8(b) show the relationship of the objective function vs. the control factors. Fit summary of Response 2: energy consumption is presented in Table 4.4.

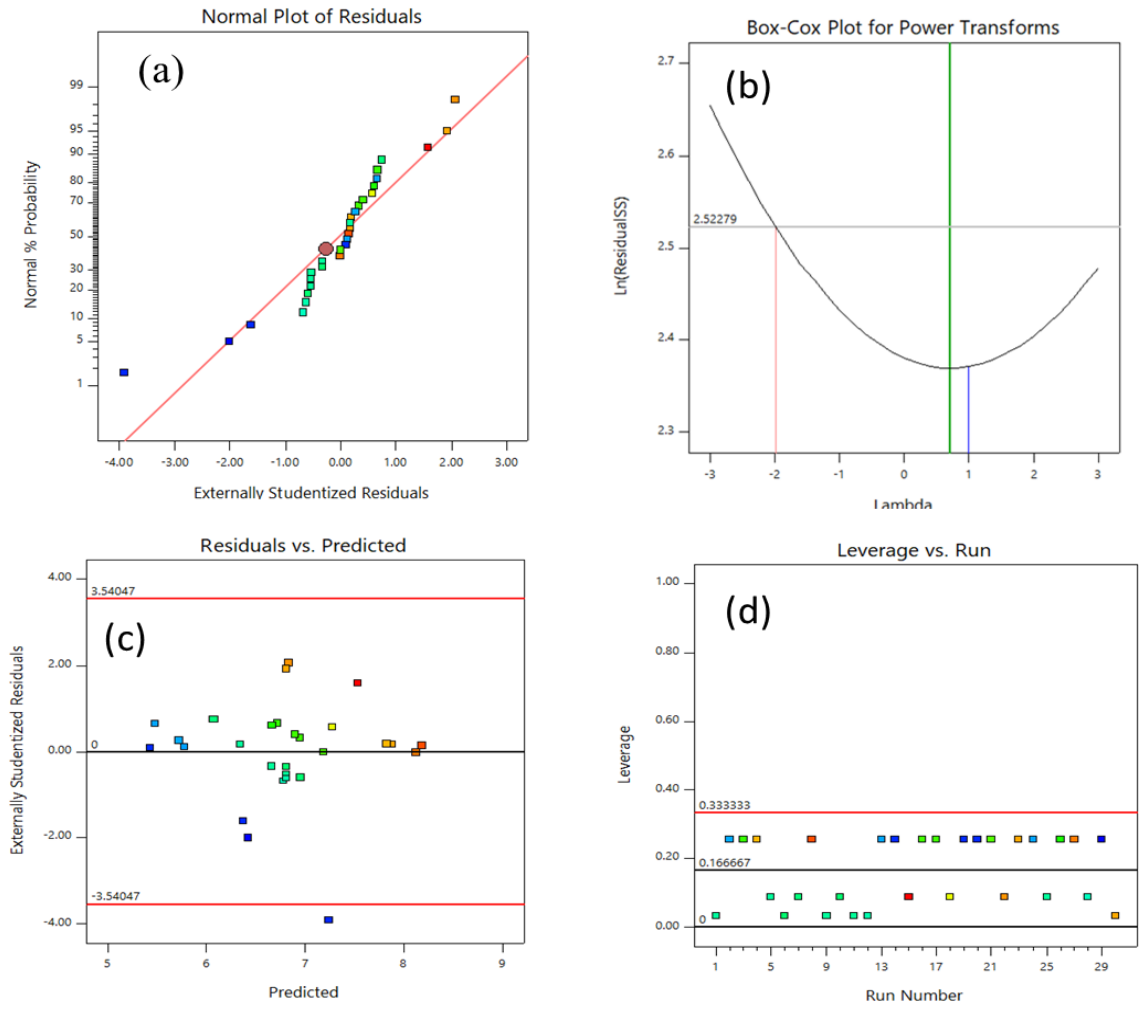

Fig 4.7 (a) Relationship of Normal probability curve vs. extremely studentized residuals (b) Box-Cox curve for power transforms (c) Relationship between residuals and predicted response (d) Relationship between residuals and run no.

The coded equation for EC can be written in the following form:

$$\text{Energy Consumption} = 6.80 - 0.732 * A + 0.1473 * B - 0.4688 * C - 0.269 * D \quad (4.2)$$

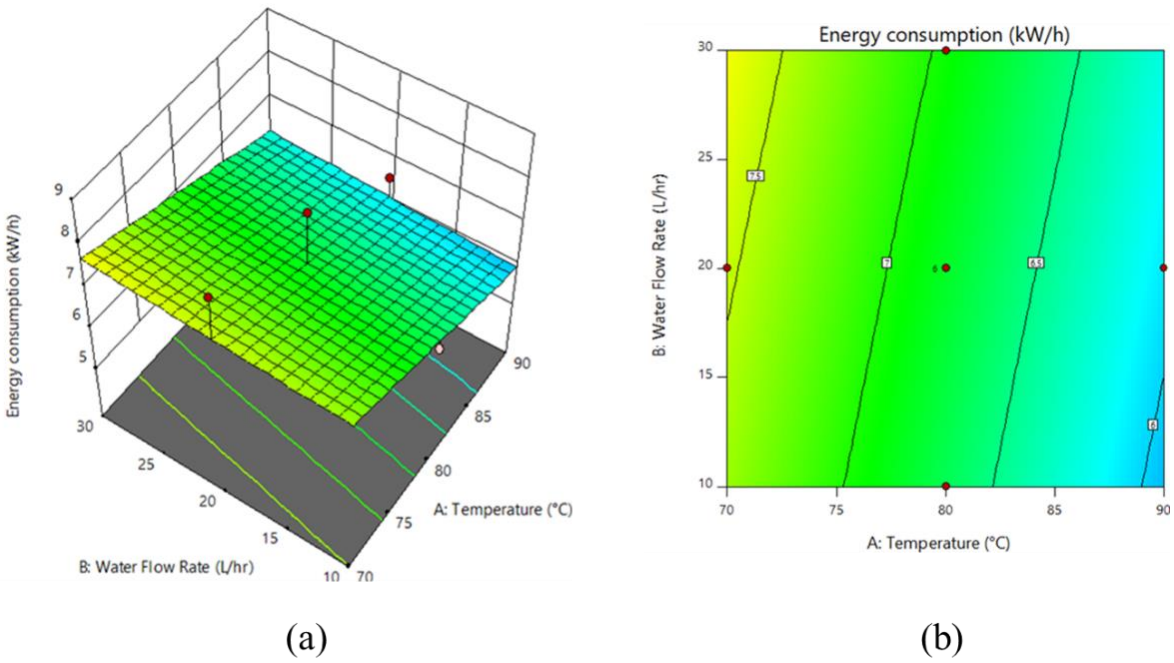

(a) (b)

Fig 4.8 Objective functions vs. the control parameters relationship

Table 4.4 Fit Summary of Response 2: Energy consumption

Source	Sequential p-value	Lack of Fit p-value	Adjusted R^2	Predicted R^2	
Linear	**0.0002**	**0.4862**	**0.4974**	**0.3530**	**Suggested**
2FI	0.0995	0.6412	0.6034	0.3739	
Quadratic	0.4759	0.6222	0.5969	0.2114	
Cubic	0.5773	0.4828	0.5678	-2.6891	Aliased

4.2.5 Shrinkage

Study of variance for shrinkage is shown in Table 4.5. Model F value is 0.7301which indicates that model is not significant. Model P value is 0.7295, which indicates the suitability of model. A, B, C, and D, are the most significant model terms in present study.

Analytical curves such as NPPP, Box-Cox plot, internally and externally studentized residual plots have been exposed in Fig 4.9 from the experimental data. The Box-Cox plot also accepted the consistent predictability of the model; later transformation to

lambda is 1 for the response completed. The style documented in Fig 4.9 makes it comprehensible that the advanced model can precisely predict the investigational data. Fig 4.10 shows the relationship of the objective function vs. the control factors. Fit summary of Response 3: shrinkage is presented in Table 4.6.

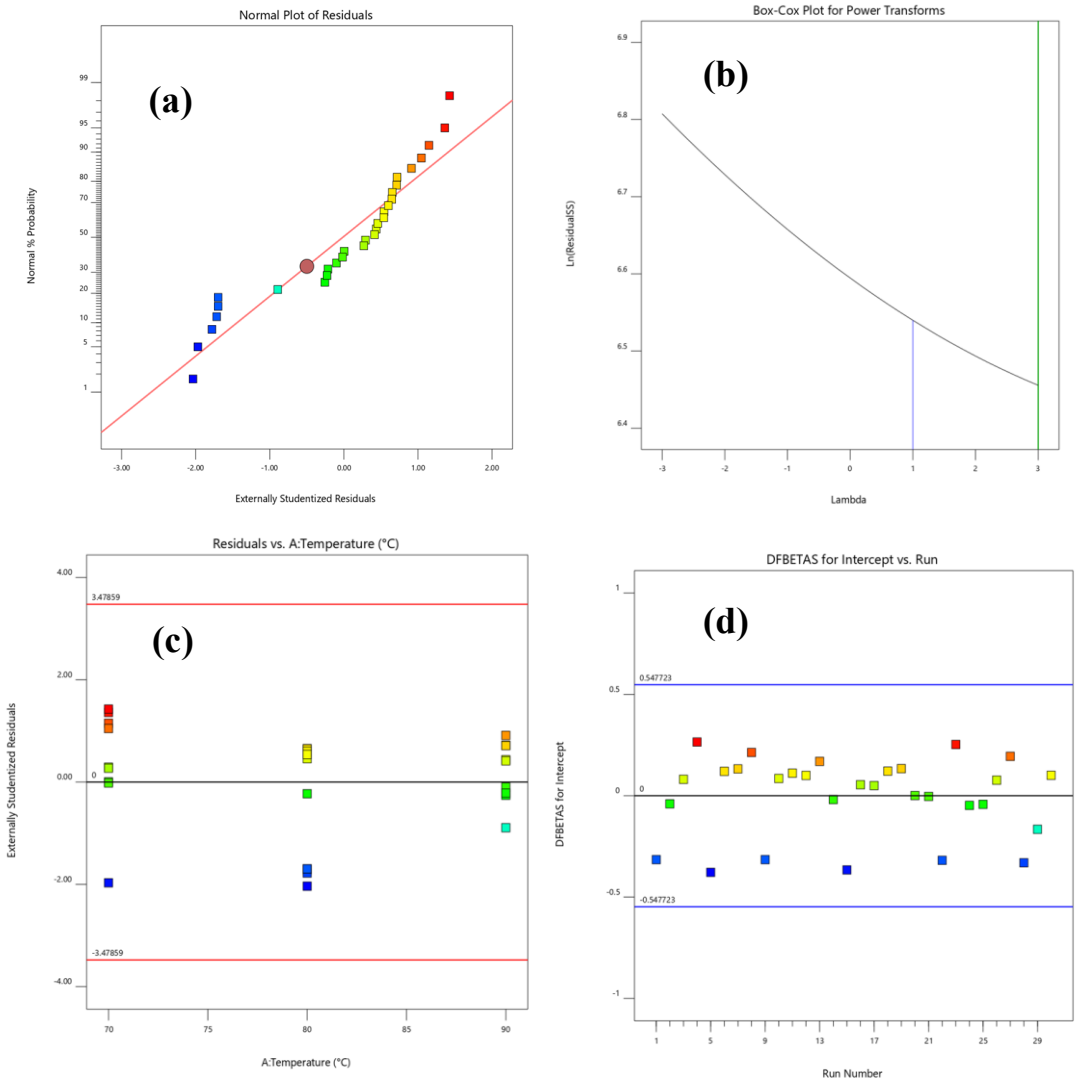

Fig 4.9 (a) Relationship of Normal probability curve vs. extremely studentized residuals(b) Box-Cox curve for power transforms (c) Relationship between residuals and predicted response (d) Relationship between residuals and run no.

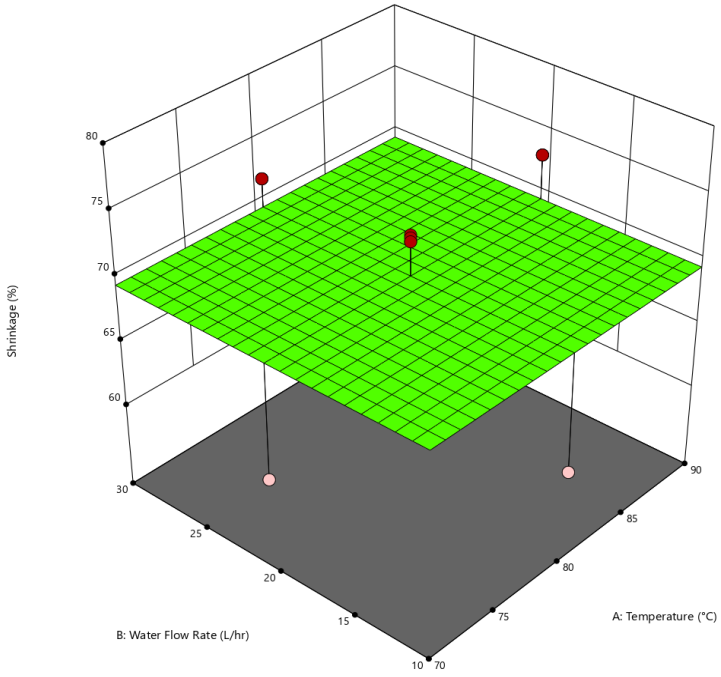

Fig 4.10 Objective functions vs. the control parameters relationship

Table 4.5 Study of variances for shrinkage

Source	**Sum of Squares**	**DOF**	**Mean Square**	**F-value**	**p-value**	
Model	0.0000	0				
Residual	692.19	29	23.87			
Lack of Fit	538.52	24	22.44	0.7301	0.7295	not significant
Pure Error	153.67	5	30.73			
Cor Total	692.19	29				

Table 4.6 Fit Summary of Response 3: shrinkage

Source	**Sequential p-value**	**Lack of Fit p-value**	**Adjusted R^2**	**Predicted R^2**	
Mean	**< 0.0001**				**Suggested**
Linear	0.9091	0.6552	-0.1160	-0.2853	
2FI	0.8748	0.5367	-0.3065	-0.9526	
Quadratic	0.1860	0.6391	-0.1229	-0.8801	
		0.4979	-0.2156	-7.9746	**Aliased**

4.2.6 Optimal condition

Out of 30 solutions created via software, one is taken as an optimal solution at maximum drying. Red-colored points indicate the optimal conditions (temperature, water flow rate, geometry of product, and mass of product), the maximum moisture content removed energy consumption, and the shrinkage factor indicated by the blue dot in Fig 4.11(a). Desirability of solution is close to 1 (0.959), as presented in Figure 4.11(b). Table 4.7 indicates the desired value for all dependent and independent factors due to optimization utilizing desirability function.

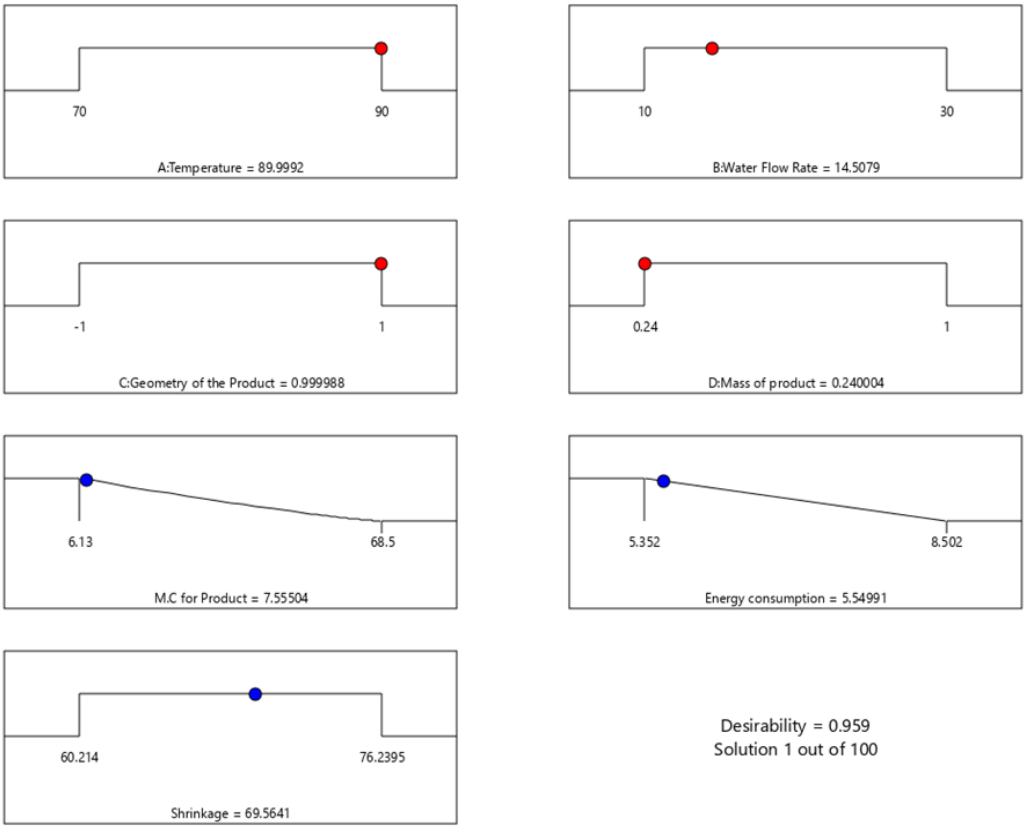

(a)

Fig 4.11(a) Optimal operating conditions

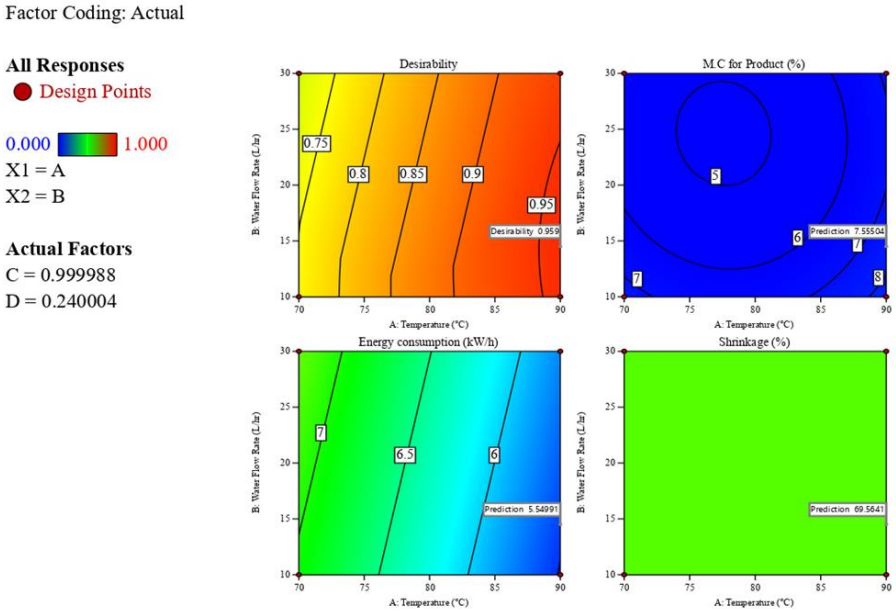

(b)

Fig 4.11 (b) Contour plot of desirability of solutions

Table 4.7 Selection of optimal point in the desirability region

	T (°C)	Water flow rate (Ltr/h)	Geometry	Mass (kg)	Moisture Content (%)	Energy consumption (kW/h)	Shrinkage (%)	Desirability
RSM Prediction	89.99	14	Circular	0.2400	7.55	5.54	69.54	0.959
Experimental					7.32	5.66	68.57	-
Error (%)	-	-	-	-	3.14	2.16	1.41	-

4.3 Thermodynamics analysis of heat exchanger-evacuated tube assisted drying system at different water flow rates (10, 20, 30 Ltr/h)

4.3.1 Experimental investigation without load condition

Performance analysis of HE-ETADS without load condition is directly proportional to the temperature attained inside the drying cabin under different ambient parameters (solar intensity, RH, and atmospheric temperature).Figs. 4.12(a),4.12(b), and 4.12(c)

show, solar intensity, RH, air temperature, and drying cabin temperature varied from 506 to 947 W/m^2, 37–49%, 25–33.63℃, and 42–79.12℃ individually at 10 Ltr/h water flow water and 408–970 W/m2, 49–56%, 25–29℃ and 39–76.2℃ respectively at 20 Ltr/h water flow rate. Likewise, the solar intensity, RH, air temperature, and cabin temperature varied from 444 to 990 W/m^2, 44–52%, 27–32℃ and 45–79.56℃ at 30 Ltr/h water flow rate.

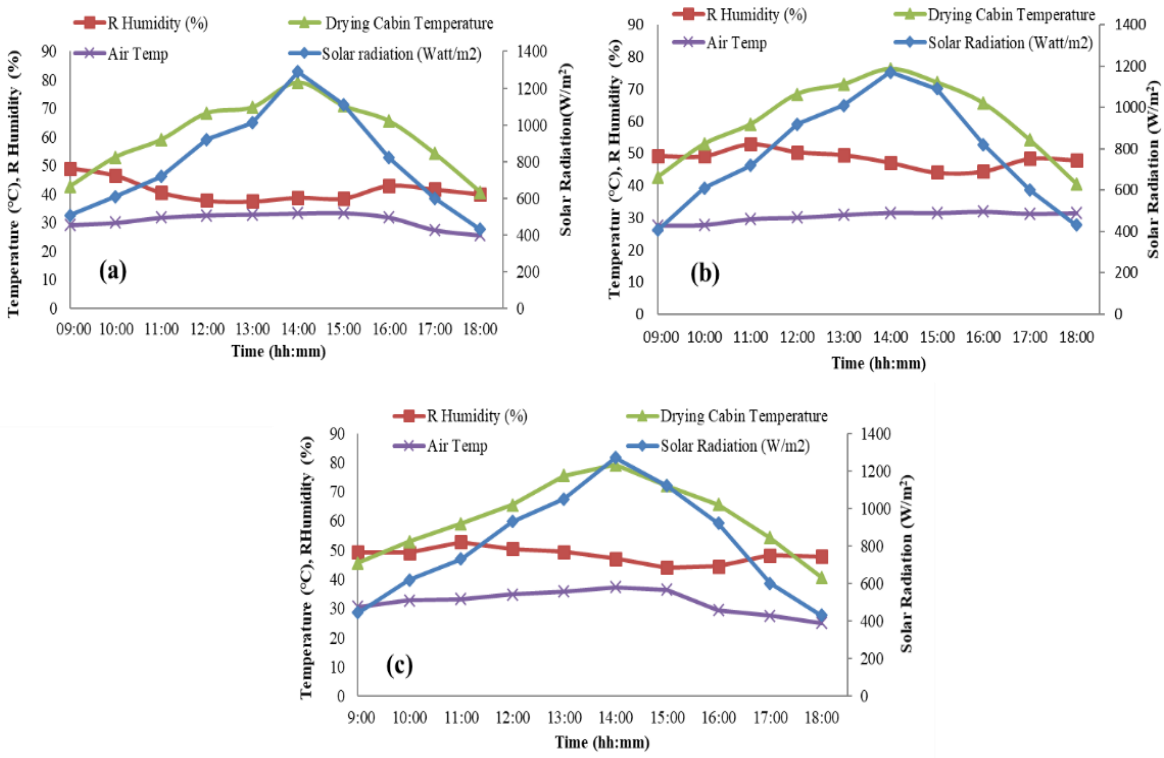

Fig 4.12 Experimental investigation without load conditions under different water flow rates (a) 10 Ltr/h, (b) 20 Ltr/h, (c) 30 Ltr/h

4.3.2 Thermal performance with full load condition

4.3.2.1 Mass of moisture removed through a drying process

Fig 4.13 shows variations in the moisture content at various water flow rates and solar intensity throughout the experimental work. The initial mass of moisture of garlic is

70% decreased by 21.33%, 13.25%, and 11.41% at 10 Ltr/h, 20 Ltr/h, and 30 Ltr/h water flow rate simultaneously in 9 hours. In the beginning, for 4 h, moisture content of product 70% decreased by 37.25%, 33.16%, and 31.21% at all experiment set.

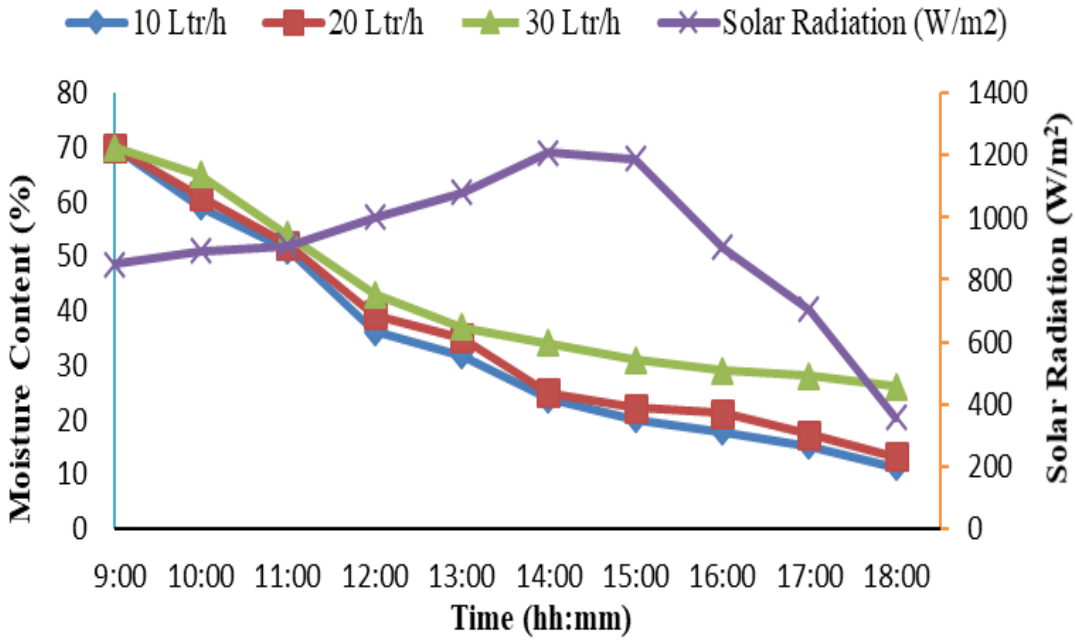

Fig 4.13 Moisture content Vs Time of the day for garlic at various water flow rates

4.3.2.2 Drying rate (DR) of garlic

Variation in DR at different water flow rates is shown in Fig 4.14. Drying rates 0.55, 0.63, and 0.65kgH_2O/kg dry solid/h are computed at water flow rates of 10 Ltr/h, 20 Ltr/h, and 30 Ltr/h, respectively. Drying rate increased up to 13:00 h and observed 0.98, 1.18, and 1.48 kgH_2O/kg dry solid/h at 10 Ltr/h, 20 Ltr/h, and 30 Ltr/h water flow rate then decreased continuously. DR was observed as 0.55, 0.63, and 0.65kgH_2O/kg dry solid/h at 10 Ltr/h, 20 Ltr/h, and 30 Ltr/h water flow rate at the end of the experiment.

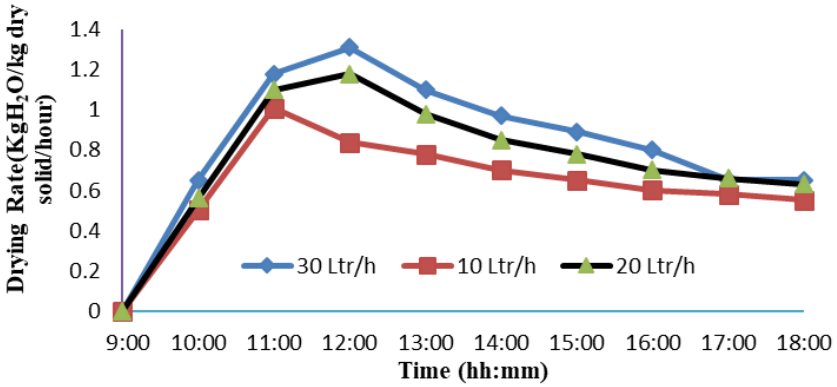

Fig 4.14 Drying rate Vs. Time of the day for garlic

4.3.2.3 Moisture ratio of garlic

Variation in moisture ratio with respect to time of the day at different water flow rate (10 Ltr/ h, 20 Ltr/h, and 30 Ltr/h) was revealed in Fig 4.15. In this investigation, the curve trend is found same at all different water flow rates. Highest moisture ratio 0.07 at a 30 Ltr/h water flow rate was obtained. In the first 3h, garlic moisture ratio deceased 1 to 0.6, 0.55, and 0.42 at all experiment sets.

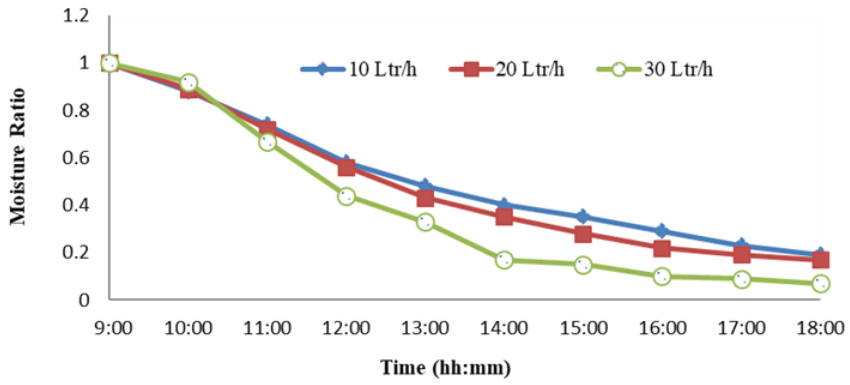

Fig 4.15 Moisture ratio Vs Time of the day for garlic at various water flow rate

4.3.2.4 Equilibrium moisture content of garlic

Relative humidity (RH) and temperature both are the main operating factors in Eq.17. Relative humidity and temperature are in the range of 14-19.8% and 35.1-45.89℃, 11.2-18.1and 36.51-52.43℃, and 10.5-18.2% and 38.66-56.72℃ for various water flow rate i.e. 10 Ltr/h, 20 Ltr/h, and 30 Ltr/h correspondingly in Fig 4.16(a). Relationship of EMC Vs. time of the day at various water flow rates i.e. 10 Ltr/h, 20 Ltr/h, and 30 Ltr/h are revealed in Fig 4.16(b). The curve trend was almost similar at all water flow rates. Equilibrium moisture content (EMC) of garlic sample is calculated using Eq.17. Equilibrium moisture content for garlic sample has been found in the range of 0.49-2.5%,0.40-2.5%, and 0.37-2.5% for various water flow rate i.e. 10 Ltr/h, 20 Ltr/h, and 30 Ltr/h correspondingly. Fresh and dehydrated garlic cloves are shown in Fig 4.17.

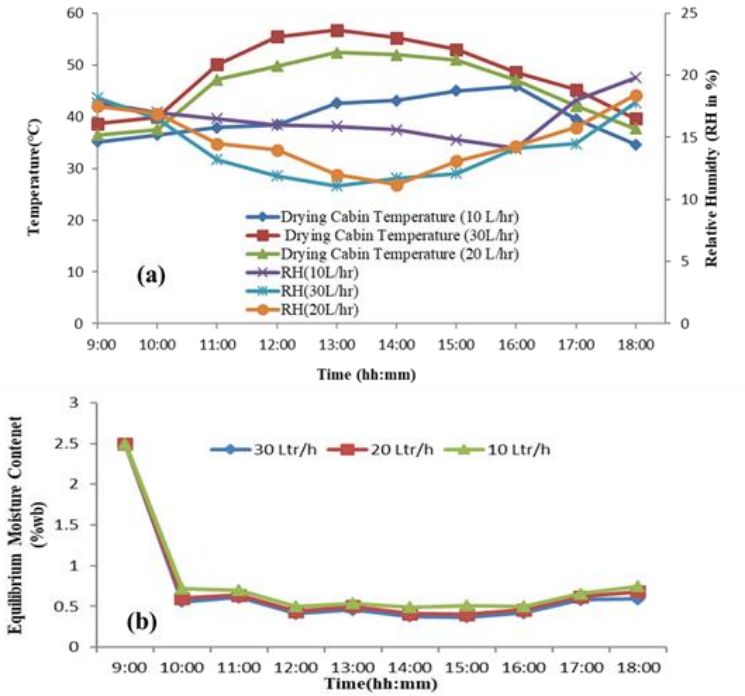

Fig 4.16(a) Relationship of RH and Temperature, (b)Equilibrium moisture content of garlic sample

(A)Fresh Garlic Sample (B) Dehydrate Garlic in HE-ETADS (C) Dehydrate Garlic in OSD

Fig 4.17 Fresh and dried product

4.3.2.5 Efficiency of ETSC

Thermal efficiency of solar collector plays a significant role in the drying system performance. Variation of collector efficiency at different water flow rates with the drying period is revealed in Fig 4.18. In the beginning, the efficiency is recorded 15.6%, 17.32%, and 18.98% at 10 Ltr/h, 20 Ltr/h, and 30 Ltr/h water flow rates respectively. A similar trend in efficiency variation at 10 Ltr/h., 20 Ltr/h and 30 Ltr/h are observed.

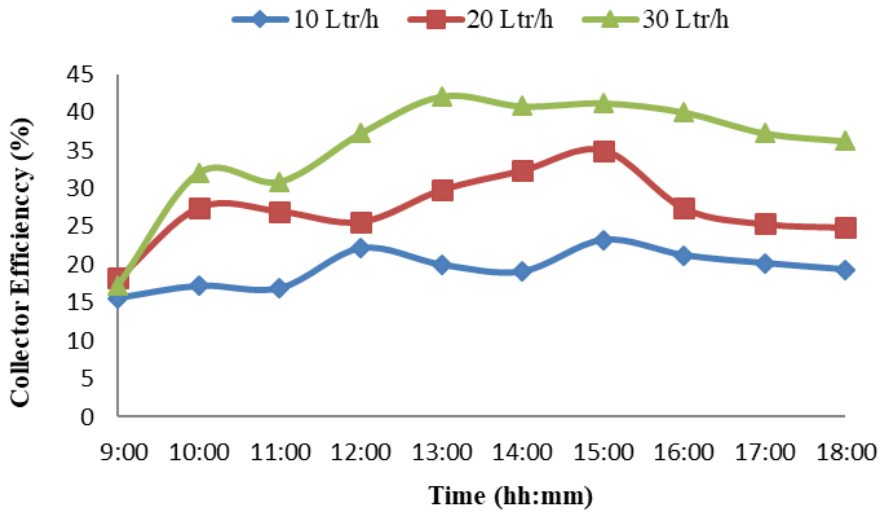

Fig 4.18 Solar collector efficiency Vs time of the day for garlic at various water flow rates

4.3.2.6 Drying system efficiency

Variations of drying system efficiency for the drying hours at water flow rates (10 Ltr/h, 20 Ltr/h, and 30 Ltr/h) are shown in Fig 4.19. Thermal efficiency 25.1%, 31.2%, and 29.1% at 10 Ltr/h, 20 Ltr/h, and 30 Ltr/h water flow rate are estimated at 9h. Maximum efficiency 55.28% at 30 Ltr/h water flow rate with solar radiations 992W/m^2 is observed. Minimum efficiency 20%, 12%, and 26% at all water flow rate throughout the process due to the beginning of decreasing the solar radiation at 14:00 h. Drying system efficiency, ETSC efficiency and overall thermal efficiency of developed HE-ETADS and earlier ETC based solar drying systems are compared in Table 4.8.

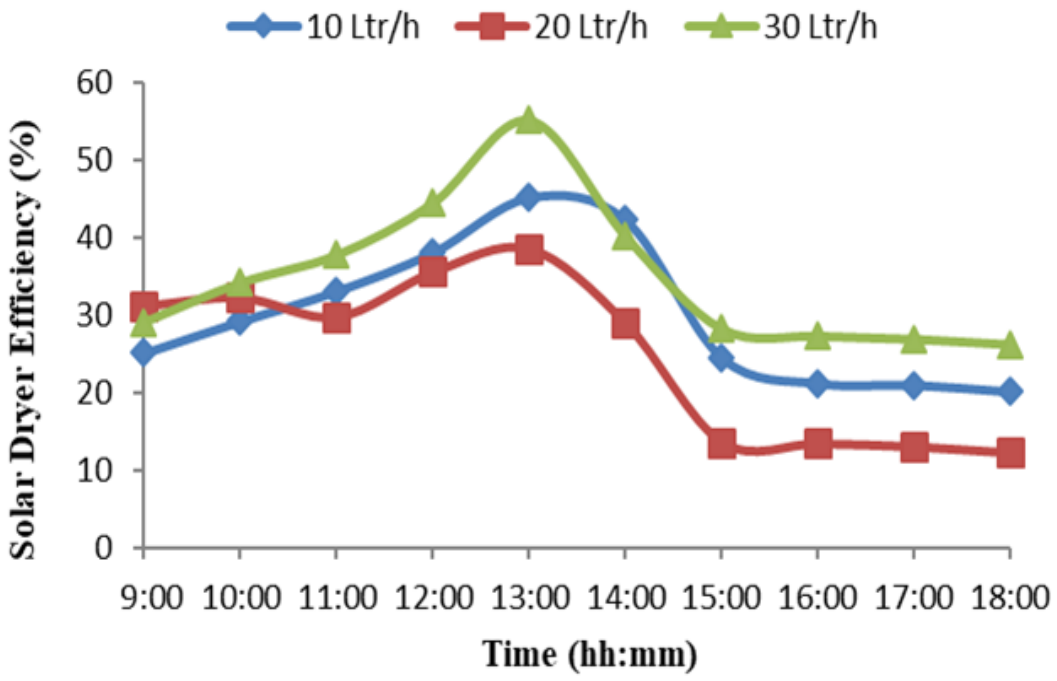

Fig 4.19 Drying system efficiency Vs Time of the day for garlic at various water flow rates

Table 4.8 Comparison of thermal performance in terms of drying system efficiency

Types of drying system (SD)	Drying system efficiency	ETSC efficiency	Electrical efficiency	Overall thermal efficiency	Years
ETC (Air as heat transfer fluid)	25.28%	30.25%	-	37.76%	2013
ETC (Air as heat transfer fluid)	27.69%	28.44%	-	39.065%	2018
ETC (Air as heat transfer fluid)	42.17%	32.15%	-	37.16%	2017
Using PCM in drying system	53.64%	-	-	48.98%	2018
ETC (Air as heat transfer fluid)	54.25%	42.36%	-	-	2021
Hybrid electric solar dryer	43.25%	-	18.65%	-	2021
ETSC (Water as heat transfer fluid)	55.28%	43.62%	-	-	-

4.3.2.7 Investigation of exergy

Variation of exergy inflow, exergy outflow, exergy loss, and energy efficiency at water flow rates (10 Ltr/h, 20 Ltr/h, and 30 Ltr/h.) are displayed in Figs 4.20(a), 4.20(b), and 4.20(c) correspondingly. A higher value of exergy inflow is obtained 13.01W, 33.23W, and 44.34 W at different water flow rates (10 Ltr/h, 20 Ltr/h, and 30 Ltr/h) respectively throughout experimental periods. Exergy inflow varied from 7.88 – 13.01W, 12.33 – 33.23W, and 8.33 – 44.34W at 10 Ltr/h, 20 Ltr/h, and 30 Ltr/h water flow rate. Average exergy data and EE are listed in Table 4.9.

Table 4.9 Exergy and energy efficiency

Water flow rate (Ltr/h)	Exergy inflow (W)	Exergy outflow (W)	Exergy loss (W)	Exergy efficiency (EE, %)
10 Ltr/h.	8.97	4.88	4.58	50.33
20 Ltr/h.	24.93	13.87	9.89	54.44
30 Ltr/h.	26.01	15.02	10.25	57.64

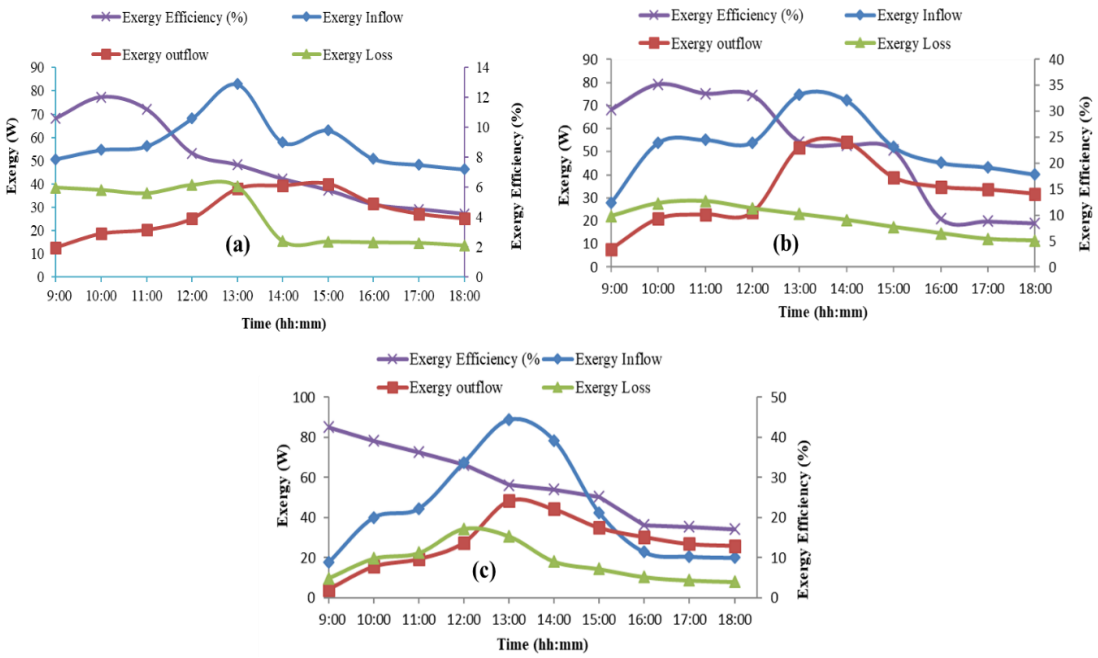

Fig 4.20 Exergy value and EE Vs Time of the day for garlic at (a) 10 Ltr/h water flow rate, (b)at 20 Ltr/h water flow rate, (c) at 30 Ltr/h water flow rate

4.4 Evaluation of drying kinetics, quality assessment, and heat and mass transfer

4.4.1 Temperature profile under unload condition

Evaluation of thermal profile of a different drying system plays an important role in confirming that the desired temperature was attained and in selecting the food items to be dried. The temperature profile of drying systems (HE-ETADS and GHSD) under unload is shown in Fig 4.21. It was observed that the variation of solar insolation, atmospheric temperature, humidity, and drying cabin temperature (HE-ETADS and GHSD) were in the range of 280-992W/m^2, 28-38.5℃, 41.2-43.8%, 38-72℃, 36-58.5℃ respectively under the unload condition. Solar insolation has a significant role in attaining the maximum temperature inside drying cabin; as the solar insolation increased (from 9 to 14h) drying cabin temperature also increased. Higher ambient and drying cabin temperature (HE-ETADS and GHSD) were noted as 38± 0.28℃, 72 ±

0.35℃, 58.5 ± 0.50℃ at maximum solar intensity of 968 ± 6.52 W/m^2 at 14h. The results varied due to atmospheric temperature fluctuations and solar radiation. Current outcomes support the idea that temperature range reached is safe for dehydrating food stuff product without affecting their nutritious content. In a low cost solar drying system, solar radiation, drying cabin temperature, and air temperature varied between 210-980W/m^2, 36–63℃, and 20-27℃, respectively [97]. Using heat pipe in a solar dryer based on ETSC improves thermal performance, consistent with previous research on improving performance by employing perforated baffles on both sides of flat plate collector [98].

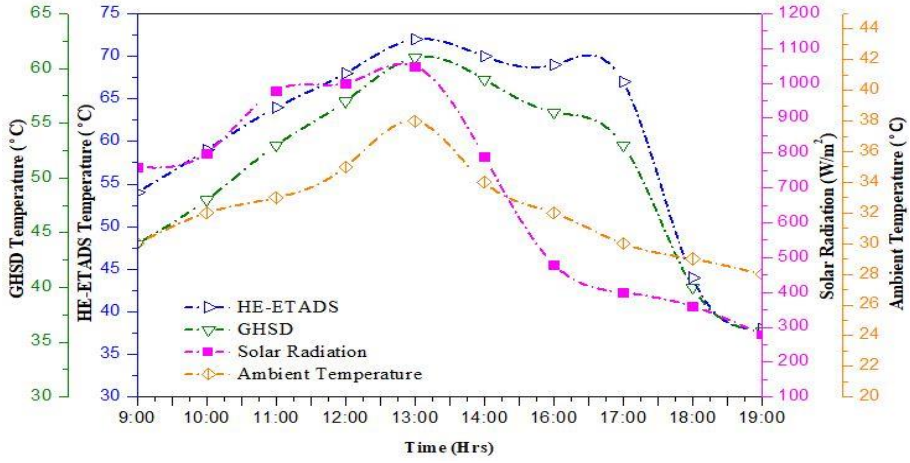

Fig 4.21 Thermal profile of drying- systems under unload condition

4.4.2 Temperature profile of HE-ETADS, GHSD, and open sun drying of banana slices

Fig 4.22 indicates ambient temperature and drying cabin temperature of drying systems (HE-ETADS and GHSD) during dehydrating banana slices. The maximum temperature was obtained as 65℃ and 58℃ for HE-ETADS and GHSD at solar radiation of 1070 ± 6.58W/m^2 for the duration of mid-noon and later, it reduces with

drying period. During the open sun drying (OSD) of banana slices, maximum air temperature was observed 40℃ at solar radiation of 970 ± 6.58W/m^2. The fluctuation of solar radiation in the range of 290-972± 6.58W/m^2 was also recorded. Average drying cabin temperature of HE-ETADS, GHSD and the surrounding air temperature in OSD was noted as 57.10℃, 51℃, and 33.65℃, respectively. Maximum and average temperature gradients for HE-ETADS and GHSD were evaluated as 29.5℃, 21.87℃, and 26.85℃, 19.85℃ respectively. Temperature gradient may be defined as a temperature difference or the rate of change with respect to drying period. The maximum surface temperature of banana slices was recorded as 52.7℃, 50.8℃, and 39.8℃ in HE-ETADS, GHSD, and OSD, as shown in Fig 4.23. The experimental results show that maximum and average temperature gradients were retained in HE-ETADS and GHSD compared to OSD. The variation of solar radiation and drying cabin temperature was recorded as 210–920W/m^2 and 34–49℃. It was also observed that average, maximum solar radiation, and drying cabin temperature 710W/m^2, 980 W/m^2, and 41℃ and 49 ℃, respectively [97].

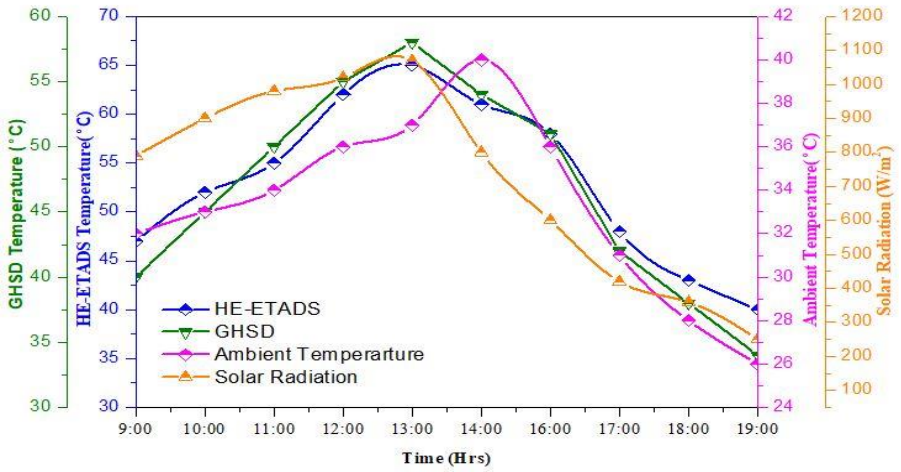

Fig 4.22 Thermal profile of drying systems under loaded condition at constant mass of 5kg banana slices

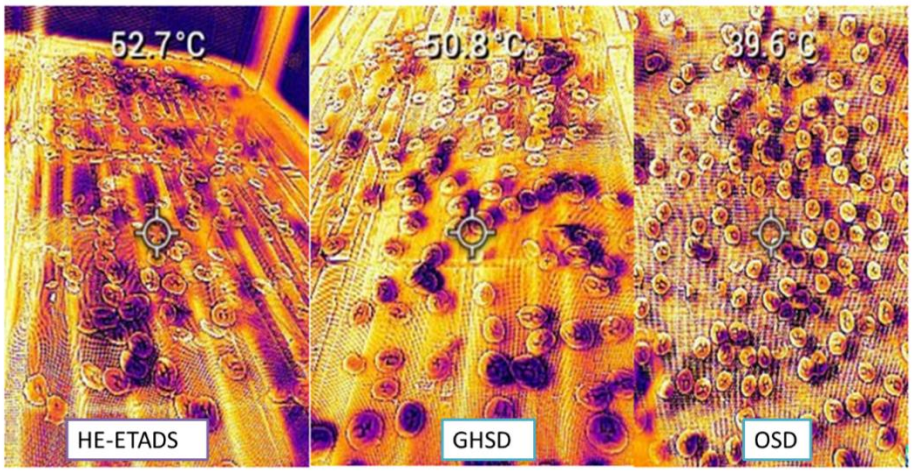

Fig 4.23 Surface temperature of banana slices

4.4.3 Moisture ratio (MR)

The variation of MR with drying hour in HE-ETADS, GHSD and OSD is presented in Fig 4.24. The trend of MR in all three drying processes with in the same manner. Final MR of 0.040, 0.049 and 0.055 was found in HE-ETADS, GHSD, and OSD, after 6 h, 8h, and 9h of drying, respectively. Same trends of reducing moisture ratio were described in various previous studies of food drying [99]-[100].

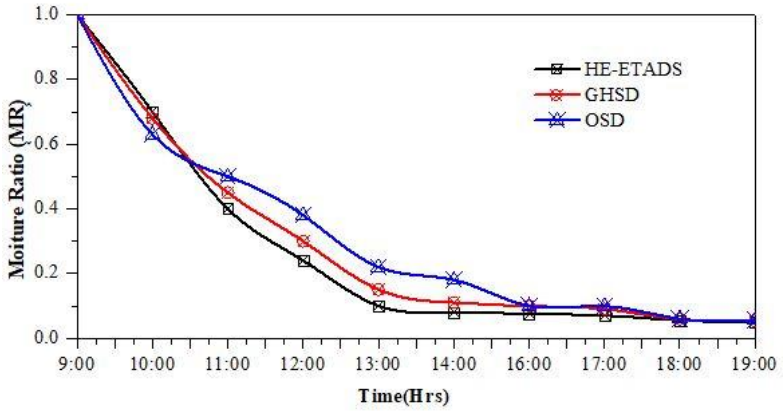

Fig 4.24 Drying curve for banana slices in HE-ETADS, GHSD, and OSD at constant mass of 5kg

4.4.4 Drying kinetics

Different thin layer models were mostly used to compute and predict drying behavior in term of drying kinetics of foods. Ten thin-layer drying kinetics models were fitted according to the MR of banana slices in all three drying systems (HE-ETADS, GHSD, and OSD). Their best fit and coefficient are illustrated in Table 4.10. All models were fitted with valid goodness of fits. It found that coefficient of determination (R^2) for all semi-empirical models was greater than 0.98, except for the Henderson model (HM) for OSD technique. Among ten fitted models discussed in Table 4.10, the Weibull model (WM) with higher R^2 (0.9927, 0.9968, and 0.99625) and lower χ^2 (0.00059381, 0.00027652, and 0.00050323) and RMSE (0.0219, 0.01487, and 0.01831) were obtained best fit to determine drying kinetics of banana slices in HE-ETADS, GHSD, and OSD respectively. Present findings align with the previous results of [32, 37], who identified that Weibull model (WM) best fit in drying kinetics modelling of garlic clove and beetroot slices, respectively. The relationship between experimental and predicted values of moisture ratio is demonstrated in Figs 4.25-4.27 with higher R^2.

Table 4.10 Coefficient of determination (R^2), Chi-square (χ^2) and RMSE for different models

Model	Methods	R^2	χ^2	RMSE
Two term	HE-ETADS	0.996681939	0.000322787	0.015384065
	GHSD	0.992486824	0.000676156	0.022519254
	OSD	0.996125636	0.000627882	0.018676815
Wang and Singh	HE-ETADS	0.874557429	0.014075746	0.110978727
	GHSD	0.880326735	0.014277783	0.111238834
	OSD	0.915147132	0.012365041	0.098067597
Weibull	**HE-ETADS**	**0.992771182**	**0.000593812**	**0.021965216**
	GHSD	**0.996870301**	**0.000276521**	**0.014873326**
	OSD	**0.996258377**	**0.000503235**	**0.018316411**
Prakash and Kumar	HE-ETADS	0.995584821	0.000511396	0.019943732
	GHSD	0.995468087	0.000372515	0.017967937

	OSD	0.990288127	0.000747097	0.025567744
	HE-ETADS	0.990501491	0.000863468	0.025447882
Midili-Kucuk	GHSD	0.995325508	0.000450483	0.018175649
	OSD	0.99323784	0.001165873	0.025450088
	HE-ETADS	0.988656824	0.001261918	0.013080809
Lewis	GHSD	0.986641225	0.001151563	0.032784017
	OSD	0.975218688	0.002124832	0.044632166
	HE-ETADS	0.995584821	0.000511396	0.019943732
Page	GHSD	0.995468087	0.000372515	0.017967937
	OSD	0.990288127	0.000747097	0.041976881
	HE-ETADS	0.988703124	0.001374784	0.032699741
Henderson	GHSD	0.987045298	0.001126807	0.031250063
	OSD	0.975109501	0.002013781	0.025567744
Modified	HE-ETADS	0.996119501	0.001048097	0.018693227
Henderson	GHSD	0.996684358	0.000394077	0.015376802
and pabis	OSD	0.992486889	0.000811387	0.225192561
	HE-ETADS	0.990288127	0.000345632	0.025567744
Verma et al.	GHSD	0.993689742	0.000321457	0.017967937
	OSD	0.985231478	0.007852134	0.018175643

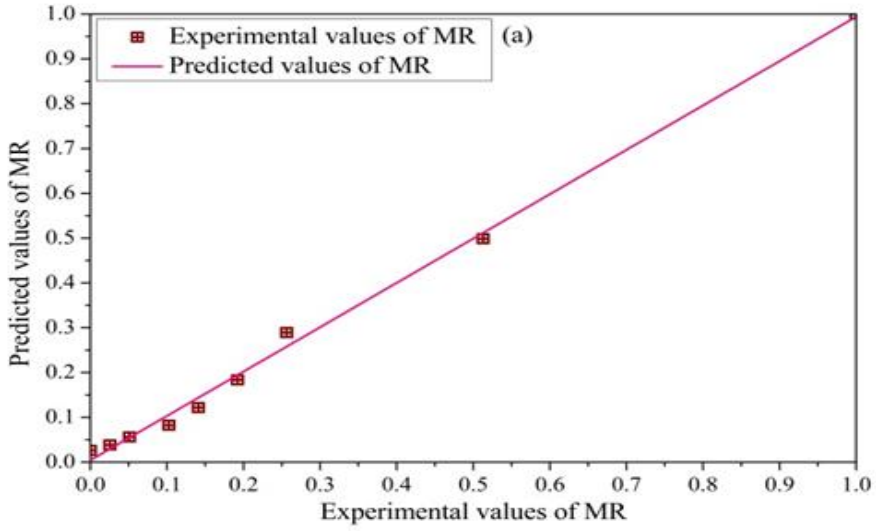

Fig 4.25 Relationship between experimental and predicted values of moisture ratio for HE-ETADS using WM at constant mass of 5kg banana slices

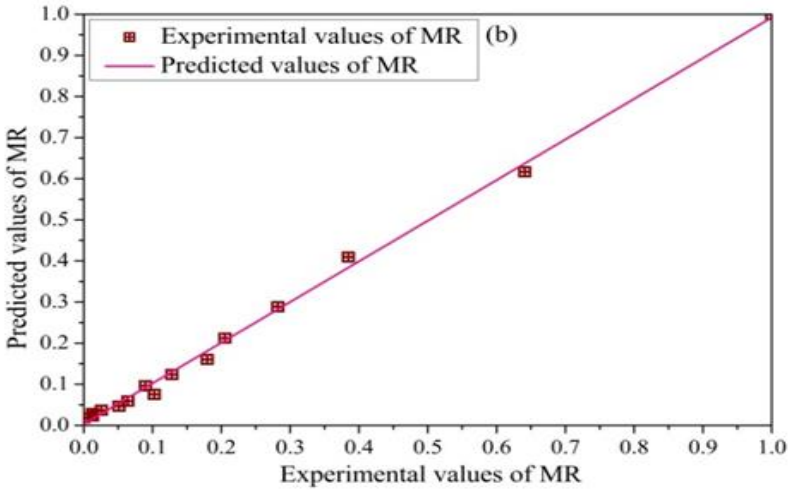

Fig 4.26 Relationship between experimental and predicted values of moisture ratio for GHSD using WM at constant mass of 5kg banana slices

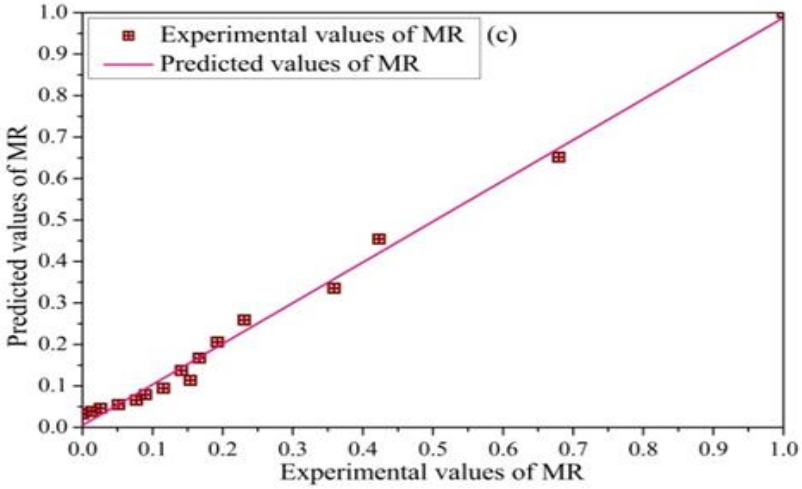

Fig 4.27 Relationship between experimental and predicted values of moisture ratio for OSD using WM at constant mass of 5kg banana slices

4.4.5 Analysis of Moisture Content and Drying Rate

Moisture content of banana slices varied throughout the drying in all three drying systems (HE-ETADS, GHSD, and OSD) as revealed in Fig 4.28. Moisture content reduced from initial (78%) to final 23.2, 25.6, and 28.8% in HE-ETADS, GHSD, and OSD respectively. Moisture content reduced to 2.4 ± 2.0% (wb) and 5.6 ± 2.0% (wb)

more in HE-ETADS than GHSD and open sun drying in the same drying period. Hence, moisture removal rate in terms of moisture content was greater in HE-ETADS compared to the other two drying systems. It also reduced the drying period of food materials due to higher temperature attained in drying cabin, and such advantage of HE-ETADS makes it more significant. While the moisture removal rate from inside of food material to the upper surface by diffusion mechanism helps to increase the difference in vapour pressure between drying air by virtue of which greater moisture evaporation occurred in HE-ETADS. The present study results align with previous investigations that reported that garlic cloves were dehydrated from 70% to 21.33%, 13.25%, and 11.41% at 10, 20 and 30Ltr/h in same drying system [82].

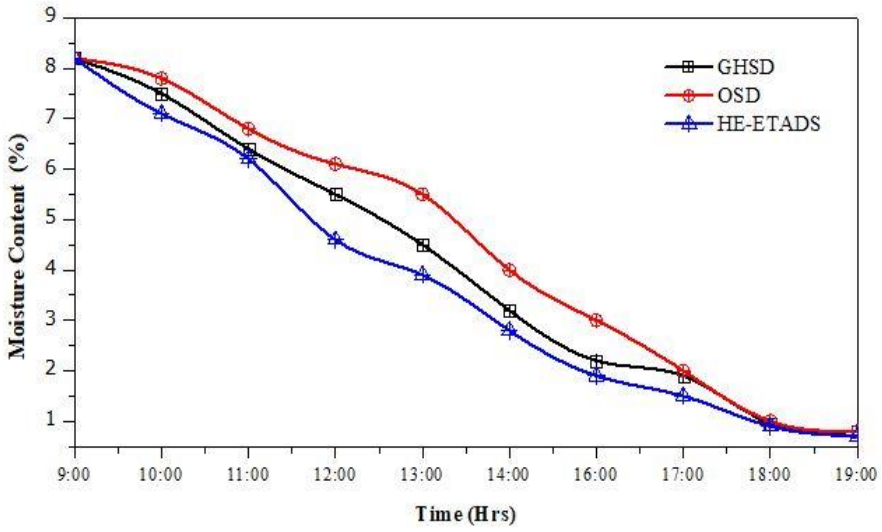

Fig 4.28 Drying curves for banana slices in HE-ETADS, GHSD, and OSD at constant mass of 5kg banana slice

Variations in DR of banana slices in all three drying systems (HE-ETADS, GHSD, and OSD) are illustrated in Fig 4.29. Solar radiation plays a significant role in drying of food products. It was observed that DR increased in the beginning with the increase in solar radiation for the first 3 hours during the drying process; subsequently, it

reduced with drying period. Highest DR of banana slices was recorded as 16.25g H_2O/g solid.h at 12h, 14.36g H_2O/g solid.h at 12:30h, and 12.76g H_2O/g solid.h at 13:00h in all three drying systems (HE-ETADS, GHSD, and OSD). Average DR was found to be 7.89g water/g solid.h, 7.65g water/g solid.h, and 7.25g water/g solid.h in HE-ETADS, GHSD, and OSD, respectively.

Maximum DR was obtained in HE-ETADS at the beginning of drying process because of maximum air temperature attained, which conveys maximum moisture diffusivity by virtue of which faster moisture removal rate is achieved from the surface of food product. From the Fig 14, it was also observed that DR continuously reduced after 12h. Current outcomes directly correlated with previous research work in which DR of garlic clove was reported as 0.55, 0.63, and 0.65kgH_2O/kg dry solid/h at different water flow rates in same drying system [82].

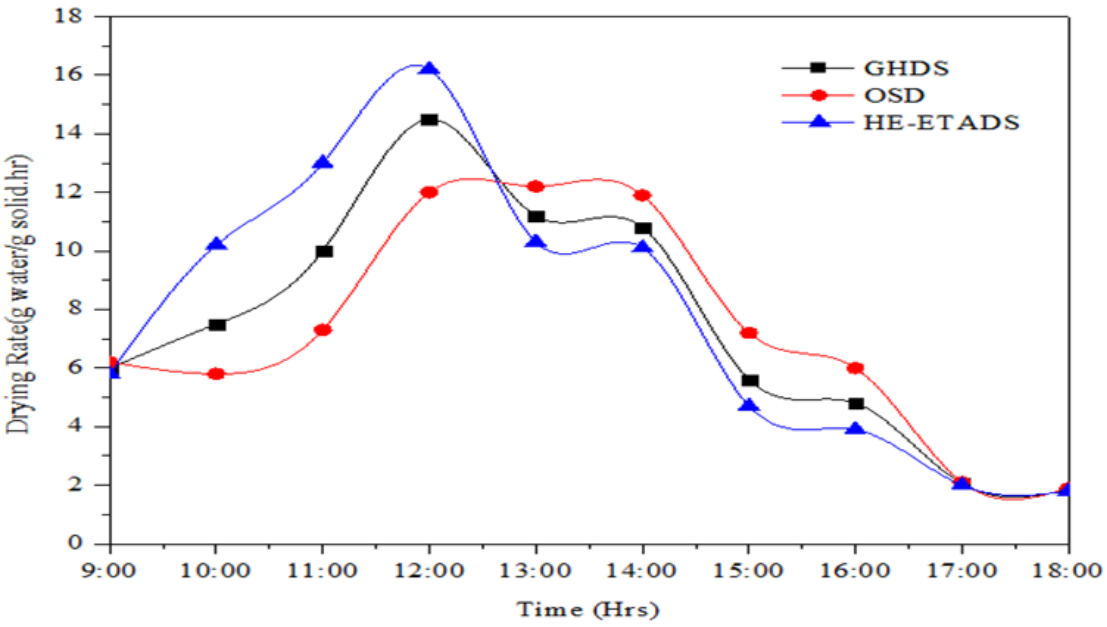

Fig 4.29 Drying rate (DR) curves for banana slices in HE-ETADS, GHSD, and OSD at constant mass of 5kg

4.4.6 Quality assessment of dried banana slices

Various kinds of quality factors are graphically demonstrated in Figs 4.30-4.32. Shrinkage factor (%) was obtained maximum in dried banana slices in HE-ETADS because of faster moisture removal rate (MRR) during drying. Inside drying cabin temperature was higher in HE-ETADS than HGSD and OSD surrounding; their shrinkage factor was 75%. The shrinkage factor was 73% and 63% in HGSD and OSD, respectively. Rehydration ratio of product depends upon on moderate range of MRR. It was observed that a higher rehydration ratio (1.73) was achieved in GHSD compared to HE-ETADS and OSD.

In deciding the hardness of dried product air temperature plays a vital role. Higher hardness of dried banana slices was noted as 373.56 in HE-ETADS due to higher inside drying cabin temperature, increasing the MRR and product became harder. Table 4.11 shows the obtained values for various quality parameters.

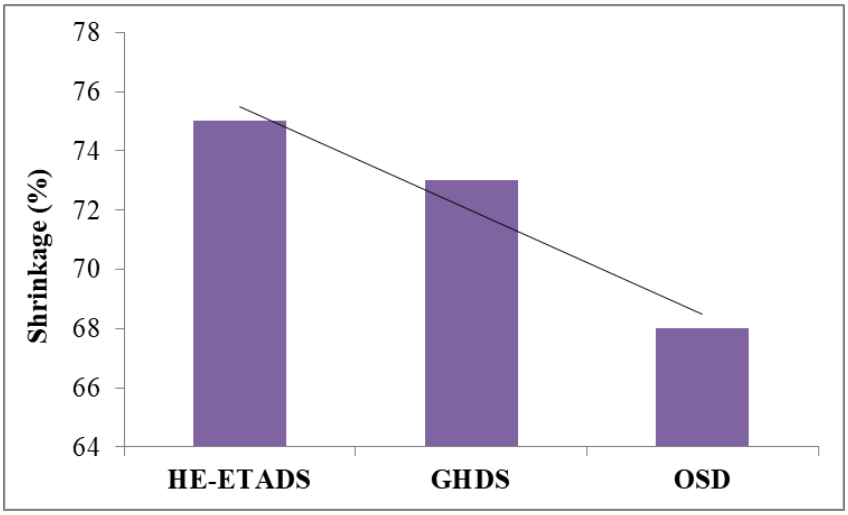

Fig 4.30 Shrinkage factor curves for dried banana slices in HE-ETADS, GHSD, and OSD at constant mass of 5kg

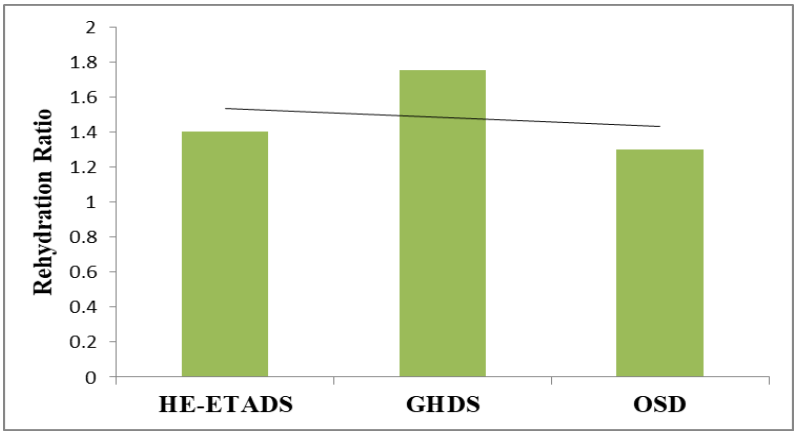

Fig 4.31 Rehydration ratio curves for dried banana slices in HE-ETADS, GHSD, and OSD at constant mass of 5kg

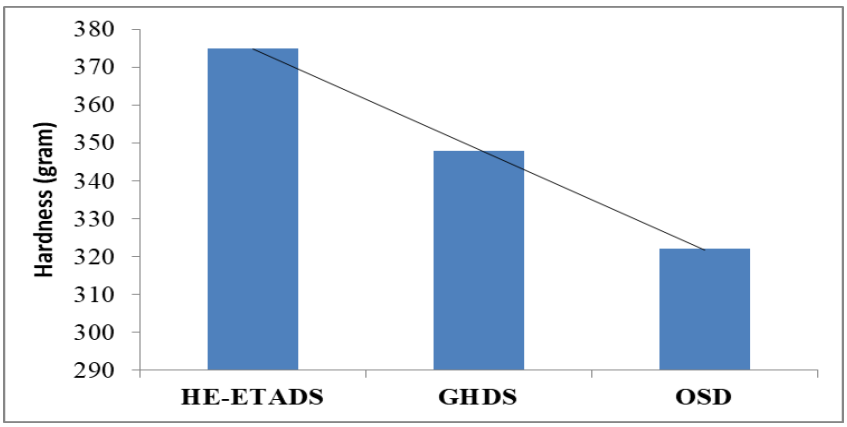

Fig 4.32 Hardness curves for dried banana slices in HE-ETADS, GHSD, and OSD at constant mass of 5kg

Table 4.11 Quality parameters for all drying conditions

Factors	Unit	Drying Methods		
		HE-ETADS	GHSD	OSD
Shrinkage	%	**75**	73	63
Hardness	g	**373.56**	348.2	321
Rehydration Ratio	-	1.41	**1.73**	1.32

Chromometer (CR-400, Minolta Co. Ltd., Japan) was used to measure the color of banana slices. During the drying process, the L, a, and b values were monitored every hour in all three drying systems and graphically presented in Figs 4.33- 4.35. Minimum changes have occurred in L- value with HE-ETADS, GHSD, and OSD throughout the experimentation. It varied from 21.98 – 27.65 in HE-ETDS, 21.98 – 27.58 in GHSD, and 21.98 – 27.46 in OSD, respectively. Hence, a and b values were reduced with time of the day in all three drying systems. Higher and lower a-values were 16.56 and 5.66 in HE-ETADS, 16.56 and 4.25 in GHSD, and 16.56- 2.12 in OSD. Also, variation in b-value in the range of 3.59 – 0.92, 3.59- 1.01, and 3.59 -1.23 in HE-ETADS, GHSD, and OSD occurred. Maximum variation in a-value and b-value was noted in mid-noon, such as 14h, because of higher air temperature.These findings are in line with past studies and also show the same pattern of color index of celery root in the term of L, a, b values from 67.32-81.35, 0.75-4.17, and 15.34-27.52 respectively dehydrated in FPC solar drying system coupled with baffles [98].

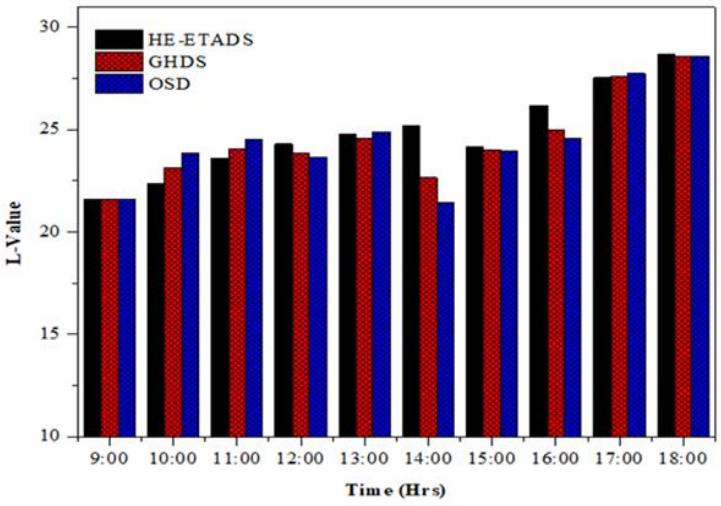

Fig 4.33 Variation in L-value for dried banana slices in HE-ETADS, GHSD, and OSD at constant mass of 5kg

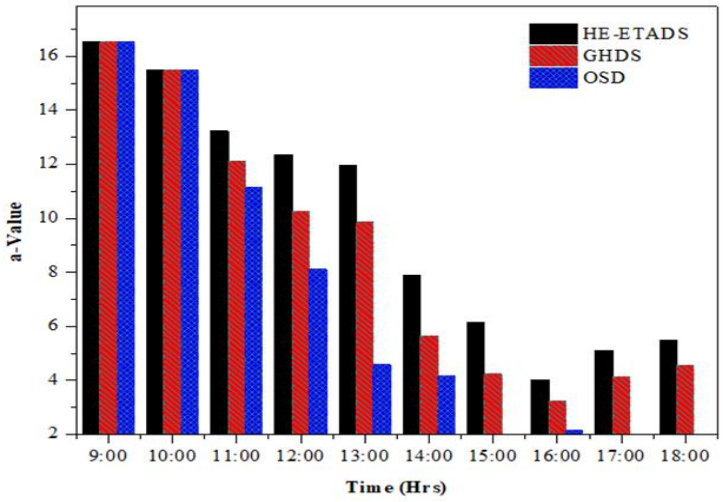

Fig 4.34 Variation in a-value for dried banana slices in HE-ETADS, GHSD, and OSD at constant mass of 5kg

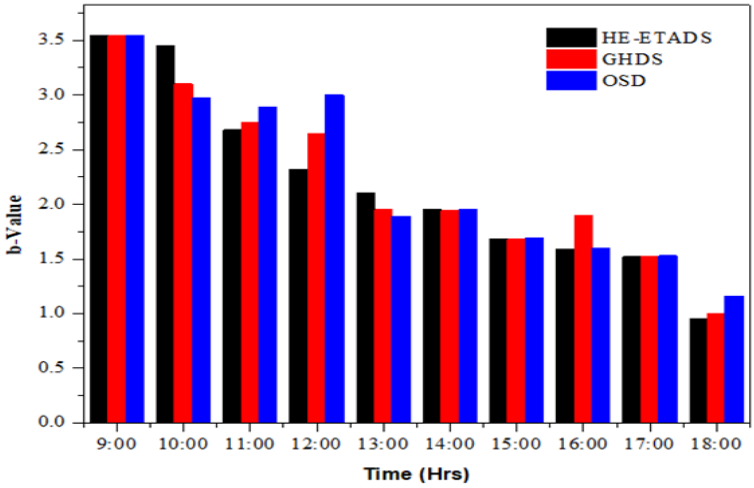

Fig 4.35 Variation in b-value for dried banana slices in HE-ETADS, GHSD, and OSD at constant mass of 5kg

The fluctuation of total color change (**Δ**E) in all three drying systems is illustrated in Fig 4.36 throughout the experiment. It was noted that in the beginning, the total color

change increased rapidly up to 13:00h and then went down continuously with drying period. The highest value of color change in HE-ETADS, GHSD and OSD was evaluated as 6.45, 6.95 and 7.51 due to increased DR with temperature and solar irradiance. More color changes occurred in OSD compared to HE-ETADS and GHSD due to higher degradation at the beginning of drying hours. Dried banana slices are demonstrated in Fig 4.37.

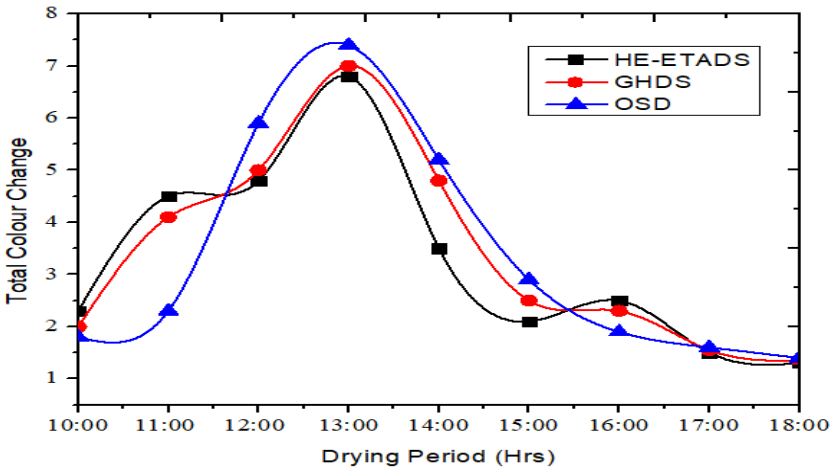

Fig 4.36 Variation in total color changes for dried banana slices in HE-ETADS, GHSD, and OSD at constant mass of 5kg

Fig 4.37 Sample of dried banana slices in all three drying methods

Water activity (A_w) plays a vital role in growth of micro-organisms and enhancing the strength of banana slices. It is defined as ratio of vapor pressure in food with respect to pure water vapor pressure. The variation of A_w throughout the experimentation in all three drying systems is summarized in Table 4.12. Initially A_w was noted 0.97, then reduced significantly with the time of day and temperature. A quick reduction in A_w was noted in HE-ETADS in comparison to GHSD and OSD due to fast DR and higher temperature maintained in drying cabin. A_w was decreased from; 0.97 to 0.33, 0.97 to 0.42, and 0.97 to 0.56 in HE-ETADS, GHSD, and OSD in 9 hours of drying time, respectively [101].

Table 4.12 Water activity (A_w) in all three drying methods

Drying Time	HE-ETADS	GHSD	OSD
9:00	0.97	0.97	0.97
10:00	0.96	0.96	0.96
11:00	0.88	0.91	0.94
12:00	0.76	0.88	0.91
13:00	0.69	0.79	0.88
14:00	0.58	0.67	0.85
15:00	0.51	0.59	0.79
16:00	0.42	0.53	0.68
17:00	0.39	0.49	0.62
18:00	0.33	0.42	0.56

4.4.7 Concept of mass transfer

4.4.7.1 Effective moisture diffusivity (D_{eff})

Effective Moisture Diffusivity (D_{eff}) is very effective in predicting the concept of mass transfer and it was measured equivalent to surface diffusion in the constant dry

rate period. Variation of Effective Moisture Diffusivity (D_{eff}) with time of the day presented in Fig 4.38. It varied from 1.11E-07 to 2.48E-07m^2s^{-1}, 1.21E-07 to 2.34E-07m^2s^{-1} and 1.3E-07 to 2.21E-07m^2s^{-1} in HE-ETADS, GHSD, and OSD respectively. Effective Moisture Diffusivity (D_{eff}) is directly proportional to the temperature and increases with the temperature increase. It was found to be maximum in HE-ETADS because forced convection occurred during drying. The inconsistency of D_{eff} is more in OSD than HE-ETADS and GHSD because solar radiation fluctuations and molecular movement mechanisms help increase the EMD at higher temperature. These findings in current work align with previous studies concluding that EMD varied from 4.8E-08 to 2.73E-07 for pumpkin chips [102], 1.13E-06 to 5.11E-06 for tomato slices dehydrated in convective drying system [103].

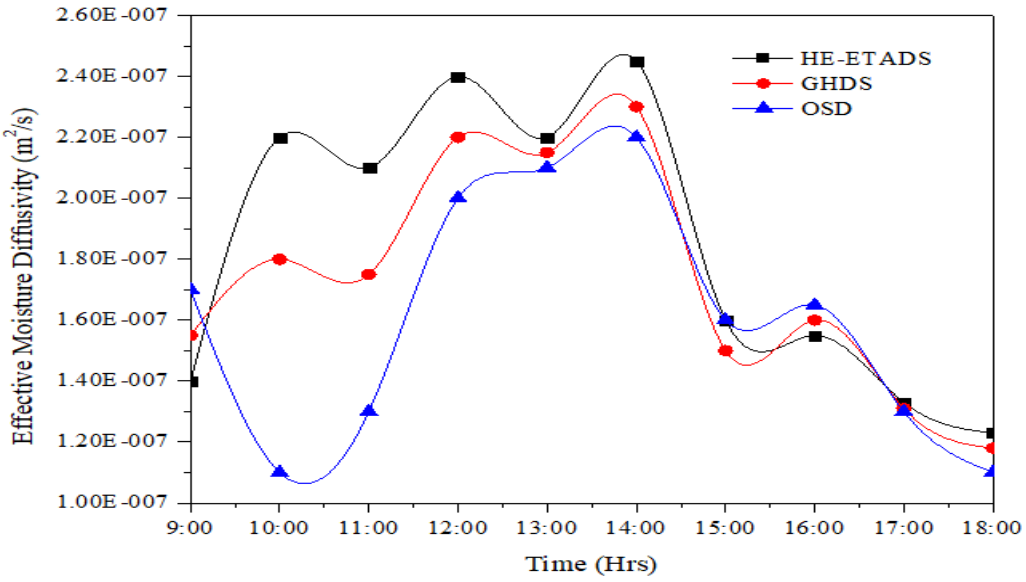

Fig 4.38 Relationship between EMD and time of the day for dried banana slices in HE-ETADS, GHSD, and OSD at constant mass of 5kg

4.7.7.2 Activation Energy (AE)

Activation Energy (AE) also plays a significant role in explaining the mass transfer concept. AE depends on the natural logarithm(ln) of diffusion coefficient, which is determined using an Arrhenius plot with a slope of ln (D_{eff}) vs. 1/T. AE was calculated as 30.25kJ/mole, 41.25kJ/mole, and 56.89kJ/mole in HE-ETADS, GHSD, and OSD, respectively. Results show that less AE is needed to initiate moisture diffusion and it also helps to enhance the DR in HE-ETADS compared to GHSD and OSD. The results are within an acceptable range of 75.6kJ/mole [104].

4.7.7.3 Convective mass transfer coefficient (CMTC)

During the dehydration of banana slices, the moisture removal rate is directly correlated with convective mass transfer coefficient (CMTC). Variation of CMTC with time of the day is demonstrated in Fig 4.39. Mass transfer coefficient varied from 3.21E-04 to 1.0E-04m/s, 3.15E-04 to1.0E-04m/s, and 3.01E-04 to1.0E-04m/s in HE-ETADS, GHSD and OSD respectively.

The maximum mass transfer coefficient was obtained in HE-ETADS due to higher moisture diffusivity as well as external forced convection flow of hot water through heat exchanger in drying cabin. Initially, the mass transfer coefficient was increased rapidly with time of the day and temperature up to 13h, then reduced continuously. The findings of current work confirmed that as the DR increased mass transfer coefficient also increased in HE-ETADS, GHSD, and OSD. The outcomes of present investigation are in the acceptable range, with the previous study estimated as 1.95E-07 to 2.11E-07m/s for kiwi slices [24], 8.53E-08 to 6.38E-05m/s for potato chips [105].

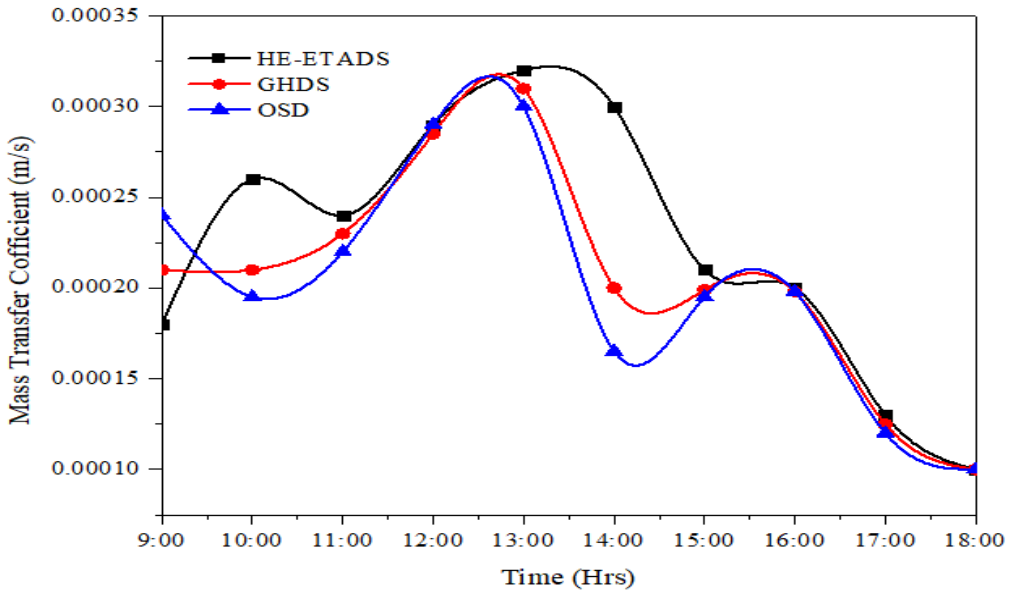

Fig 4.39 Relationship between mass transfer coefficient and time of the day for dried banana slices in HE-ETADS, GHSD, and OSD at constant mass of 5kg

4.5 Environmental analysis

The novel Heat Exchanger –Evacuated Assisted Drying System (HE-ETADS) was found appropriate for dehydrating hygroscopic crops. The effectiveness of advanced drying system was tested by dehydrating the three different hygroscopic crops (garlic clove, banana slices, and peppermint leaves). All these crops were dehydrated instantaneously inside drying cabin up to target moisture level on wet basis. The internal structure of each crop plays a significant role in dehydration and time would be estimated in drying up to final moisture level. Because of these phenomena, all crops have different drying periods. Since garlic cloves are granular, there is less evaporation of moisture. Hence, it consumes more drying period than the remaining two crops.

4.5.1 Drying behaviour

The trend of dehydrating three different hygroscopic crops (garlic cloves, banana slices, and peppermint leaves) was displayed in Fig 40(a). The drying period of garlic clove, banana slices, and peppermint leaves was decreased by 18, 17 and 22 hours in Case-I, correspondingly compared to Case-II. Drying period varied for Case-I and Case-II throughout the experiment, as illustrated in Fig 4.40(b). The higher drying cabin temperature plays a significant role in increasing moisture diffusion from top surface of crops. As cabin temperature increases crop's surface temperature also rises. Therefore, evaporation of moisture from crop surface also improved. Due to this concept, Case-I consumes less drying period compared to Case-II. Fig 4.40(a) indicates that in Case-I, banana slices and peppermint leaves attain their target moisture level of 10% in single day. While the same crops consume approximately three days in Case-II.

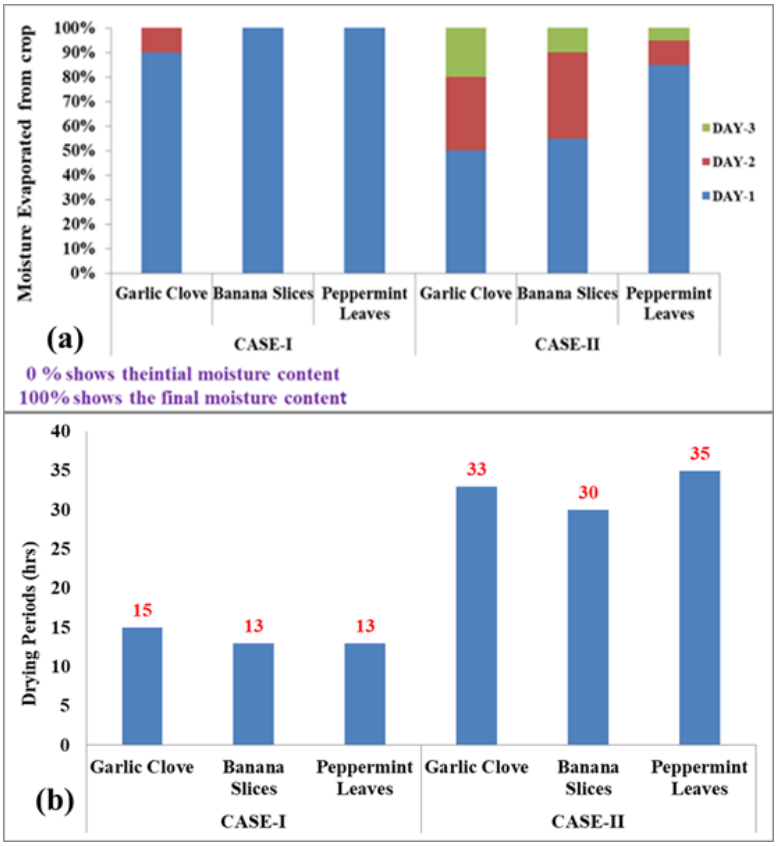

Fig 4.40 (a) Representation of drying behavior for different crops in Case-I & Case-II **(b)** Drying period for different crops for Case-I & Case-II

4.5.2 Environmental analysis

The calculation of embodied energy for proposed novel HE-ETADS and hybrid drying system is given in Table 3.5. The use of ETSC with drying system enhances the value of embodied energy by 84.68% in comparison to hybrid drying system. Therefore, it is mandatory to check cost of novel HE-ETADS from an environmental perspective. Equally, the environmental variables of the drying system depend generally on the moisture removal rate for specific crops. Hence, environmental analysis of the proposed drying system was evaluated for 03 different crops for both Cases. Embodied energy plays a significant role in emission of CO_2 for any system. Therefore, the novel HE-ETADS emits 70.09% carbon/year more in Case-I compared to Case-II. Because

in Case-I drying system coupled with some auxiliary devices such as ETSC and wire & tube type heat exchanger and increase the embodied energy. CO_2 mitigation is directly proportional to moisture removal inside drying system yearly for certain products. As the moisture evaporation was faster in Case-I than in Case II, the Case-I drying system mitigated 117%, 141%, and 247% CO_2 more for three different crops (garlic clove, banana slices, and peppermint leaves) during the experiment. Computed environmental analysis results for proposed HE-ETADS for both cases are discussed in Table 4.13.

Table 4.13. Environmental parameters for Case-I and Case-II

Environmental factors	Unit	Case-I			Case-II		
		Garlic clove	Banana slices	Peppermint leaves	Garlic clove	Banana slices	Peppermint leaves
EPBT	Year	4.25	7.5	3.20	5.10	8.6	5.65
Carbon Credit Earned	$	1421	857	2100	853	502	708
CO_2 Emitted	kg/year	493.62	493.62	493.62	290.2	290.2	290.2
CO_2 Mitigation	kg/year	3381	1873	4402	1562	775	1266
Net CO_2 Mitigation (Lifetime)	Tons	77	45.52	126	42.68	24.62	39.21

Fig 4.41 demonstrates the performance evaluation of advanced drying system from an environmental perspective for both Cases. EPBT was obtained lower in Case-I compared to Case-II for three different crops (garlic clove, banana slices, and peppermint leaves) during the experiment due to high value of annual thermal energy because of rapid moisture evaporation. Average value of EPBT was obtained as 4.99 and 6.47 years for Case-I and Case-II, respectively. Usually, its value depends on the

volume of drying system. System capacity was 10kg /batch. Further, the volume of mass increased, and the value of EPBT reduced. Hence, adding more mass reduced the moisture evaporation as more thermal energy was consumed inside the drying cabin to remove water from the upper surface of the products.

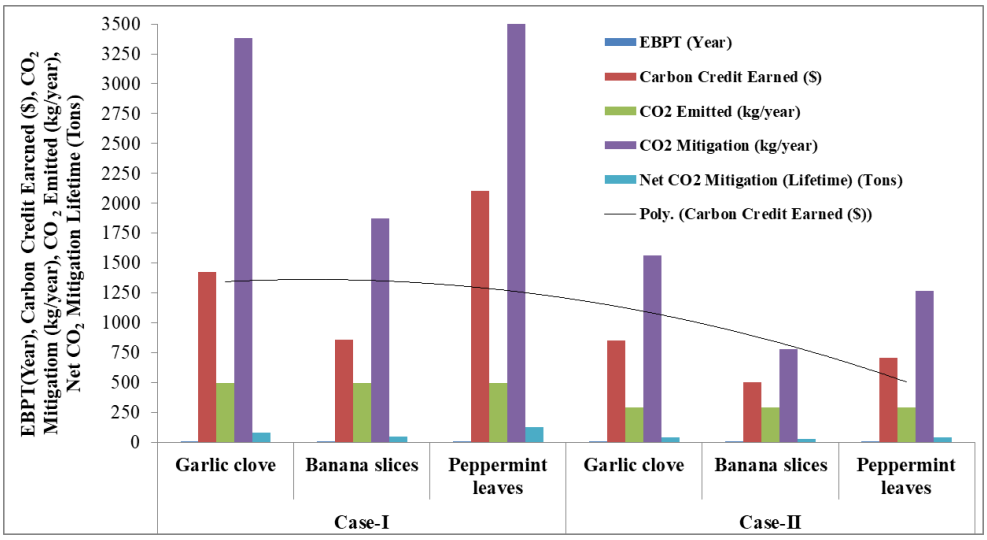

Fig 4.41 EPBT, CO_2 mitigation, net CO_2 mitigation, carbon credit earned, and CO_2 emission, for both Cases

Therefore, capacity can be optimized for novel drying system. The newly proposed HE-ETADS can decrease 34.32, 20.91, and 86.79 tons of CO_2 more for Case-I compared to Case-II in its whole life used for garlic clove, banana slices, and peppermint leaves correspondingly. This indicates the perfectness of HE-ETADS for ecosystem in Case-I. As a result, CO_2 mitigation was higher in Case-I as the earned carbon credits from the drying system were also higher in Case-I. It also depends on the size of the system and drying period of products. Carbon credit was taken as $14.80 for one ton of CO_2. Table 4.14 summarizes previous studies on hybrid drying systems to validate current research outcomes.

Table 4.14 Comparison with previous studies

Type of drying system	Product to be dried	Comparison of ground (floor) area with present system	EPBT (Year)	Net CO_2 mitigation lifetime	References
Tunnel type drying system	Peppermint	2.98 times more	1.98	29.85	[106]
Cabinet type greenhouse drying system		5.12 times more	0.96	98.65	[11]
Drying system with phase change material	Strawberry	1.02 times more	5.12	92.61	[107]
PVT integrated hybrid drying system	Grapes	0.86 times more	2.98	41.23	[65]
Even span roof type drying system with insulated north wall	Bitter ground flakes	3.95 times more	2.19	29.89	[64]

4.5.3 Exergetic based sustainability analysis

Environmental sustainability of energy systems is a key factor for environmentalists and researchers. Therefore, an energy system with high efficiency and minimum waste energy emission is more sustainable. Sustainability index of novel HE-ETADS for both Cases is shown in Fig 4.42. Drying system was highly sustainable in Case-I with a higher value of ESI 2.92, while the Case-II drying system had a lower value of ESI 1.25. That indicated the poor utilization of energy in Case-II. The energy generated, especially from biomass heaters, must be absorbed if it is to be consumed.

Another factor, EEF, also indicates the effect of unusable energy on the atmosphere.

Therefore, higher the waste energy, higher the EEF. Exergetic indicators indicate that novel drying system will have lower ecosystem damage in Case-I, while system in Case-II would harm the environment more. Fig 4.42 shows the same trend of environmental destruction coefficient (ED C) as EEF. System efficiency will be improved by recycling waste energy outputs through recovery. The values of EDC were theoretically varied from 0 to 1. When EDC method 1, there was a higher chance to increase system efficiency. The values of EEF and EDC varied within the range 0.98 to 15.36 and 1.47 to 16.43 for Case-I and Case-II, respectively.

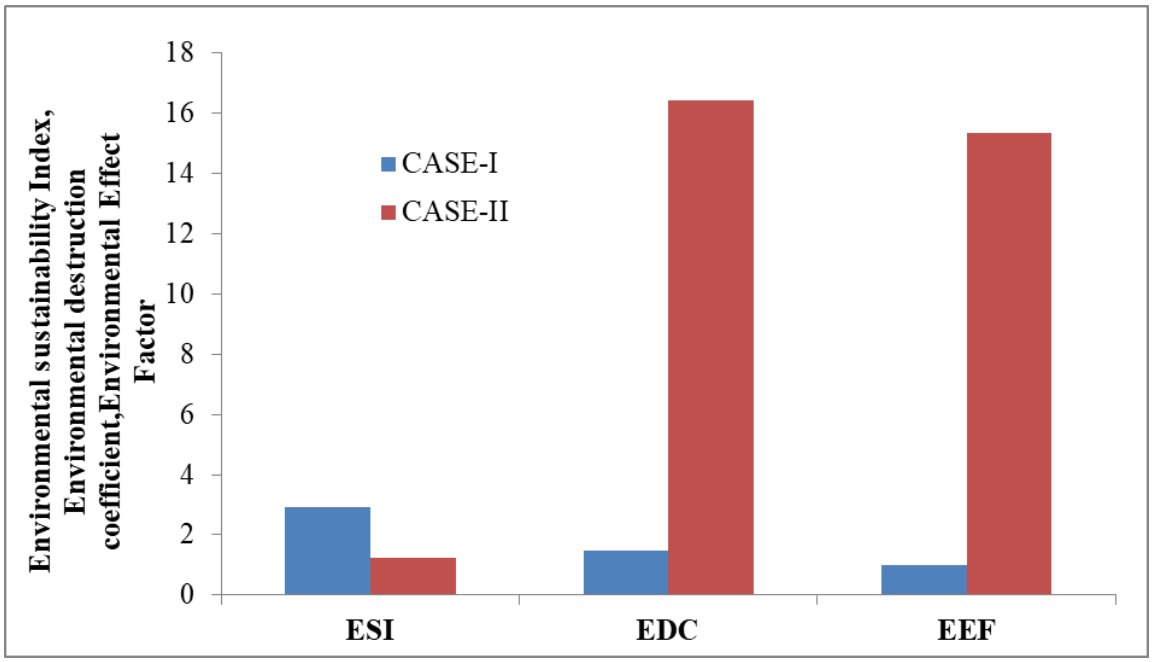

Fig 4.42 Variation of ESI, EDC, and EEF for Case-I and Case-I

CHAPTER-5

5. Conclusion and Future Scope

Performance analysis and optimization of drying parameters of a novel HE-ETADS were evaluated under unloaded and loaded conditions (for dehydrating the banana slices) respectively. Thin layer drying kinetics, quality assessment, and mass transfer phenomena were compared in all three drying systems (HE-ETADS, GHSD, and OSD). Following concluding remarks address the drying properties and quality stability of dried products in a novel Heat exchanger- evacuated tube-assisted drying system.

i. In current research work, the performance evaluation of novel drying system in active mode under unload conditions has been conducted in three different categories. CHTC of north wall insulated greenhouse dryer (NWIGHD) for ground to drying cabin air was 46.622W/m^2°C, while for advanced HE-ETADS it was found 47.542 W/m^2°C, that is 1.98% greater than NWIGHD. This indicates the higher thermal performance or efficiency of proposed HE-ETADS.

ii. HE-ETADS was more effective for dehydrating agricultural products than previously developed greenhouse dryers. 61.23°C higher drying cabin temperature and 3.99% lower inside relative humidity for greenhouse during the experimentation, which is acceptable dehydrating condition for most agricultural products.

iii. Heat exchanger evacuated tube assisted drying system was analyzed in terms of drying parameters such as drying rate, solar collector, and drying system

efficiency for a sample. Performance investigation was done at different water flow rate i.e. 10 Ltr/h, 20 Ltr/h, and 30 Ltr/h throughout the sunlight periods between 09:00 h to 18:00 h. Better performance of drying system was enhanced at 30 Ltr/h water flow rate was observed throughout the experimentation.

iv. The required moisture content for safe storage of dehydrated garlic was attained in 9 h. Maximum drying rate of the sample was achieved 1.48 kgH_2O/kg dry solid/h at 30 Ltr/h water flow rate. Its value reduces with an increasing drying period.

v. Highest solar collector and drying system efficiency values were recorded as 43.62% and 55.28%, correspondingly at 30 Ltr/h water flow rate. EE and average minimum exergy loss were calculated 57.64% at 30 Ltr/h water flow rate and 4.58 W at 10 Ltr/h water flow rate.

vi. Average drying cabin temperature of HE-ETADS was 65.25℃ and 59.32℃ under unload and loaded conditions, respectively. It is appropriate for banana slice drying.

vii. Higher DR was 16.25, 14.36, and 12.56g H_2O/g dry solid.h in HE-ETADS, GHSD, and OSD, respectively. Hence, average DR is more in HE-ETADS compared to GHSD and OSD.

viii. Weibull model (WM) is best fitted to define the thin layer drying kinetics of banana slices in all three drying systems.

ix. A high rehydration ratio of 1.73 was achieved un GHSD due to moderate moisture removal from banana surface.

x. Higher and lower a-values were 16.56 and 5.66 in HE-ETADS, 16.56 and 4.25 in GHSD and 16.56- 2.12 in OSD. While variation in b-value in the range of 3.59 – 0.92, 3.59- 1.01, and 3.59 -1.23 in HE-ETADS, GHSD, and OSD has occurred.

xi. Bananas were dehydrated from initial MC to the final MC in the range of 3.33gm water/gm dry to 0.03 gm water/gm dry using a solar drying process. The experimentation work was carried out in range of temperature 70-90℃, water flow rate varies from 10-30Ltr/h., geometry of product (rectangular and circle), and mass of product (1kg) considered as independent factors, using the Response surface methodology with central composite design (CCD).

xii. Moisture content, energy consumption, and shrinkage factor were responses that have been enhanced. Water flow rate and ambient temperature remarkably affected all the yield or response. Regression model Eq. was effectively advanced to effectively predict the quality factors of banana slices' solar dehydration. The Model F-value of 8.18 suggests the model is significant. There is only a 0.02% casual that an F-value this large could occur due to noise. P-values < 0.0500 specify model terms are significant. Optimal operational parameters are observed 89.99℃ (drying cabin temperature), 14.0Ltr/h (water flow rate), 0.9998(circular geometry), and 0.24004kg (mass of product). Optimum responses were 7.55 % (moisture content), 5.54kW/h (energy consumption), and 69.54% (shrinkage).

xiii. Further, experiment was conducted at optimal operating conditions, and the results indicate good consistency between predicted and experimental data with a deviation of 3.14%, 2.16% and, 1.41% for the minimum moisture,

energy consumption and, shrinkage, correspondingly. Hence, this is very helpful in further research on optimizing process parameters for hybrid indirect drying system for banana slices.

xiv. CO_2 emission normally depends on the embodied energy of material used for fabricating 0.98 kg per kWh in the drying system. In Case-I auxiliary devices are attached compared to Case-II; therefore, CO_2 emission is 84.68% more in Case I.

xv. CO_2 mitigation and earned carbon credit from the drying system depend on type of product selected for dehydration. As for all 03 selected crops, the CO_2 mitigation is higher for Case- I compared to Case-II because of rapid moisture evaporation in Case I.

Future Scope:

The experimental study has demonstrated the effectiveness of the Heat Exchanger-Evacuated Tube-Assisted Drying System in reducing drying time and producing high-quality dried banana slices. However, the current system is primarily suitable for moderate temperature drying applications.

Future research can focus on enhancing the performance of this system by integrating different types of solar collectors, exploring the use of phase change materials to improve energy efficiency, and implementing wall insulation to further optimize the drying process. These enhancements have the potential to extend the applicability of the system to a wider range of drying conditions and contribute to more sustainable and efficient drying technologies for agricultural products like banana slices.

By incorporating these improvements, future studies can build upon the current findings and advance the development of innovative drying systems that offer increased performance and reliability across various operational scenarios.

REFERENCES

[1] A. Kumar and G. N. Tiwari, "Thermal modeling of a natural convection greenhouse drying system for jaggery: An experimental validation," *Sol. Energy*, vol. 80, no. 9, pp. 1135–1144, 2006, doi: 10.1016/j.solener.2005.09.011.

[2] A. Arabhosseini, H. Samimi-akhijahani, and M. Motehayyer, "Increasing the energy and exergy efficiencies of a collector using porous and recycling system," *Renew. Energy*,vol.125(c), pp. 308-325, 2018, doi: 10.1016/j.renene.2018.07.132.

[3] M. Rashidi, A. Arabhosseini, H. Samimi-Akhijahani, and A. M. Kermani, "Acceleration the drying process of oleaster (Elaeagnus angustifolia L.) using reflectors and desiccant system in a solar drying system," *Renew. Energy*, vol. 171, pp. 526–541, 2021, doi: 10.1016/j.renene.2021.02.094.

[4] H. Ghasemkhani, A. Keyhani, M. Aghbashlo, S. Rafiee, and A. S. Mujumdar, "Improving exergetic performance parameters of a rotating-tray air dryer via a simple heat exchanger," *Appl. Therm. Eng.*, vol. 94, pp. 13–23, 2016, doi: 10.1016/j.applthermaleng.2015.10.114.

[5] R. Trostle, "A Report from the Economic Research Service Global Agricultural Supply and Demand : Factors Contributing to the Recent Increase in Food," *Agric. Outlook*, 2008.

[6] G. Akmak and C. Yildiz, "The drying kinetics of seeded grape in solar dryer with PCM-based solar integrated collector," *Food Bioprod. Process.*, vol. 89, no. 2, pp. 103–108, 2011, doi: 10.1016/j.fbp.2010.04.001.

[7] T. Koyuncu, I. Tosun, and Y. Pinar, "Drying characteristics and heat energy

requirement of cornelian cherry fruits (Cornus mas L.)," *J. Food Eng.*, vol. 78, no. 2, pp. 735–739, 2007, doi: 10.1016/j.jfoodeng.2005.09.035.

[8] P. Singh, V. Shrivastava, and A. Kumar, "Recent developments in greenhouse solar drying: A review," *Renew. Sustain. Energy Rev.*, vol. 82, pp. 3250-3262, 2017, doi: 10.1016/j.rser.2017.10.020.

[9] I. S. Afolabi, "Moisture Migration and Bulk Nutrients Interaction in a Drying Food Systems: A Review," *Food Nutr. Sci.*, vol. 05, no. 08, pp. 692–714, 2014, doi: 10.4236/fns.2014.58080.

[10] S. Vijayan, T. V. Arjunan, and A. Kumar, "Exergo-environmental analysis of an indirect forced convection solar dryer for drying bitter gourd slices," *Renew. Energy*, vol. 146, pp. 2210–2223, 2020, doi: 10.1016/j.renene.2019.08.066.

[11] V. Saini, S. Tiwari, and G. N. Tiwari, "Environ economic analysis of various types of photovoltaic technologies integrated with greenhouse solar drying system," *J. Clean. Prod.*, vol. 156, pp. 30–40, 2017, doi: 10.1016/j.jclepro.2017.04.044.

[12] J. Banout, P. Ehl, J. Havlik, B. Lojka, Z. Polesny, and V. Verner, "Design and performance evaluation of a Double-pass solar drier for drying of red chilli (Capsicum annum L.)," *Sol. Energy*, vol. 85, no. 3, pp. 506–515, 2011, doi: 10.1016/j.solener.2010.12.017.

[13] E. A. Mewa, M. W. Okoth, C. N. Kunyanga, and M. N. Rugiri, "Experimental evaluation of beef drying kinetics in a solar tunnel dryer," *Renew. Energy*, vol. 139, pp. 235–241, 2019, doi: 10.1016/j.renene.2019.02.067.

[14] A. Kumar and G. N. Tiwari, "Effect of mass on convective mass transfer coefficient during open sun and greenhouse drying of onion flakes," *J. Food*

Eng., vol. 79, no. 4, pp. 1337–1350, 2007, doi: 10.1016/j.jfoodeng.2006.04.026.

[15] S. Vijayavenkataraman, S. Iniyan, and R. Goic, "A review of solar drying technologies," *Renew. Sustain. Energy Rev.*, vol. 16, no. 5, pp. 2652–2670, Jun. 2012, doi: 10.1016/j.rser.2012.01.007.

[16] E. K. Akpinar, "Drying of mint leaves in a solar dryer and under open sun: Modelling, performance analyses," *Energy Convers. Manag.*, vol. 51, no. 12, pp. 2407–2418, 2010, doi: 10.1016/j.enconman.2010.05.005.

[17] A. ELkhadraoui, S. Kooli, and A. Farhat, "Study on effectiveness of mixed mode solar greenhouse dryer for drying of red pepper," *Int. J. Sci. Res. Eng. Technol.*, vol. 3, no. 2, pp. 143–146, 2015.

[18] I. N. Ramos, T. R. S. Brandão, and C. L. M. Silva, "Simulation of solar drying of grapes using an integrated heat and mass transfer model," *Renew. Energy*, vol. 81, pp. 896–902, 2015, doi: 10.1016/j.renene.2015.04.011.

[19] R. O. Lamidi, L. Jiang, P. B. Pathare, Y. D. Wang, and A. P. Roskilly, "Recent advances in sustainable drying of agricultural produce: A review," *Applied Energy*, vol. 233–234. Elsevier Ltd, pp. 367–385, Jan. 2019. doi: 10.1016/j.apenergy.2018.10.044.

[20] A. Fudholi, S. Mat, D. F. Basri, M. H. Ruslan, and K. Sopian, "Performances analysis of greenhouse solar dryer with heat exchanger," *Contemp. Eng. Sci.*, vol. 9, no. 3, pp. 135–144, 2016, doi: 10.12988/ces.2016.512322.

[21] O. Prakash and A. Kumar, "Historical review and recent trends in solar drying systems," *Int. J. Green Energy*, vol. 10, no. 7, pp. 690–738, 2013, doi: 10.1080/15435075.2012.727113.

[22] L. Semple, R. Carriveau, and D. S. K. Ting, "A techno-economic analysis of

seasonal thermal energy storage for greenhouse applications," *Energy Build.*, vol. 154, pp. 175–187, 2017, doi: 10.1016/j.enbuild.2017.08.065.

[23] P. Singh and M. K. Gaur, "Heat transfer analysis of hybrid active greenhouse solar dryer attached with evacuated tube solar collector," *Sol. Energy*, vol. 224, no. January, pp. 1178–1192, 2021, doi: 10.1016/j.solener.2021.06.050.

[24] I. Mohammadi, R. Tabatabaekoloor, and A. Motevali, "Effect of air recirculation and heat pump on mass transfer and energy parameters in drying of kiwifruit slices," *Energy*, vol. 170, pp. 149–158, 2019, doi: 10.1016/j.energy.2018.12.099.

[25] A. EL khadraoui, I. Hamdi, S. Kooli, and A. Guizani, "Drying of red pepper slices in a solar greenhouse dryer and under open sun: Experimental and mathematical investigations," *Innov. Food Sci. Emerg. Technol.*, vol. 52, no. November 2016, pp. 262–270, 2019, doi: 10.1016/j.ifset.2019.01.001.

[26] W. Wang, M. Li, R. H. E. Hassanien, Y. Wang, and L. Yang, "Thermal performance of indirect forced convection solar dryer and kinetics analysis of mango," *Appl. Therm. Eng.*, vol. 134, no. February, pp. 310–321, 2018, doi: 10.1016/j.applthermaleng.2018.01.115.

[27] D. Jain and G. N. Tiwari, "Effect of greenhouse on crop drying under natural and forced convection I: Evaluation of convective mass transfer coefficient," *Energy Convers. Manag.*, vol. 45, no. 5, pp. 765–783, 2004, doi: 10.1016/S0196-8904(03)00178-X.

[28] P. Gbaha, H. Yobouet Andoh, J. Kouassi Saraka, B. Kaménan Koua, and S. Touré, "Experimental investigation of a solar dryer with natural convective heat flow," *Renew. Energy*, vol. 32, no. 11, pp. 1817–1829, 2007, doi:

10.1016/j.renene.2006.10.011.

[29] M. Mohanraj and P. Chandrasekar, “Performance of a forced convection solar drier integrated with gravel as heat storage material,” *Proc. IASTED Int. Conf. Sol. Energy, SOE 2009*, no. May, pp. 51–54, 2009.

[30] M. Mohanraj and P. Chandrasekar, “Performance of a forced convection solar drier integrated with gravel as heat storage material for chili drying,” *J. Eng. Sci. Technol.*, vol. 4, no. 3, pp. 305–314, 2009.

[31] Hamdani, T. A. Rizal, and Z. Muhammad, “Fabrication and testing of hybrid solar-biomass dryer for drying fish,” *Case Stud. Therm. Eng.*, vol. 12, pp. 489–496, Sep. 2018, doi: 10.1016/j.csite.2018.06.008.

[32] O. Prakash, A. Kumar, and V. Laguri, “Performance of modified greenhouse dryer with thermal energy storage,” *Energy Reports*, vol. 2, pp. 155–162, 2016, doi: 10.1016/j.egyr.2016.06.003.

[33] S. Tiwari, G. N. Tiwari, and I. M. Al-Helal, “Performance analysis of photovoltaic–thermal (PVT) mixed mode greenhouse solar dryer,” *Sol. Energy*, vol. 133, pp. 421–428, 2016, doi: 10.1016/j.solener.2016.04.033.

[34] K. Jitjack, S. Thepa, K. Sudaprasert, and P. Namprakai, “Improvement of a rubber drying greenhouse with a parabolic cover and enhanced panels,” *Energy Build.*, vol. 124, pp. 178–193, 2016, doi: 10.1016/j.enbuild.2016.04.030.

[35] A. O. Omolola, A. I. O. Jideani, and P. F. Kapila, “Drying kinetics of banana (Musa spp.),” *Interciencia*, vol. 40, no. 6, pp. 374–380, 2015.

[36] A. O. Omolola, A. I. O. Jideani, and P. F. Kapila, “Modeling of thin layer drying characteristics of banana cv.Luvhele,” *Bulg. J. Agric. Sci.*, vol. 21, no. 2, pp. 342–348, 2015.

[37] Om Prakassh and A. Kumar., *Solar Drying Systems*. CRC Press , Taylor & Francis, 2019. doi: https://doi.org/10.1201/9780429299353.

[38] Om Prakassh and A. Kumar., *Solar drying systems*, vol. 0, no. 9789811038327. 2017. doi: 10.1007/978-981-10-3833-4_2.

[39] Nidhi, "Drying Characteristics of vermicelli in a Slant height greenhouse Dryer," *IOSR J. Mech. Civ. Enggineering*, pp. 1–6, 2015.

[40] M. R. Nukulwar and V. B. Tungikar, "Thin-layer mathematical modeling of turmeric in indirect natural conventional solar dryer," *J. Sol. Energy Eng. Trans. ASME*, vol. 142, no. 4, pp. 1–7, 2020, doi: 10.1115/1.4045828.

[41] A. A. Hassanain, "Simple Solar Drying System for Banana Fruit," *World J. Agric. Sci.*, vol. 5, no. 4, p. 10, 2009.

[42] B. M. A. Amer, M. A. Hossain, and K. Gottschalk, "Design and performance evaluation of a new hybrid solar dryer for banana," *Energy Convers. Manag.*, vol. 51, no. 4, pp. 813–820, 2010, doi: 10.1016/j.enconman.2009.11.016.

[43] A. Lingayat, V. P. Chandramohan, and V. R. K. Raju, "Design, Development and Performance of Indirect Type Solar Dryer for Banana Drying," *Energy Procedia*, vol. 109, no. November 2016, pp. 409–416, 2017, doi: 10.1016/j.egypro.2017.03.041.

[44] C. P. Genobiagon and F. B. Alagao, "Performance of low-cost dual circuit solar assisted cabinet dryer for green banana," *J. Mech. Eng. Res. Dev.*, vol. 42, no. 1, pp. 42–45, 2019, doi: 10.26480/jmerd.01.2019.42.45.

[45] P. Pruengam, S. Pathaveerat, and P. Pukdeewong, "Fabrication and testing of double-sided solar collector dryer for drying banana," *Case Stud. Therm. Eng.*, vol. 27, no. March, p. 101335, 2021, doi: 10.1016/j.csite.2021.101335.

[46] A. Lingayat and V. P. Chandramohan, “Numerical investigation on solar air collector and its practical application in the indirect solar dryer for banana chips drying with energy and exergy analysis,” *Therm. Sci. Eng. Prog.*, vol. 26, no. August, p. 101077, 2021, doi: 10.1016/j.tsep.2021.101077.

[47] C. Lamnatou, E. Papanicolaou, V. Belessiotis, and N. Kyriakis, “Experimental investigation and thermodynamic performance analysis of a solar dryer using an evacuated-tube air collector,” *Appl. Energy*, vol. 94, pp. 232–243, 2012, doi: 10.1016/j.apenergy.2012.01.025.

[48] A. Mahesh, C. E. Sooriamoorthi, and A. K. Kumaraguru, “Performance study of solar vacuum tubes type dryer,” *J. Renew. Sustain. Energy*, vol. 4, no. 6, 2012, doi: 10.1063/1.4767934.

[49] A. B. Ubale, D. Pangavhane, and A. Auti, “Performance analysis of forced convection evacuated tube solar collector used for grape dryer,” *J. Eng. Sci. Technol.*, vol. 12, no. 1, pp. 42–53, 2017.

[50] P. Singh, S. Vyas, and A. Yadav, “Experimental comparison of open sun drying and solar drying based on evacuated tube collector,” *Int. J. Sustain. Energy*, vol. 38, no. 4, pp. 348–367, 2019, doi: 10.1080/14786451.2018.1505726.

[51] H. Majdi and J. A. Esfahani, “Energy and drying time optimization of convective drying: Taguchi and LBM methods,” *Dry. Technol.*, vol. 37, no. 6, pp. 722–734, 2019, doi: 10.1080/07373937.2018.1458036.

[52] Z. Šumić, A. Vakula, A. Tepić, J. Čakarević, J. Vitas, and B. Pavlić, “Modeling and optimization of red currants vacuum drying process by response surface methodology (RSM),” *Food Chem.*, vol. 203, pp. 465–475, 2016, doi: 10.1016/j.foodchem.2016.02.109.

[53] Q. H. Han, L. J. Yin, S. J. Li, B. N. Yang, and J. W. Ma, “Optimization of process parameters for microwave vacuum drying of apple lices using response surface method,” *Dry. Technol.*, vol. 28, no. 4, pp. 523–532, 2010, doi: 10.1080/07373931003618790.

[54] J. A. Esfahani, H. Majdi, and E. Barati, “Analytical two-dimensional analysis of the transport phenomena occurring dur- ing convective drying: apple slices,” *J. Food Eng.*, vol. S0260-8774, no. JFOE 7566, pp. 1–32, 2013.

[55] Emmanuel C. Nwadike. | Matthew N. Abonyi. | Joseph T. Nwabanne. | Pascal E. Ohale, “Optimization of Solar Drying of Blanched and Unblanched Aerial Yam using Response Surface Methodology,” *Int. J. Trend Sci. Res. Dev.*, vol. 4, no. 3, pp. 659–666, 2020.

[56] E. E. Abano and L. K. Sam-Amoah, “Effects of different pretreatments on drying characteristics of banana slices,” *ARPN J. Eng. Appl. Sci.*, vol. 6, no. 3, pp. 121–129, 2011.

[57] A. Abdeen, A. A. Serageldin, M. G. E. Ibrahim, A. El-Zafarany, S. Ookawara, and R. Murata, “Solar chimney optimization for enhancing thermal comfort in Egypt: An experimental and numerical study,” *Sol. Energy*, vol. 180, no. October 2018, pp. 524–536, 2019, doi: 10.1016/j.solener.2019.01.063.

[58] T. B. Gorji and A. A. Ranjbar, “Geometry optimization of a nanofluid-based direct absorption solar collector using response surface methodology,” *Sol. Energy*, vol. 122, pp. 314–325, 2015, doi: 10.1016/j.solener.2015.09.007.

[59] O. I. Obajemihi, J. O. Olaoye, J. O. Ojediran, J. H. Cheng, and D. W. Sun, *Model development and optimization of process conditions for color properties of tomato in a hot-air convective dryer using box–behnken design*, vol. 44, no.

10. 2020. doi: 10.1111/jfpp.14771.

[60] M. J. Dalvand, S. S. Mohtasebi, and S. Rafiee, “Optimization on drying conditions of a solar electrohydrodynamic drying system based on desirability concept,” *Food Sci. Nutr.*, vol. 2, no. 6, pp. 758–767, 2014, doi: 10.1002/fsn3.168.

[61] Y. I. Sallam, M. H. Aly, A. F. Nassar, and E. A. Mohamed, “Solar drying of whole mint plant under natural and forced convection,” *J. Adv. Res.*, vol. 6, no. 2, pp. 171–178, 2015, doi: 10.1016/j.jare.2013.12.001.

[62] P. P. Tripathy, “Investigation into solar drying of potato: effect of sample geometry on drying kinetics and CO_2 emissions mitigation,” *J. Food Sci. Technol.*, vol. 52, no. 3, pp. 1383–1393, 2015, doi: 10.1007/s13197-013-1170-0.

[63] S. Singh and S. Kumar, “Solar drying for different test conditions: Proposed framework for estimation of specific energy consumption and CO_2 emissions mitigation,” *Energy*, vol. 51, pp. 27–36, 2013, doi: 10.1016/j.energy.2013.01.006.

[64] O. Prakash and A. Kumar, “Environomical analysis and mathematical modelling for tomato flakes drying in a modified greenhouse dryer under active mode,” *Int. J. Food Eng.*, vol. 10, no. 4, pp. 669–681, 2014, doi: 10.1515/ijfe-2013-0063.

[65] S. Tiwari and G. N. Tiwari, “Thermal analysis of photovoltaic thermal integrated greenhouse system (PVTIGS) for heating of slurry in potable biogas plant: An experimental study,” *Sol. Energy*, vol. 155, pp. 203–211, 2017, doi: 10.1016/j.solener.2017.06.021.

[66] Ndukwu, M.C., Ibeh, M.I., Ugwu, E., Ekop, I., Etim, P., Igbojionu, D., Abam, F., Lamrani, B., Simo-Tagne, M. and Bennamoun, L., "Environmental Effects Environmental sustainability and exergy return on investment of selected solar dryer designs based on standard and extended exergy approaches," *Energy Sources, Part A: Recovery, Utilization, And Environmental Effects,*vol. 44, no.4, pp.10647-10664, 2022, doi: 10.1080/15567036.2022.2156636.

[67] P. Singh and M. K. Gaur, "Environmental and economic analysis of novel hybrid active greenhouse solar dryer with evacuated tube solar collector," *Sustain. Energy Technol. Assessments*, vol. 47, no. June, p. 101428, 2021, doi: 10.1016/j.seta.2021.101428.

[68] A. Gupta, B. Das, A. Biswas, and J. D. Mondol, "An environmental and economic evaluation of solar photovoltaic thermal dryer," *Int. J. Environ. Sci. Technol.*, vol. 19, no. 11, pp. 10773–10792, 2022, doi: 10.1007/s13762-021-03739-8.

[69] M. Simo-tagne and M. Ndi-azese, "Thermal , economic , and environmental analysis of a novel solar dryer for firewood in various temperate and tropical climates," *Sol. Energy*, vol. 226, no. August, pp. 348–364, 2021, doi: 10.1016/j.solener.2021.08.060.

[70] S. Madhankumar, K. Viswanathan, and W. Wu, "Energy, exergy and environmental impact analysis on the novel indirect solar dryer with fins inserted phase change material," *Renew. Energy*, vol. 176, no. 176, p. 280e294 Contents, 2021, doi: 10.1016/j.renene.2021.05.085.

[71] R. H. E. Hassanien, M. Li, and Y. Tang, "The evacuated tube solar collector assisted heat pump for heating greenhouses," *Energy Build.*, vol. 169, pp. 305–

318, 2018, doi: 10.1016/j.enbuild.2018.03.072.

[72] O. Prakash and A. Kumar, “Performance evaluation of greenhouse dryer with opaque north wall,” *Heat Mass Transf. und Stoffuebertragung*, vol. 50, no. 4, pp. 493–500, 2014, doi: 10.1007/s00231-013-1256-2.

[73] O. Prakash and A. Kumar, “Annual performance of a modified greenhouse dryer under passive mode in no-load conditions,” *Int. J. Green Energy*, vol. 12, no. 11, pp. 1091–1099, 2015, doi: 10.1080/15435075.2014.961461.

[74] O. Prakash, A. Kumar, and V. Laguri, “Performance of modified greenhouse dryer with thermal energy storage,” *Energy Reports*, vol. 2, no. July, pp. 155–162, 2016, doi: 10.1016/j.egyr.2016.06.003.

[75] A. Kushwah, A. Kumar, M. Kumar, and A. Pal, “Performance analysis of heat exchanger- evacuated tube assisted drying system (HE-ETADS) under unload condition,” *Sustain. Energy Technol. Assessments*, vol. 53, no. PB, p. 102589, 2022, doi: 10.1016/j.seta.2022.102589.

[76] A. Kushwah, A. Kumar, M. K. Gaur, and A. Pal, “Garlic dehydration inside heat exchanger-evacuated tube assisted drying system: Thermal performance, drying kinetic and color index,” *J. Stored Prod. Res.*, vol. 93, no. May, 2021, doi: 10.1016/j.jspr.2021.101852.

[77] D. Kumar, S. Prasad, and G. S. Murthy, “Optimization of microwave-assisted hot air drying conditions of okra using response surface methodology,” *J. Food Sci. Technol.*, vol. 51, no. 2, pp. 221–232, 2014, doi: 10.1007/s13197-011-0487-9.

[78] S. K. Giri and S. Prasad, “Optimization of microwave-vacuum drying of button mushrooms using response-surface methodology,” *Dry. Technol.*, vol. 25, no.

5, pp. 901–911, 2007, doi: 10.1080/07373930701370407.

[79] E. Veeramanipriya and A. R. Umayal Sundari, “Performance evaluation of hybrid photovoltaic thermal (PVT) solar dryer for drying of cassava,” *Sol. Energy*, vol. 215, no. January, pp. 240–251, 2021, doi: 10.1016/j.solener.2020.12.027.

[80] M. S. Seveda, “Design and Development of Walk-In Type Hemicylindrical Solar Tunnel Dryer for Industrial Use,” *ISRN Renew. Energy*, vol. 2012, pp. 1–9, 2012, doi: 10.5402/2012/890820.

[81] P. S. Chauhan, A. Kumar, C. Nuntadusit, and S. S. Mishra, “Drying Kinetics, Quality Assessment, and Economic Analysis of Bitter Gourd Flakes Drying Inside Forced Convection Greenhouse Dryer,” *J. Sol. Energy Eng. Trans. ASME*, vol. 140, no. 5, pp. 1–10, 2018, doi: 10.1115/1.4039891.

[82] A. Kushwah, A. Kumar, M. Kumar, and A. Pal, “Garlic dehydration inside heat exchanger-evacuated tube assisted drying system : Thermal performance , drying kinetic and color index,” *J. Stored Prod. Res.*, vol. 93, no. May, p. 101852, 2021, doi: 10.1016/j.jspr.2021.101852.

[83] P. S. Chauhan, A. Kumar, and C. Nuntadusit, “Thermo-environomical and drying kinetics of bitter gourd flakes drying under north wall insulated greenhouse dryer,” *Sol. Energy*, vol. 162, no. April 2017, pp. 205–216, 2018, doi: 10.1016/j.solener.2018.01.023.

[84] A. Kushwah, A. Kumar, and M. K. Gaur, “Drying kinetics, performance, and quality assessment for banana slices using heat pump–assisted drying system (HPADS),” *J. Food Process Eng.*, vol. 45, no. 3, pp. 1–10, 2022, doi: 10.1111/jfpe.13964.

[85] R. Daghigh, R. Shahidian, and H. Oramipoor, “A multistate investigation of a solar dryer coupled with photovoltaic thermal collector and evacuated tube collector,” *Sol. Energy*, vol. 199, no. February, pp. 694–703, 2020, doi: 10.1016/j.solener.2020.02.069.

[86] A. Kushwah, A. Kumar, A. Pal, and M. Kumar, “Materials Today : Proceedings Experimental analysis and thermal performance of evacuated tube solar collector assisted solar dryer,” *Mater. Today Proc.*, no. xxxx, 2021, doi: 10.1016/j.matpr.2021.04.243.

[87] J. W. Westwater and H. G. Drickamer, “The Mathematics of Diffusion,” *J. Am. Chem. Soc.*, vol. 79, no. 5, pp. 1267–1268, 1957, doi: 10.1021/ja01562a072.

[88] A. O. Dissa, H. Desmorieux, J. Bathiebo, and J. Koulidiati, “A comparative study of direct and indirect solar drying of mango,” *Glob. J. Pure Appl. Sci.*, vol. 17, no. 3, pp. 273-294–294, 2011.

[89] P. S. Chauhan, A. Kumar, and C. Nuntadusit, “Thermo-environomical and drying kinetics of bitter gourd flakes drying under north wall insulated greenhouse dryer,” *Sol. Energy*, vol. 162, no. November 2017, pp. 205–216, 2018, doi: 10.1016/j.solener.2018.01.023.

[90] M. Kumar, R. K. Sahdev, S. Tiwari, H. Manchanda, and A. Kumar, “Enviro-economical feasibility of groundnut drying under greenhouse and indoor forced convection hot air dryers,” *J. Stored Prod. Res.*, vol. 93, no. November 2020, p. 101848, 2021, doi: 10.1016/j.jspr.2021.101848.

[91] T.Chowdhury, H.Chowdhury, M.Thirugnanasambandam, S.Hossain, P.Barua, J.U.Ahamed, R.Saidur, and S.M Sait, “Is the commercial sector of Bangladesh sustainable? – Viewing via an exergetic approach,” *J. Clean. Prod.*, vol. 228,

pp. 544–556, 2019, doi: 10.1016/j.jclepro.2019.04.270.

[92] T.Chowdhury, H.Chowdhury, P.Chowdhury, S.M.Sait, A.Paul, J.U. Ahamed, and R.Saidur,"A case study to application of exergy-based indicators to address the sustainability of Bangladesh residential sector," *Sustain. Energy Technol. Assessments*, vol. 37, no. November 2019, p. 100615, 2020, doi: 10.1016/j.seta.2019.100615.

[93] A. Midilli and H. Kucuk, "Assessment of exergetic sustainability indicators for a single layer solar drying system," *Int. J. Exergy*, vol. 16, no. 3, pp. 278–292, 2015, doi: 10.1504/IJEX.2015.068227.

[94] P. S. Chauhan and A. Kumar, "Performance analysis of greenhouse dryer by using insulated north-wall under natural convection mode," *Energy Reports*, vol. 2, no. May, pp. 107–116, 2016, doi: 10.1016/j.egyr.2016.05.004.

[95] R. Kant and A. Kumar, "Process optimization of conventional steam distillation system for peppermint oil extraction," *Energy Sources, Part A Recover. Util. Environ. Eff.*, vol. 44, no. 2, pp. 3960–3980, 2022, doi: 10.1080/15567036.2022.2069886.

[96] A. Fudholi, R. Yendra, D. F. Basri, M. H. Ruslan, and K. Sopian, "Energy and exergy analysis of hybrid solar drying system," *Contemp. Eng. Sci.*, vol. 9, no. 5, pp. 215–223, 2016, doi: 10.12988/ces.2016.512323.

[97] S. Poonia, A. K. Singh, P. Santra, and D. Mishra, "Design, Development and Performance Evolution of a Low-Cost Solar Dryer," pp. 219–223, 2018, doi: 10.1007/978-981-10-4576-9_20.

[98] A. Khanlari, H.O. Güler, A.D. Tuncer, C.Sirin, Y.C. Bilge, Y.Yılmaz, and A. Gungor, "Experimental and numerical study of the effect of integrating plus-

shaped perforated baffles to solar air collector in drying application," *Renew. Energy*, vol. 145, pp. 1677–1692, 2020, doi: 10.1016/j.renene.2019.07.076.

[99] A. Dasore, T. Polavarapu, R. Konijeti, and N. Puppala, "Convective hot air drying kinetics of red beetroot in thin layers," *Front. Heat Mass Transf.*, vol. 14, no. June, pp. 1–8, 2020, doi: 10.5098/hmt.14.23.

[100] S. V. Gokhale and S. S. Lele, "Dehydration of red beet root (Beta vulgaris) by hot air drying: Process optimization and mathematical modeling," *Food Sci. Biotechnol.*, vol. 20, no. 4, pp. 955–964, 2011, doi: 10.1007/s10068-011-0132-4.

[101] S. Malakar, M. Alam, and V. K. Arora, "Evacuated tube solar and sun drying of beetroot slices: Comparative assessment of thermal performance, drying kinetics, and quality analysis," *Sol. Energy*, vol. 233, no. October 2021, pp. 246–258, 2022, doi: 10.1016/j.solener.2022.01.029.

[102] R. P. F. Guiné, S. Pinho, and M. J. Barroca, "Study of the convective drying of pumpkin (Cucurbita maxima)," *Food Bioprod. Process.*, vol. 89, no. 4, pp. 422–428, 2011, doi: 10.1016/j.fbp.2010.09.001.

[103] B. Dianda, M. Ousmane, S. Kam, and T. Ky, "Experimental study of the kinetics and shrinkage of tomato slices in convective drying," *African J. Food Sci.*, vol. 9, no. 5, pp. 262–271, 2015, doi: 10.5897/ajfs2015.1298.

[104] O. Badaoui, S. Hanini, A. Djebli, B. Haddad, and A. Benhamou, "Experimental and modelling study of tomato pomace waste drying in a new solar greenhouse: Evaluation of new drying models," *Renew. Energy*, vol. 133, pp. 144–155, 2019, doi: 10.1016/j.renene.2018.10.020.

[105] C. Ilicali and F. Icier, "Modified Dincer and Dost Method for Predicting the

Mass Transfer Coefficients in Solids," *Int. J. Food Eng.*, vol. 12, no. 1, pp. 101–105, 2016, doi: 10.1515/ijfe-2015-0095.

[106] M. A. Eltawil, M. M. Azam, and A. O. Alghannam, "Solar PV powered mixed-mode tunnel dryer for drying potato chips," *Renew. Energy*, vol. 116, pp. 594–605, 2018, doi: 10.1016/j.renene.2017.10.007.

[107] H. Atalay and E. Cankurtaran, "Energy, exergy, exergoeconomic and exergo-environmental analyses of a large scale solar dryer with PCM energy storage medium," *Energy*, vol. 216, p. 119221, 2021, doi: 10.1016/j.energy.2020.119221.

Publications

Paper published in International peer reviewed journals

1. **Anand Kushwah,** Anil Kumar, Manoj Kumar Gaur, Pranshu Srivastava. "Environmental Sustainability and Exergetic Based Sustainability Indicators for Heat Exchanger-Evacuated Tube Assisted Drying System (HE-ETADS)" Sustainable Energy Technologies and Assessments. https://doi.org/10.1016/j.seta.2023.103277. **SCI Impact Factor 7.632**
2. **Anand Kushwah**, Anil Kumar, Manoj Kumar Gaur, Amit Pal. Heat and Mass Transfer, Quality, Performance Analysis, and Modeling of Thin Layer Drying Kinetics of Banana Slices. ASME. J. Sol. Energy Eng. October 2023; 145(5): 051010. https://doi.org/10.1115/1.4062447. **SCI Impact Factor 2.83**
3. **Anand Kushwah**, Anil Kumar and Manoj Kumar Gaur. Optimization of Drying Parameters for Hybrid Indirect Solar Dryer for Banana Slices Using Response Surface Methodology. Process Safety and Environmental Protection-Elsevier Volume 170, February 2023, Pages 176-187. https://doi.org/10.1016/j.psep.2022.12.003. **SCI Impact Factor 7.926**
4. **Anand Kushwah**, Anil Kumar, Manoj Kumar Gaur, Amit Pal. Performance Analysis of Heat Exchanger- Evacuated Tube Assisted Drying System (HE-ETADS) Under Unload Condition. Sustainable Energy Technologies and Assessments. Volume 53, Part B, October 2022, 102589. https://doi.org/10.1016/j.seta.2022.102589. **SCI Impact Factor 7.632**
5. **Anand Kushwah**, Anil Kumar, Manoj Kumar Gaur and Amit Pal. Garlic Dehydration inside Heat Exchanger-Evacuated Tube Assisted Drying System: Thermal Performance, Drying Kinetic and Color Index. Journal of Stored

Products Research, Volume 93, September 2021, 101848. https://doi.org/10.1016/j.jspr.2021.101852. **SCI Impact Factor: 2.831**

Participation/Paper published in International conferences

1 **Anand Kushwah**, Anil Kumar, Amit Pal and Manoj Kumar Gaur. Experimental analysis and thermal performance of evacuated tube solar collector assisted solar dryer. Materials Today: Proceedings. Volume 47, Part 17, 2021, Pages 5846-5851. https://doi.org/10.1016/j.matpr.2021.04.243

2 **Anand Kushwah**, Anil Kumar, Amit Pal and Manoj Kumar Gaur. Experimental Investigation on Heat Exchanger- Evacuated Tube Assisted Drying System (HE-ETADS) Under Unload Condition. Paper presented in international conferences on Advances in **Heat Transfer and Fluid Dynamics (AHTFD-22),** organized by Department of Mechanical Engineering, Z.H. College of Engineering & Technology, AMU, Aligarh, 1-3rd Dec 2022

3 **Anand Kushwah**, Anil Kumar, and Manoj Kumar Gaur. Thermal Performance of Heat Exchanger- Evacuated Tube Assisted Drying System (HE-ETADS) with Single and Double Evacuated Tube Solar Collector Under no-load. Paper presented in international conferences on Sustainable Energy and Green Technology (SEGT-2023), Ho Chi Minh City, Vietnam,10-13th Dec 2023.

Brief Bio-Data

Mr. Anand Kushwah

anand.kuswah1989@gmail.com

Mailing/Permanent Address:

93-D, Sankat Mochan Nagar , Behind M.E.S Power House, Parsdai Ka Pura,Cantt Area Morar, Gwalior-474006, INDIA.

Contact No: **+91-7999671338**, +91-8982295774,

ACADEMIC QUALIFICATION

- **Ph. D. (Thermal Engg.)** Pursuing **Jan-2021**, **Delhi Technological University**, Delhi 110042, INDIA.
- **M.Tech.** (**Automobile Engg.),** June **2017**, **Rutam Ji Institute of Technology, B.S.F Academy** Tekanpur Gwalior**,** INDIA.
- **B.Tech. (Mech. Engg)**, June **2014**, Rajiv Ghandi Technical University, Bhopal, INDIA.
- **Intermediate** June 2010 M.P. Board, INDIA, with Physics, Chemistry, and Mathematics.
- SSC: (10^{th}) June 2004, M.P. Board, INDIA, with Science, Math, English, Technical Drawing and Hindi.

Sustainable Energy Technologies and Assessments 57 (2023) 103277

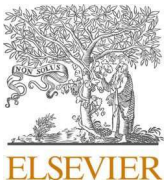

Contents lists available at ScienceDirect

Sustainable Energy Technologies and Assessments

journal homepage: www.elsevier.com/locate/seta

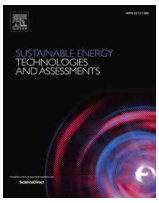

Environmental Sustainability and Exergetic Based Sustainability Indicators for Heat Exchanger-Evacuated Tube Assisted Drying System (HE-ETADS)

Anand Kushwah [a], Anil Kumar [a,b,*], Manoj Kumar Gaur [c], Pranshu Shrivastava [d]

[a] Department of Mechanical Engineering, Delhi Technological University, Delhi-110 042, India
[b] Centre for Energy and Environment, Delhi Technological University, Delhi-110 042, India
[c] Department of Mechanical Engineering, Madhav Institute of Technology & Science, Gwalior-474 005, India
[d] Bioenergy and Catalysis Research Unit (BCRU), Faculty of Engineering, Thammasat University, Khlongluang-12120, Thailand

ARTICLE INFO

Keywords:
Drying Systems
Environmental sustainability index
CO_2 emission
Embodied energy
Energy payback time

ABSTRACT

Exergetic based sustainability indicators of advanced Heat Exchanger-Evacuated Tube Assisted Drying System (HE-ETADS) are evaluated in this research. Exergetic based sustainability indicators include environmental sustainability index, environmental destruction coefficient and environmental effect factor. Experiments are conducted on advanced drying system for 03 selected crops to check environmental suitability. Crops of hygroscopic nature i.e., garlic clove, banana slices, and peppermint leaves, are evaluated. Throughout the experiment, the highest drying cabin temperature is 87°C and 61°C in Case-I and Case-II. Novel drying system decreases the drying period of garlic clove, banana slices, and peppermint leaves by 45%, 43%, and 62%, respectively. The system mitigates 77, 45.52, and 126 tons of CO_2 & 42.68, 24.62, and 39.21 tons of CO_2 in its lifetime for Case-I and Case-II for garlic cloves, banana slices and peppermint leave correspondingly. Energy payback time for garlic cloves, banana slices, and peppermint leaves is 0.85, 1.1 and 2.45 years less in Case-I compared to Case-II. The drying system is more sustainable in Case-I, with a higher Environmental Sustainability Index (ESI) value of 2.92, while in Case-II, the drying system has a lower value (1.25).

Introduction

The emission of greenhouse gases is one of the leading causes of contaminating environment. International treaty has been contracted with Kyoto Protocol that came into action in 2005 to decrease the emission of greenhouse gases i.e., carbon monoxide, hydrocarbons, methane, carbon dioxide, Sulphur hexafluoride, hydrofluorocarbons, and nitrous oxides [1]. Carbon credit is a certification allotted to commercial and specific customers to release 01 ton of carbon or other comparable greenhouse gases into the environment. The certification may be obtained by decreasing 1 ton of carbon footmark from the environment or procuring from others with extra carbon credits. The European Union Emissions Trading System observed that the carbon credits rate fluctuates between US$7.75 and US$25.21 [2].

Solar drying systems have become a sustainable solution to space heating [3]. These systems also play a significant role in decreasing carbon footprints because renewable energy sources operate them. The demand for foods can be sustainably met by increasing population with these drying systems. Due to some limitations, such as lower drying cabin temperature, low drying rate, these drying systems have lower efficiency. To overcome these limitations, hybrid drying systems were introduced. Hybrid drying systems can produce higher drying cabin temperature than existing conventional greenhouse solar dryers, increase moisture removal rate from top surface of foodstuffs, and decrease drying hours [4–6]. Another resource of thermal energy storage can be used with solar energy in a hybrid drying system. By this, these systems remain in operational condition with auxiliary sources of energy such as solar collectors (FPC, ETC) and phase change materials in sunset periods. Several investigations have been carried out to specify these systems' environmental suitability [7].

Tripathy et al. evaluated that mixed mode type drying system will decrease the 23% CO_2 emission and also analyzed that conventional energy consumption can be minimized in the range of 28–81% with a minimum of 39% efficient solar drying system [8]. Singh and Tiwari developed a mixed-mode type solar drying system and observed that maximum CO_2 mitigation was attained using solar energy in place of coal. This drying system mitigates CO_2 178–612 kg annually with a volumetric dimension of 0.19 m^2 [9]. Prakash et al. fabricated a greenhouse solar dying system and computed the CO_2 mitigation as well

* Corresponding author at: Department of Mechanical Engineering, Delhi Technological University, Delhi-110 042, India.
E-mail address: anilkumar76@dtu.ac.in (A. Kumar).

https://doi.org/10.1016/j.seta.2023.103277
Received 31 December 2022; Received in revised form 30 April 2023; Accepted 3 May 2023

Process Safety and Environmental Protection 170 (2023) 176–187

Contents lists available at ScienceDirect

Process Safety and Environmental Protection

journal homepage: www.journals.elsevier.com/process-safety-and-environmental-protection

Optimization of drying parameters for hybrid indirect solar dryer for banana slices using response surface methodology

Anand Kushwah [a], Anil Kumar [a,b,*], Manoj Kumar Gaur [c]

[a] Department of Mechanical Engineering, Delhi Technological University, Delhi 110042, India
[b] Centre for Energy and Environment, Delhi Technological University, Delhi 110042, India
[c] Department of Mechanical Engineering, Madhav Institute of Technology & Science, Gwalior 474005, India

ARTICLE INFO

Keywords:
RSM
Shrinkage
Banana
Energy consumption
Moisture content
Solar drying

ABSTRACT

Present research work focuses on applying response surface methodology (RSM) in optimization and modeling dried banana slices in a hybrid indirect solar dryer. The relationship of independent variables in terms of mass of banana slices (kg), drying chamber temperature (°C), water flow rate (L/hr), and geometry (cm^2). Therefore, responses of interest or dependent variable consisting of moisture content (% db), energy consumption (kW/h), and shrinkage (%) utilization are concluded. A short drying period and energy consumption are seen as the optimizing drying parameters of banana slices. Response surface methodology with central composite design (CCD) was applied to optimize the dependent variable. Experimentally observed data are adjusted by applying a second-order polynomial regression model. The predicted R^2 in the range of 0.9828–0.9530, adjusted R^2 value (0.9571–0.9974), and model F value (08.18) for banana slices were calculated. Optimal operational parameters are observed 89.99 °C (drying cabin temperature), 14.0 L/hr (water flow rate), 0.9998 (circular geometry), and 0.24004 kg (product mass). Optimum responses were 7.55% db (moisture content, MC), 5.54 kW/h (energy consumption), and 69.54% (shrinkage). Further, experiment was conducted at optimal operating conditions, and the results indicate good consistency between predicted and experimental data with a deviation of 3.14%, 2.16% and, 1.41% for the minimum moisture content (wb), energy consumption and, shrinkage, respectively.

1. Introduction

Since ancient times, preserving fruits and vegetables has played a vital role in human history. It has been practiced for centuries by the sun's power to preserve food and other agricultural products. In traditional method of drying, crops are generally dehydrated directly in sunlight under open sun. Compared to drying by heat effect generated by conventional energy sources, it is a popular and affordable method of food preservation and is still generally utilized in most underdeveloped countries. Drying is also one more necessary process in many food handling plants. If drying is not completed properly, it will introduce several critical inadequacies in the quantity and quality of the dried products. It required significant energy utilization in various segments of the production processes of various outputs. About 60% of collective energy produces by dried products (Prakash and Kumar, 2017, 2020; Zomorodian et al., 2007).

Moisture content (MC) of agricultural products (fruits and vegetables) is high, in the range of 80–85%, and both are considered very unpreserved products (Pasban et al., 2017). Hence, fruit and vegetables are dehydrated to improve storing capacity, reduce packing necessities and minimize transport weight (Sagar and Suresh Kumar, 2010). The most common application of convective dryers in the food industries reduces the drying period and enhances effective drying. Operating variables affecting the drying method and the dehydrated conditions are the thermo physical properties of food products, including ambient temperature, relative humidity (Rh), and air flow rate (Majdi and Esfahani, 2019). Drying is a commonly accepted method of preserving food products. Banana is necessary raw material for several food products. Banana plantation is cultivated throughout the whole world. Thus, it is critical to find out the operating parameters in which the possessions of fresh banana can be conserved and to set optimum conditions to store and use again. In dehydrating banana slices, minimizing the dehydration cost is one of the most considered parameters. Second, the parameters that offer the lowest expenses conflict with the outcome in the maximum eminence, as optimal parameters of heat and mass transfer do not match those for optimal eminence (Bai et al., 2002).

Majdi and Esfahani proposed a novel technique for numerical

* Corresponding author at: Department of Mechanical Engineering, Delhi Technological University, Delhi 110042, India.
E-mail address: anilkumar76@dtu.ac.in (A. Kumar).

https://doi.org/10.1016/j.psep.2022.12.003
Received 5 October 2022; Received in revised form 1 December 2022; Accepted 1 December 2022
Available online 5 December 2022

ASME Journal of Solar Energy Engineering
Online journal at:
https://asmedigitalcollection.asme.org/solarenergyengineering

Anand Kushwah
Department of Mechanical Engineering,
Delhi Technological University,
Delhi 110042, India
e-mail: anand.kushwah1989@gmail.com

Anil Kumar[1]
Department of Mechanical Engineering,
Delhi Technological University,
Delhi 110042, India;
Centre for Energy and Environment,
Delhi Technological University,
Delhi 110042, India
e-mail: anilkumar76@dtu.ac.in

Manoj Kumar Gaur
Department of Mechanical Engineering,
Madhav Institute of Technology and Science,
Gwalior 474005, India
e-mail: gmanojkumar@rediffmail.com

Amit Pal
Department of Mechanical Engineering,
Delhi Technological University,
Delhi 110042, India
e-mail: amitpal@dce.ac.in

Heat and Mass Transfer, Quality, Performance Analysis, and Modeling of Thin Layer Drying Kinetics of Banana Slices

In this study, experimental works were carried out in three different drying methods named heat exchanger-evacuated tube-assisted drying system (HE-ETADS), greenhouse solar dryer (GHSD), and open sun drying (OSD) to compare thin-layer drying kinetics, concept of mass transfer, and quality assessment of banana slices. Initial moisture content (MC) of banana slices was obtained as 78 ± 2.0% (wb), which decreased to 23.2 ± 2.0% (wb), 25.6 ± 2.0% (wb), and 28.8 ± 2.0% (wb) in all three drying systems, respectively, in 9 h of drying time. Average drying rate was evaluated as 7.89, 7.65, and 7.25 g water/g solid h in HE-ETADS, GHSD, and OSD, respectively. Weibull model (WM) defines thin-layer drying kinetics of banana slices in all three drying processes. Maximum hardness and shrinkage factor of dried banana slices were obtained as 373.6 g and 75%, respectively, in HE-ETADS. Effective moisture diffusivity, activation energy, and mass transfer coefficient were computed as 1.11–2.48 × 10^{-07} m^2 s^{-1}, 30.25 kJ/mole, and 3.21–1.0 × 10^{-04} m/s, in HE-ETADS. Similarly, in GHSD and OSD, these factors were observed as 1.21–2.34 × 10^{-07} m^2 s^{-1}, 41.25 kJ/mole, 3.15–1.0 × 10^{-04} m/s and 1.3–2.21 × 10^{-07} m^2 s^{-1}, 56.89 kJ/mole, 3.01–1.0 × 10^{-04} m/s. Maximum total color changes were noted in OSD. Hence, HE-ETADS can potentially dry high moisture content crops effectively within a minimum drying period. [DOI: 10.1115/1.4062447]

Keywords: banana slices, HE-ETADS, GHSD, OSD, quality assessment, mass transfer, collector, drying, heat transfer, solar

1 Introduction

Banana is a major fruit crop in tropical–subtropical and contributes significantly to the economy of many countries. Sweet bananas have become very popular in modern western diets. They are popular for their taste, texture, and convenience value, being easy to peel and eat. Bananas contribute to Vitamins A, C, and B_6 diet content and are an important and immediate energy source often consumed by players or athletes during competitions. They are also cholesterol-free and rich in fiber. A medium sized banana contains 280 kJ energy, greater than deciduous and citrus fruits. They are mainly eaten raw as a dessert because they are sweet when ripe and are easily digested. Bananas have medicinal value in many special diets. Ripe mashed banana is an excellent food for children due to its easy digestibility, vitamin content, and minerals [1]. For old people, fruit can be consumed in large quantities without causing fattening or digestive disturbances.

Bananas are low in sodium, contain very little fat, and no cholesterol. Hence, it is useful in managing patients with hypertension and heart diseases. Bananas can neutralize free hydrochloric acid (HCl), which suggests its use in the treatment of peptic ulcers [2]. Fully ripe banana mixed with milk powder is especially advised for ulcer patients. It is an excellent source of energy. That is why it is consumed worldwide from one form to another. Recently, research has focused and interested in bananas due to their nutritional and economic importance. Common foods obtained from bananas are chips, pasta and noodles, etc.

Drying process of a crop can be described as a series of steps in which drying rate (DR) plays a significant role. Figure 1 displays a typical drying rate curve for a constant drying condition. Point B represents equilibrium temperature conditions of the product surface. Sections B and C of curve, called constant rate periods, represent removal of unbound water from the crop. The water acts as if the solid is not present. The surface of crop is very wet and watery. The constant rate period continues as long as the amount of water that evaporates equals the amount of water supplied to the crop surface (banana slices). The falling rate period is attained when the drying rate starts to reduce and the surface water activity (A_w) >1. Rate of drying is governed by internal flow of liquid or vapor. This point is represented by C in the curve. At this point, there is insufficient water on the surface to maintain an $A_w = 1$. The falling rate period can be categorized into two steps. A first falling drying rate occurs when wetted spots in the surface continually diminish until the surface is dried (point D). The second

[1]Corresponding author.

Contributed by the Solar Energy Division of ASME for publication in the Journal of Solar Energy Engineering: Including Wind Energy and Building Energy Conservation. Manuscript received September 11, 2022; final manuscript received April 17, 2023; published online May 18, 2023. Assoc. Editor: Prathap Ramamurthy.

Sustainable Energy Technologies and Assessments 53 (2022) 102589

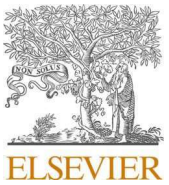

Contents lists available at ScienceDirect

Sustainable Energy Technologies and Assessments

journal homepage: www.elsevier.com/locate/seta

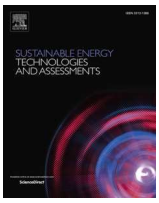

Performance analysis of heat exchanger- evacuated tube assisted drying system (HE-ETADS) under unload condition

Anand Kushwah [a], Anil Kumar [a,b,*], Manoj Kumar Gaur [c], Amit Pal [a]

[a] Department of Mechanical Engineering, Delhi Technological University, Delhi, India
[b] Centre for Energy and Environment, Delhi Technological University, Delhi, India
[c] Department of Mechanical Engineering, Madhav Institute of Technology & Science, Gwalior, India

ARTICLE INFO

Keywords:
Diffusion coefficient
Coefficient of performance
Heat consumption factor
Dryer
Unload

ABSTRACT

A prototype heat exchanger-evacuated tube assisted drying system (HE-ETADS) has been fabricated and tested under unload conditions in active mode at different water flow rates (10, 20, and 30Ltr/hr). Experimental work was conducted in three different categories. Category-I: drying system in stagnation condition, Category-II: all fans are in operating condition and Category-III: ventilation window is open. Coefficient of performance, heat consumption factor, convective heat transfer coefficient (CHTC) and diffusion coefficient have been calculated in thermal performance analysis of advanced system. Highest coefficient of diffusivity (0.19) was on third day of experimentation under Category-III at 30Ltr/hr water flow rate. Maximum heat consumption factor (0.60) was calculated during the second day for Category-I at 20Ltr/hr and for Category-II it was 0.775 during third day of experimentation at 30Ltr/hr, whereas in Category-III it was 0.782 at 10Ltr/hr water flow rate during first day of experiment. Higher coefficient of performance was 0.902 on third day of experiment for Category-I at 30Ltr/hr water flow rate whereas 0.940 was on first day of experimentation for Category-II at 10Ltr/hr flow rate. Category-III achieved 0.97 at 10Ltr/hr water flow rate during first day of experiment. CHTC of north wall insulated greenhouse dryer (NWIGHD) for ground to drying cabin air was 46.622 W/m^{2}°C, while for advanced HE-ETADS it was found 47.542 W/m^{2}°C, which is 1.98% greater than NWIGHD. Hence, HE-ETADS has potential to enhance drying rate and reduce payback period.

Introduction

According to previous investigations, energy utilization in the whole world is increased (doubled) every 20 years [1]. Therefore, the expenditure on renewable energy is still less than fossil fuel, which is responsible for several environmental pollution and problems worldwide. Hence, the need for renewable energy, particularly solar power (solar energy), has grown recently [2]. Significant amount of whole world energy, nearly 30%, is consumed in farming areas and around 3.59% is utilized in dehydrating crops and foodstuffs [3–5].

One suitable technique for preserving farming products such as fresh vegetables and fruits is dehydrating them via well-designed machines with optimal energy utilization. It could be in the absence of dehydrating process and free water is responsible for spoils or rots in the foodstuff. Hence, removing free water in terms of moisture from the surface of vegetables and fruits improves the shelf life of the agricultural products and makes those products easy to package and transport. Solar dehydrating is one of the greatest techniques for dehydrating farming produce that comprises two industrial as well as traditional processes. In traditional ways, because of dehydrating agricultural products in the front of sun on open roof or floor, the quality of dried products in terms of color index is less than industrial technique [6].

In another way, it is used worldwide due to the availability of sun power in terms of solar energy and easy design or fabrication of solar dryer (SD). Despite the advantages of using solar power for dehydrating farming produces, such as low price and accessibility, little advancement in these dryers has taken place because of lower efficiency. Therefore, many studies have been done to enhance the thermal performance of SD. Several varieties of solar collectors are generally coupled with SD. One of them, solar cabinet types dryer, is widely used. In this dryer, drying cabin and source of heat in the form of thermal energy are parted and food materials are not in direct contact with sunlight, preserving product quality and color index [7–8].

It is observed from literature that, due to abundant, low cost and unlimited amount of solar energy, it is being used in dehydrating

* Corresponding author at: Department of Mechanical Engineering, Delhi Technological University, Delhi, India.
E-mail address: anilkumar76@dtu.ac.in (A. Kumar).

https://doi.org/10.1016/j.seta.2022.102589
Received 20 April 2022; Received in revised form 14 July 2022; Accepted 25 July 2022

Journal of Stored Products Research 93 (2021) 101852

Contents lists available at ScienceDirect

Journal of Stored Products Research

journal homepage: www.elsevier.com/locate/jspr

Garlic dehydration inside heat exchanger-evacuated tube assisted drying system: Thermal performance, drying kinetic and color index

Anand Kushwah [a], Anil Kumar [a,b,*], Manoj Kumar Gaur [c], Amit Pal [a]

[a] Department of Mechanical Engineering, Delhi Technological University, Delhi, 110042, India
[b] Centre for Energy and Environment, Delhi Technological University, Delhi, 110042, India
[c] Department of Mechanical Engineering, Madhav Institute of Technology & Science, Gwalior, 474005, India

ARTICLE INFO

Keywords:
Solar dryer
Evacuated tube solar collector
Drying rate
Efficiency
Exergy

ABSTRACT

An experimental investigation was done on an advanced evacuated tube-assisted solar drying system without and with load conditions at various water flow rates (10 L/h, 20 L/h, and 30 L/h) to evaluate its performance analysis. 79.56 °C maximum greenhouse air temperature was recorded without load at 30 L/h water flow rate with an average solar intensity of 850 W/m^2. Highest value of drying rate (DR) is 1.48 kgH_2O/kg dry solid/h and the maximum efficiency of solar collector (SC) and solar dryer (SD) is 43.62% and 55.28%, respectively, at 30 L/h water flow rate. Garlic was dehydrating from 70% to 8% (wb) moisture content (MC). The maximum exergy efficiency (EE) and minimum exergy loss were 57.64% at 30 L/h water flow rate and 4.58 W at 10 L/h water flow rate. Quality assessment is also carried out for dried garlic samples in the heat exchanger –evacuated tube assisted drying system (HE-ETADS). Color conservation (indices) of dehydrated garlic sample is best in HE-ETADS (L_o = 60.42, a_o = −0.92, and b_o = 11.54) in comparison to old-style (traditional) drying process (L_o = 58.89, a_o = - 0.67, and b_o = 5.99). Therefore, the developed drying system represented not only good financial returns but also better product quality. The present system provides interesting options for the entry of this type of collectors in medium-scale applications in the agricultural and industrial sectors.

1. Introduction

Food is one of the essential requirements of living beings for their existence. With the increase in population, the food requirement also increases. Produced food needs to be conserved by reducing the various post-harvest losses to meet the food requirement. Solar dryers are the setup to harness solar energy for drying crops or grains or other non-agricultural products. Edible items (fruits, vegetables, cereals, etc.) are mostly spoiled due to their high moisture content. Effective method to preserve the crop from being deteriorated is drying them up to a safe moisture level (Koyuncu et al., 2007; Singh et al., 2018a,b; Stegou-Sagia and Fragkou, 2015, 2018). During drying, the moisture level at which the crop is considered safe for storage with a minimum loss in its nutritious qualities is termed as a safe moisture level (Afolabi, 2014). Dried agricultural produces had various advantages like better quality, low after harvest losses, and longer storage time (Vijayan et al., 2020; Tiwari et al., 2017). Various artificial dryers are developed, providing the required velocity and temperature to achieve good quality products in less time (Banout et al., 2011). However, these dryers consume energy generated from conventional sources and are not eco-friendly (Mewa et al., 2019). Solar drying is considered a proficient method of using solar insolation for drying purposes (Janjai et al., 2007; Chauhan Singh et al., 2015; Prakash and Kumar, 2017, 2020) as the energy from the Sun is a clean source of energy and available in ample quantity (Kumar and Tiwari, 2007; Bhardwaj et al., 2019). Solar drying is not a very new concept as from ancient times. Natural sun drying is used for drying crops and other non-agricultural produce (Vijayavenkataraman et al., 2012; Cerci and Akpinar, 2016). Open sun drying requires less investment, but the dried product contaminates easily by birds, insects, pests, dirt, grit, rain, etc. (ELkhadraoui et al., 2015; Ramos et al., 2015; Lamidi et al., 2019). Hence, the solar dryers were developed to prevent crop deterioration and store it for a longer time (Fudholi et al., 2016). Solar dryers are also sustainable as they emit very low or even negligible carbon (Prakash and Kumar, 2013; Singh et al., 2018a). Solar dryers are classified into direct, indirect, and mixed-mode types (Semple et al., 2017). Greenhouse dryer (direct type) emerges as the best means to utilize solar energy for bulk drying and space heating (Singh and Gaur, 2020). The greenhouse solar dryers function on the greenhouse effect principle as enclosing material like glass, polythene, polycarbonate

* Corresponding author. Department of Mechanical Engineering, Delhi Technological University, Delhi, 110042, India.
E-mail address: anilkumar76@dtu.ac.in (A. Kumar).

https://doi.org/10.1016/j.jspr.2021.101852
Received 6 May 2021; Received in revised form 19 May 2021; Accepted 21 June 2021

Materials Today: Proceedings xxx (xxxx) xxx

Contents lists available at ScienceDirect

Materials Today: Proceedings

journal homepage: www.elsevier.com/locate/matpr

Experimental analysis and thermal performance of evacuated tube solar collector assisted solar dryer

Anand Kushwah [a], Anil Kumar [a,b,*], Amit Pal [a], Manoj Kumar Gaur [c]

[a] Department of Mechanical Engineering, Delhi Technological University, Delhi 110 042, India
[b] Centre for Energy and Environment, Delhi Technological University, Delhi 110 042, India
[c] Mechanical Engineering Department, Madhav Institute of Technology and Science, Gwalior 474 005, India

ARTICLE INFO

Article history:
Available online xxxx

Keywords:
Solar drying
Drying rate
Temperature
Heating
Evacuated tube solar collector assisted solar drying system

ABSTRACT

The solar drying of agricultural products is considered the most excellent green and sustainable agricultural product conservation method. The advancement of effective drying system design and agricultural products drying characteristics will increase product conservation. The current research work focuses on the investigation analysis of evacuated tube assisted solar dryer in eliminating the moisture ratio present in the crops. The temperature can be controlled and maintained by regulating the flow rate of flowing hot water inside the drying chamber with heat exchanger. The thermal performance of evacuated tube solar collector assisted solar dryer and open sun drying method were compared. Due to advancements in solar dryers, its drying cabin temperature increased. Consequences indicated that using a hybrid greenhouse solar dryer decreased the drying period while equating to open sun drying. All the experiments are performed under the environmental condition of Gwalior-India (26.2183° N, 78.1828° E) during the days of February 25, 2021 and February 26, 2021. The temperature difference between drying methods during the experiment was recorded 14.35℃ and 13.95℃ on the first day and second day of experiments, respectively. Also the relative humidity of open sun drying method is more in comparison to hybrid greenhouse solar drying. Time need to reduce moisture by using advanced solar dry systems recorded 7 h, while in open sun drying 10 h. The results show that drying time is 30% more in open sun drying.

Selection and peer-review under responsibility of the scientific committee of the Technology Innovation in Mechanical Engineering-2021.

1. Introduction

Using the Sun's power to preserve foodstuff and other products from agriculture has been in practice for centuries. In the traditional drying technique, agricultural products are generally dried directly in the Sun under the open sky. This is a popular and economical method of agricultural product preservation, compared to drying by the heating effect produced by conventional energy sources, and is still frequently used in most developing countries. The most important drawback of the mentioned conventional method is that the goods are exposed to dirt, animals, insects, wind and open atmospheric effects and need to be covered every time during adverse climatic conditions like rain or dew. In addition to these limitations, drying results are dependent on good weather conditions [1]. The latest solar drying approaches have good efficiency, provide hygiene, and keep agricultural products safe from damage. Solar drying carried out in solar dryers uses the thermal energy received from the Sun in the form of solar radiation to dry the products. These solar dryers manage controlled drying by maintaining the main influencing parameters such as moisture content, solar dryer temperature, humidity, and airflow rate. Sufficient drying helps preserve the food's flavour, texture, and color, ultimately providing a better-quality product [2]. Prakash and Kumar [3] developed an adapted greenhouse drying system for dehydration of tomato flakes in active mode and performed thermal investigation. The efficiency of the greenhouse drying system was increased by using black color polycarbonate sheet to cover the drying system. In the beginning, the MC (moisture content) was 96.0% in the product on wet basis and after the drying MC reduced up to 9.08% on wet basis for 15 h. Kumar and Tiwari [4] developed thermal modeling of drying systems in forced convection mode for jaggery. The value of the coefficient of correlation

* Corresponding author at: Department of Mechanical Engineering, Delhi Technological University, Delhi 110 042, India.
E-mail address: anilkumar76@dtu.ac.in (A. Kumar).

https://doi.org/10.1016/j.matpr.2021.04.243
2214-7853/
Selection and peer-review under responsibility of the scientific committee of the Technology Innovation in Mechanical Engineering-2021.

PAPER NAME

Anand PhD 05_12_2023.docx

AUTHOR

Anand Kushwah

WORD COUNT

22013 Words

CHARACTER COUNT

120926 Characters

PAGE COUNT

118 Pages

FILE SIZE

15.3MB

SUBMISSION DATE

Dec 15, 2023 11:47 AM GMT+5:30

REPORT DATE

Dec 15, 2023 11:49 AM GMT+5:30

7% Overall Similarity

The combined total of all matches, including overlapping sources, for each database.

- 3% Internet database
- 6% Publications database
- Crossref database
- Crossref Posted Content database
- 2% Submitted Works database

Excluded from Similarity Report

- Bibliographic material
- Quoted material
- Cited material
- Small Matches (Less then 12 words)
- Manually excluded sources